

**For Reference**

---

**NOT TO BE TAKEN FROM THIS ROOM**

Ex libris  
UNIVERSITATIS  
ALBERTAEENSIS













THE UNIVERSITY OF ALBERTA

RELEASE FORM

NAME OF AUTHOR .....STEPHEN C. CHATWIN.....

TITLE OF THESIS .....PERMAFROST AGGRADATION AND DEGRADATION.....

.....IN A SUB-ARCTIC PEATLAND.....

DEGREE FOR WHICH THESIS WAS PRESENTED .....MASTER OF SCIENCE.....

YEAR THIS DEGREE GRANTED .....1981.....

Permission is hereby granted to The UNIVERSITY OF ALBERTA  
LIBRARY to reproduce single copies of this thesis and to lend or  
sell such copies for private, scholarly or scientific research  
purposes only.

The author reserves other publication rights, and neither  
the thesis nor extensive extracts from it may be printed or  
otherwise reproduced without the author's written permission.



THE UNIVERSITY OF ALBERTA

PERMAFROST AGGRADATION AND DEGRADATION

IN A SUB-ARCTIC PEATLAND

by



STEPHEN C. CHATWIN

A THESIS

SUBMITTED TO THE FACULTY OF GRADUATE STUDIES AND RESEARCH

IN PARTIAL FULFILLMENT OF THE REQUIREMENTS FOR THE DEGREE

OF MASTER OF SCIENCE

DEPARTMENT OF GEOLOGY

EDMONTON, ALBERTA

Fall, 1981





61F-3

THE UNIVERSITY OF ALBERTA  
FACULTY OF GRADUATE STUDIES AND RESEARCH

The undersigned certify that they have read, and recommend to the Faculty of Graduate Studies and Research, for acceptance, a thesis entitled Permafrost Aggradation and Degradation in a Sub-Arctic Peatland submitted by Stephen C. Chatwin in partial fulfilment of the requirements for the degree of Master of Science.



## ABSTRACT

A detailed field and laboratory investigation was made of a palsa complex near Fort Simpson, Northwest Territories, in order to characterize and determine the origin of the landform. Permafrost is discontinuous in the area, occurring mainly in peatlands that have developed over glacio-lacustrine sediments. Regionally the development of permafrost has been relatively recent, probably not occurring before 3500 years Before Present. Paleoclimatic information, obtained by oxygen isotope analysis of peat cellulose, indicates that past temperatures have not been an impediment to permafrost aggradation. There is no evidence for temperatures warmer than present day values over the past 10,000 years. The absence of permafrost in the early Holocene is attributed to the high water levels in the peatlands. Stratigraphic investigations show the peatland has evolved through five distinct vegetative phases, each phase being attributable to increasingly efficient peatland drainage. It was not until water table divides formed, creating local ombrotrophic conditions, that extensive Sphagnum bogs developed. As water levels in the bogs dropped, possibly aided by a period of intense dessication, the unique thermal properties of Sphagnum led to permafrost development. Isotopic evidence indicates there has been continuous upward moisture migration through the permafrost ever since its initial aggradation.

Stratigraphic evidence indicates that permafrost became areally extensive, but not continuous, covering at least 5 km<sup>2</sup> in the study





area. The greatest development of segregated ice occurred along the former margins of the glacial lakes, especially in areas with slightly elevated mineral soil. With climatic warming, beginning approximately 300 years B.P., rapid thermal degradation of the permafrost occurred. Over the last 30 years, the areal extent of frozen ground has decreased by approximately 25%. There is no evidence for cyclical aggradational-degradational periods.

The palsa complex is not a frost heave feature, but rather is a relic thermo-erosional landform. Melting of the segregated ice in the mineral soil only accounts for approximately one-half of the observed relief in a fen-palsa peatland. The remaining relief is due to normal consolidation of the uplifted peat as it thaws. The end result of a melted palsa is a shallow circular pond.



## ACKNOWLEDGMENTS

This project was initiated by Dr. Owen Hughes, of the Geological Survey of Canada. His suggestion of the topic and of a suitable study location, his aid in obtaining logistical support for the fieldwork, as well as his ideas expressed in many fruitful discussions are gratefully acknowledged.

A number of organizations have financially contributed to the field work and laboratory expenses. Appreciation is expressed to the Boreal Institute (at the University of Alberta) and the former Northern Engineering Ltd. (Canadian Arctic Gas) for providing funds and to the Terrain Sciences Division, Geological Survey of Canada, for loaning equipment and manpower for the winter drilling program.

Special thanks are due to a number of people who assisted during various phases of this work: Mark Nixon for his drilling expertise, often under very trying conditions; Susan Preston, Jack Wong and Domino Smith for their summer field assistance; and to Susan Preston for her help with manuscript preparation.

Finally, I thank my committee for their patience and guidance and my thesis advisor, Dr. Nat Rutter, for his encouragement and advice.



## TABLE OF CONTENTS

|  | <u>PAGE</u> |
|--|-------------|
| CHAPTER 1 INTRODUCTION                     | 1           |
| 1.1 Objectives                             | 2           |
| 1.2 Location of Study Site                 | 3           |
| 1.3 Field Methods                          | 7           |
| 1.4 Previous Theories of Palsa Development | 8           |
| <br>CHAPTER 2 TERRAIN CHARACTERISTICS      | <br>11      |
| 2.1 Climate                                | 12          |
| 2.2 Glacial History and Geology            | 12          |
| 2.3 Landscape Position                     | 13          |
| 2.4 Morphology                             | 17          |
| 2.5 Vegetation                             | 24          |
| 2.6 Stratigraphy                           | 24          |
| 2.7 Permafrost Configuration               | 28          |
| 2.8 Ground Thermal Regime                  | 28          |
| 2.9 Ground Ice Characteristics             | 32          |





|  | <u>PAGE</u> |
|--|-------------|
| 2.91 Description                                 | 32          |
| 2.92 Ionic Chemistry                             | 36          |
| 2.93 Environmental Isotopes                      | 44          |
| 2.931 Tritium                                    | 46          |
| 2.932 Stable Isotopes                            | 48          |
| 2.10 Hydrogeology of the Palsa Complex           | 55          |
| CHAPTER 3 PALEOCLIMATIC DETERMINATION            | 58          |
| 3.1 Introduction                                 | 59          |
| 3.2 Previous Investigations                      | 60          |
| 3.3 Methods of Analysis                          | 63          |
| 3.4 Results                                      | 64          |
| 3.41 Effect of Different Plant Species           | 67          |
| 3.42 Effect of Humification on Isotope Values    | 70          |
| 3.43 Temperature Effects                         | 70          |
| 3.5 Paleoclimatic Interpretations                | 71          |
| CHAPTER 4 EVOLUTION OF THE PEATLAND LANDSCAPE    | 78          |
| 4.1 Introduction                                 | 79          |
| 4.2 Environmental Sequences                      | 80          |
| CHAPTER 5 Permafrost Aggradation and Degradation | 85          |
| 5.1 Introduction                                 | 86          |
| 5.2 Ground Ice Aggradation                       | 87          |
| 5.21 Processes and Controls                      | 87          |
| 5.211 Climatic Controls                          | 87          |
| 5.212 Vegetational and Hydrological Controls     | 88          |



|   | <u>PAGE</u> |
|---|-------------|
| 5.213 Influence of Mineral Soil Topography                        | 90          |
| 5.3 Ground Ice Degradation  | 101         |
| 5.31 Processes and Controls                                       | 101         |
| 5.311 Surface Processes   | 101         |
| 5.312 Bottom Melting  | 102         |
| 5.313 Lateral Erosion   | 102         |
| 5.32 Former Extent of Permafrost                                  | 105         |
| 5.33 Rates of Ground Ice Degradation                              | 109         |
| 5.4 The Effect on Palsa Relief                                    | 110         |
| CHAPTER 6 Concluding Remarks                                      | 117         |
| 6.1 Regional Permafrost Development in the Fort Simpson Peatlands | 118         |
| 6.2 The Palsa Complex: A Relic Thermo-erosional Landform          | 121         |
| 6.3 Open System Moisture Migration in Permafrost                  | 123         |
| 6.4 Further Research  | 127         |
| BIBLIOGRAPHY  | 129         |
| APPENDIX 1 Thermistor Construction                                | 142         |
| APPENDIX 2 Water Chemistry Results                                | 144         |
| APPENDIX 3 Thaw Consolidation Results                             | 147         |
| APPENDIX 4 Testing Methods: Thaw Consolidation                    | 153         |





|   | <u>PAGE</u> |
|---|-------------|
| APPENDIX 5    Stefan's Equation                                 | 155         |
| APPENDIX 6    Frost heave test methods                          | 156         |
| APPENDIX 7    Frost heave characteristics of the palsa<br>soils | 157         |



## LIST OF TABLES

| TABLE  | PAGE |
|--|------|
| 1. Peatland types and vegetation communitie  | 25   |
| 2. Peat types and modern growth environments   | 26   |
| 3. Major ion chemistry of surface waters and groundwaters  | 38   |
| 4. Environmental tritium analysis  | 47   |
| 5. Oxygen and hydrogen isotope ratios in ground ice, surface water and groundwater                                 | 49   |
| 6. Peat oxygen isotope results   | 66   |
| 7. Isotopic composition of modern peat forming plants  | 69   |
| 8. Summary of thaw consolidation relationships   | 97   |
| 9. Total thaw settlement of the mineral soil and observed frozen soil relief in the palsa complex                  | 98   |
| 10. The elevations of the mineral soil surface beneath unfrozen bogs and sinkholes relative to the fen water level | 100  |
| 11. Chemical analysis of peat and peat forming vegetation  | 107  |
| 12. Empirical relationships predicting thaw settlement in peat   | 113  |
| 13. Thaw settlement of the frozen peat cores and comparison with mineral soil settlement                           | 115  |



## LIST OF FIGURES

| FIGURE   | PAGE |
|--|------|
| 1. Location of study site  | 4    |
| 2. Map of palsa complex site   | 6    |
| 3. Distribution of peatland types and associated beach deposits in the Ft. Simpson area  | 15   |
| 4. Topographic profile, ground ice configuration, geophysical resistivity response, peat stratigraphy, and vegetation distribution for transect E - E' | 19   |
| 5. Topographic profile, ground ice configuration, geophysical resistivity response, peat stratigraphy, and vegetation distribution for transect S - S' | 20   |
| 6. Topographic profile, ground ice configuration, geophysical resistivity response, peat stratigraphy, and vegetation distribution for transect N - N' | 21   |
| 7. Temperature profile in frozen palsa   | 29   |
| 8. Temperature profile in unfrozen peat bog  | 30   |
| 9. Ground ice profiles from two transects across the palsa complex   | 34   |
| 10. Ground ice conductivity profiles   | 40   |
| 11. Major ion chemistry for core E-11  | 41   |
| 12. Major ion chemistry for core E-3   | 42   |
| 13. Major ion chemistry for core S-78  | 43   |
| 14. Oxygen isotope profile with depth, core E-11   | 50   |
| 15. Relationship between oxygen- 18 and deuterium, core S-78   | 51   |
| 16. Conceptual model for isotope exchange in ground ice under a temperature gradient   | 54   |



| FIGURE |  | PAGE |
|--------|--|------|
| 17.    | Isopotentials and local groundwater flow due to a perched collapse bog, site E-3   | 57   |
| 18.    | Flow chart for peat cellulose extraction   | 65   |
| 19.    | Showing the relationship between peat stratigraphy carbon-14 age of the peat, and oxygen isotopic value of the peat cellulose with depth, core E-3 | 68   |
| 20.    | Change in oxygen isotope content of modern <u>Sphagnum</u> moss with the mean annual temperature of their place of growth                          | 73   |
| 21.    | Geothermal profile near Ft. Providence   | 76   |
| 22.    | Thaw settlement parameter, A, for mineral soil related to frozen bulk density  | 93   |
| 23.    | Total thaw strain: frozen bulk density relationship for mineral soil   | 94   |
| 24.    | Coefficient of compressibility - frozen bulk density relationship for mineral soils  | 94   |
| 25.    | Moisture content - frozen bulk density relationship for mineral soil   | 95   |
| 26.    | Initial thaw settlement parameter - water content relationship for mineral soil  | 95   |
| 27.    | Relationship between total heave in mineral soil and initial mineral soil relief   | 96   |
| 28.    | Total thaw strain - frozen bulk density relationship for organic soils   | 113  |
| 29.    | Total thaw strain - volumetric ice content relationship for organic soils  | 113  |





## CHAPTER 1: INTRODUCTION



## 1.1 Objectives

Permafrost is defined as earth materials having a temperature below  $0^{\circ}\text{C}$ . for two or more years (Brown, 1963). Brown (1968) has delineated various zones of permafrost in Canada, on the basis of the distribution and frequency of perennially frozen ground. In the southern part of the Discontinuous Zone, permafrost occurs almost exclusively in peatlands.

The most common permafrost body in a subarctic peatland is the palsa, a circular to elongate mound of peat and mineral soil with a perennially frozen core. Individual palsas are generally less than 100 meters across and 1 to 7 meters in height (Sjors, 1961; Forsgren, 1968), but may coalesce, forming a palsa complex greater than  $1\text{ km}^2$  in area.

Past research emphasis on palsas has been on their morphology and plant ecology, with very little work on the internal structure, ground ice characteristics, or thermal and hydrological regimes. An assumption often made in previous studies is that the gross peatland environment was very similar in the past. Local edaphic factors were therefore assumed to be the controlling factors. This has naturally led to the notion of localized and cyclical permafrost dynamics in peatlands.

The hypothesis of this thesis is that modern peatland environments may be significantly different from those of the past because of regional changes in the climatic and hydrological regimes. To understand



permafrost dynamics, in subarctic peatlands, not only the modern terrain characteristics but also the history of the peatland environment must be established. The physical and chemical characteristics of the peat and ground ice may contain information on the peatland paleoenvironment.

The objectives of this thesis are:

1. To characterize the terrain of a palsa complex peatland;
2. To investigate the genesis of the palsa complex within the context of the evolution of the entire peatland;
3. To determine the role of regional climatic fluctuations in permafrost genesis in the Upper Mackenzie Valley;
4. To determine whether the formation of palsas is a dynamic and cyclic process or whether palsas are relic and erosive landforms;
5. To develop a conceptual model of permafrost aggradation and degradation in a subarctic peatland.

## 1.2 Location of Study Site

The palsa complex is located approximately 40 km southeast of Fort Simpson, N.W.T. about midway between the Mackenzie and Liard Rivers ( $61^{\circ} 28' \text{ N}$ ,  $120^{\circ} 55' \text{ E}$ ; Fig. 1).

The study site is located on a large speckled bog (Reid, 1977) palsa complex that is approximately 2000 m by 250 m in size. A



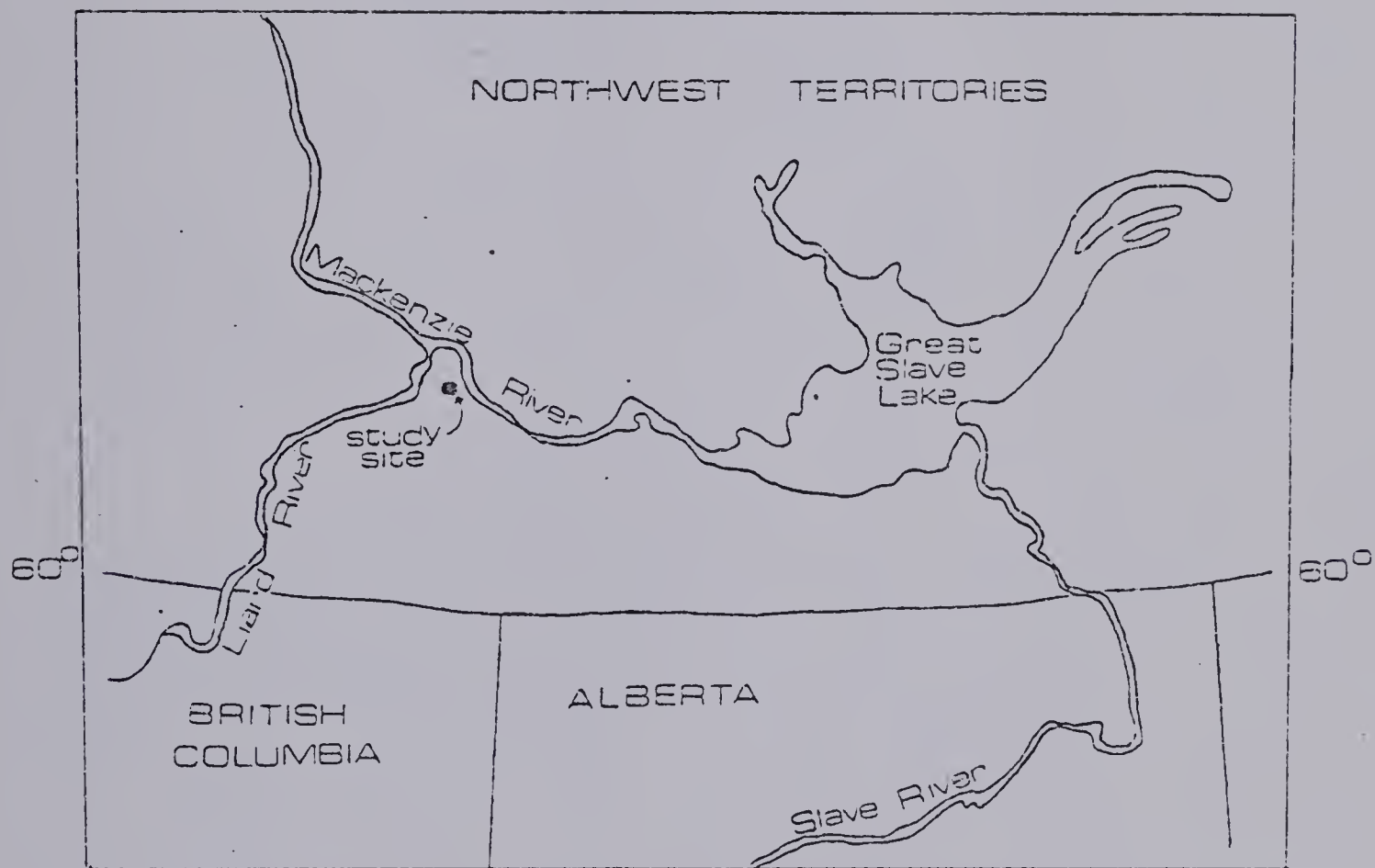


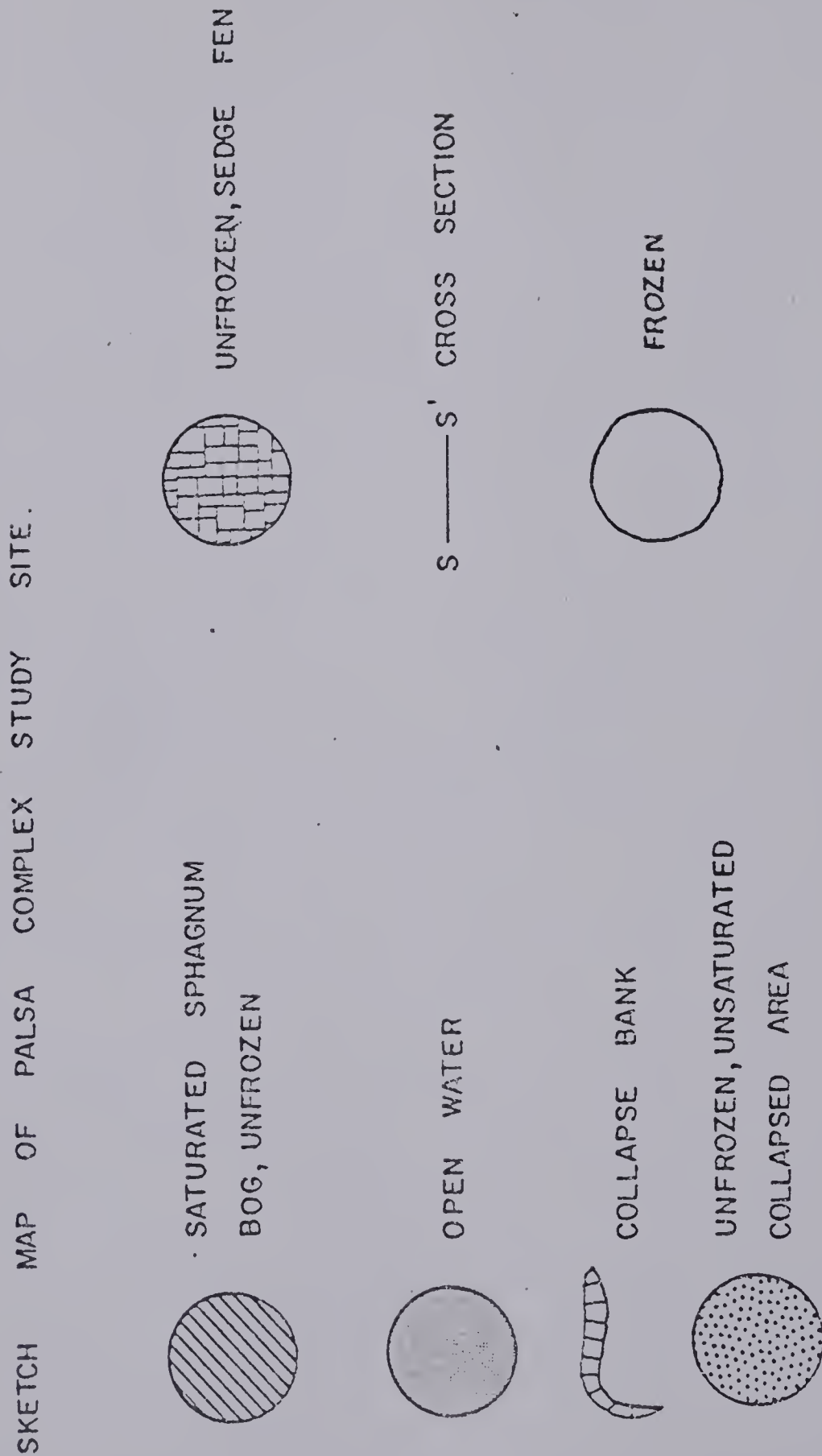
FIGURE 1 : Location of the study site

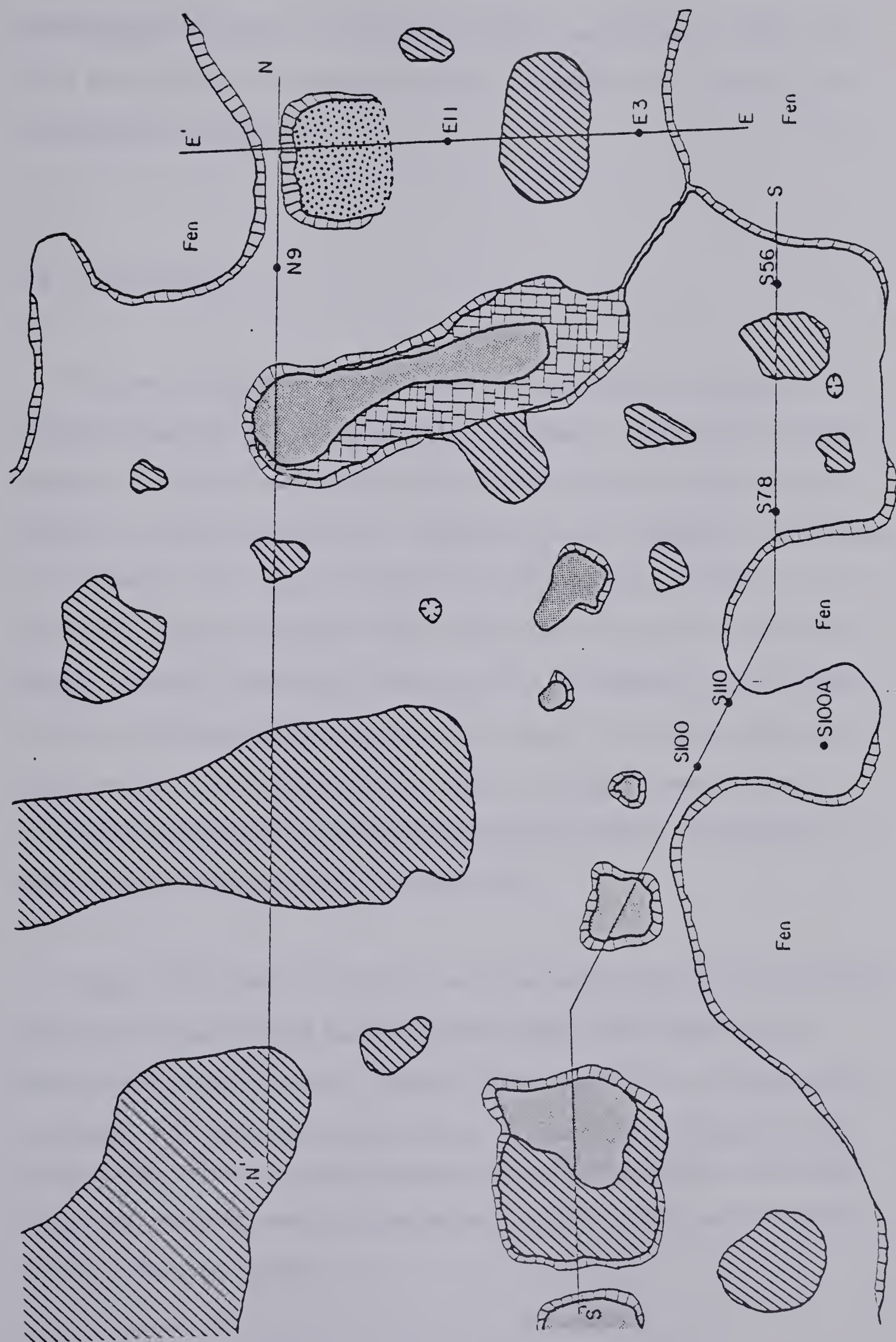






# FIGURE 2







representative section of the palsa complex, approximately 200 m by 100 m was selected for detailed study. A sketch map of the site is illustrated in figure 2.

### 1.3 Field Methods

The preservation of frozen cores is essential if chemical and isotopic analysis of the ground ice is planned. The winter drilling program was carried out with an all terrain vehicle mounted drill, similar to that described by J. Veillette (1975), capable of obtaining 9 cm diameter core using a standard permafrost coring barrel. The cores were sealed in plastic film then packed with snow in foam insulated crates. The cores, shipped by air to Edmonton, were exposed to above freezing temperatures for less than 8 hours and suffered no deterioration. The drill was also used to install seven pneumatic groundwater piezometers and three thermistor cables. Descriptions of these systems are included in chapter two.

Summer field work took place over two months during 1975 and 1976. Frozen peat stratigraphy and permafrost depths were determined by coring with a Hoffer probe. Unfrozen peat samples were obtained with a standard 5 cm diameter piston corer. Permafrost configuration was extrapolated between cores by means of electroresistivity profiling. Vegetation sampling was by a random point method developed by Braun-Blanquet (Kershaw, 1969).





#### 1.4 Previous Theories of Palsa Development

The role of vegetation, especially mosses of the genus Sphagnum, in creating a micro-climate conducive to permafrost aggradation is central to most theories of palsa formation. In North America, the role of Black Spruce in establishing a local negative heat balance has been emphasized (Sjors, 1963; Brown, 1968; Zoltai, 1971; and Zoltai and Tarnocai, 1975). By shading underlying peat from snow accumulation, there is deeper penetration of the winter frost front. As summer melting is reduced by the insulative properties of the peat and the shading provided by the spruce, small ice lenses may remain throughout the year. The coalescing of these frozen hummocks creates a peat plateau. The process is believed to initiate with a single Black Spruce seedling growing on a small, individual, slightly raised and drier hummock of Sphagnum.

In Fennoscandia and Labrador-Ungava, palsas are found north of the tree line, apparently developing without the aid of Black Spruce. Under treeless conditions, wind erosion of the protective snow cover on exposed palsa summits allows deeper propagation of the frost front (Salmi, 1970). While this theory explains the maintenance of the feature, it does not explain the initiation.

The presence of lichen communities on palsas has led to the hypothesis that albedo is an important factor in maintaining a negative heat balance. Lundqvist (1951) and Sjors (1961) have proposed that the high albedo of Sphagnum fuscum and Cladonia alpestris is sufficient





in northern regions to cause development of an ice core. Railton (1973) in a heat balance study of a palsa in the Hudson Bay Lowland discovered no evidence for this and found variations in heat balance from evapotranspiration to be of more importance.

A major controversy in palsa formation is whether the formation of palsas is a cyclic process, as first advocated by Lundqvist (1951) or whether palsas are relic features, formed in a past period of climatic deterioration. Lundqvist's theory of cyclical aggradation and degradation has been advanced in North America by Sjors (1963), Brown (1968), Zoltai (1971), Zoltai and Tarnocai (1971 and 1975), Payette and Samson (1976), Railton (1973), and Reid (1977). Zoltai and Tarnocai (1975) have applied the terms incipient, young, mature and over-mature to the developmental stages of palsas and peat plateaus. The incipient and young peat plateaus are considered to be an aggrading stage. The mature plateau is in a state of equilibrium which upon reaching the degrading stage is referred to as overmature. In contrast to this theory, Vorren (1972) and Sollid and Sorbel (1974) support the idea that palsas are relic landscape features which are out of phase with present climatic conditions, and that the ground ice is protected only by the insulating peat layer.

Further controversy in palsa development is that of a dynamic versus an erosive origin. The dynamic theory, first postulated by Lundqvist (1951), involves the progressive growth of a small Sphagnum frost hummock to a mature palsa. The previously mentioned process involving a Black Spruce initiated micro-climate, is a dynamic process.



This theory has received wide spread support both in Europe and in North America (Sjors, 1961; Zoltai, 1971; Zoltai and Tarnocai, 1975).

A theory first suggested by Cajuander (1913) is that palsas might be erosional features in the process of degrading. The region where present day palsas are found is thought to have once been covered by a broad area of polygonal frozen ground. Climatic warming has produced ground ice degradation and thermokarsting. Palsas are interpreted as erosional remnants of the once more extensive permafrost. More recently, Vorren (1972) has advocated an erosive origin for palsas in the northern part of Norway.



## CHAPTER 2: TERRAIN CHARACTERISTICS



## 2.1 Climate

The study site is within the Sub-Boreal Forest Climatic Zone (Burns, 1973). Mean daily temperature at Fort Simpson, 40 km to the north-west, is  $-4.1^{\circ}$  C.; the mean July temperature is  $16^{\circ}$  C.; and a mean temperature of  $-29^{\circ}$  C. is recorded for January. The number of freezing degree-days (below  $32^{\circ}$  F.) is 6300 and the number of thawing degree-days (above  $32^{\circ}$  F.) is 3450. Precipitation averages 34.5 cm of which 40% falls as snow.

## 2.2 Glacial History and Geology

The area was invaded at least twice from the east by Laurentide Ice (Rutter et al, 1974). The first advance is recorded by a grey-black basal stony till with erratics found up to an elevation of 1500 m in the Mackenzie Mountains to the west. The second, lesser, advance believed to be Classical Wisconsin, deposited a light grey-brown stony till (Rutter et al, 1973).

Retreat of the ice sheet was northeastward, damming natural drainage outlets and creating large glacial lakes along the Mackenzie and Liard River Valleys. Glacial Lake McConnell was the largest of these lakes, remaining until at least 11,500 years B.P. (Rutter et al, 1973). Large fluctuations in lake levels created well defined beach ridges.





The study site is located approximately 250 meters north of one of the prominent beach ridges. The beaches, composed of fine to medium grained sands with occasional gravel, are up to 6 m in height. To the north, is a broad silty clay glaciolacustrine plain capped uniformly with organic deposits. Occasional sand dunes provide the only relief. Surficial sediment is underlain by Lower Cretaceous shales of the Ft. St. John group and by Upper Devonian cryptocrystalline and clastic limestones of the Dunvegan formation.

### 2.3 Landscape Position

The areal distribution of six peatland types is superimposed on the surficial geology map of the area (Rutter, et al, 1973; Fig. 3).

The peatland types are:

1. fen
2. fen with scattered peat plateaus
3. peat plateau
4. 'speckled bog'
5. 'speckled bog' palsa complex
6. collapse scars and ponds.

They are subdivided on the basis of ground ice development, but mapped by air photo identification of associated surface characteristics (see legend, Figure 3).

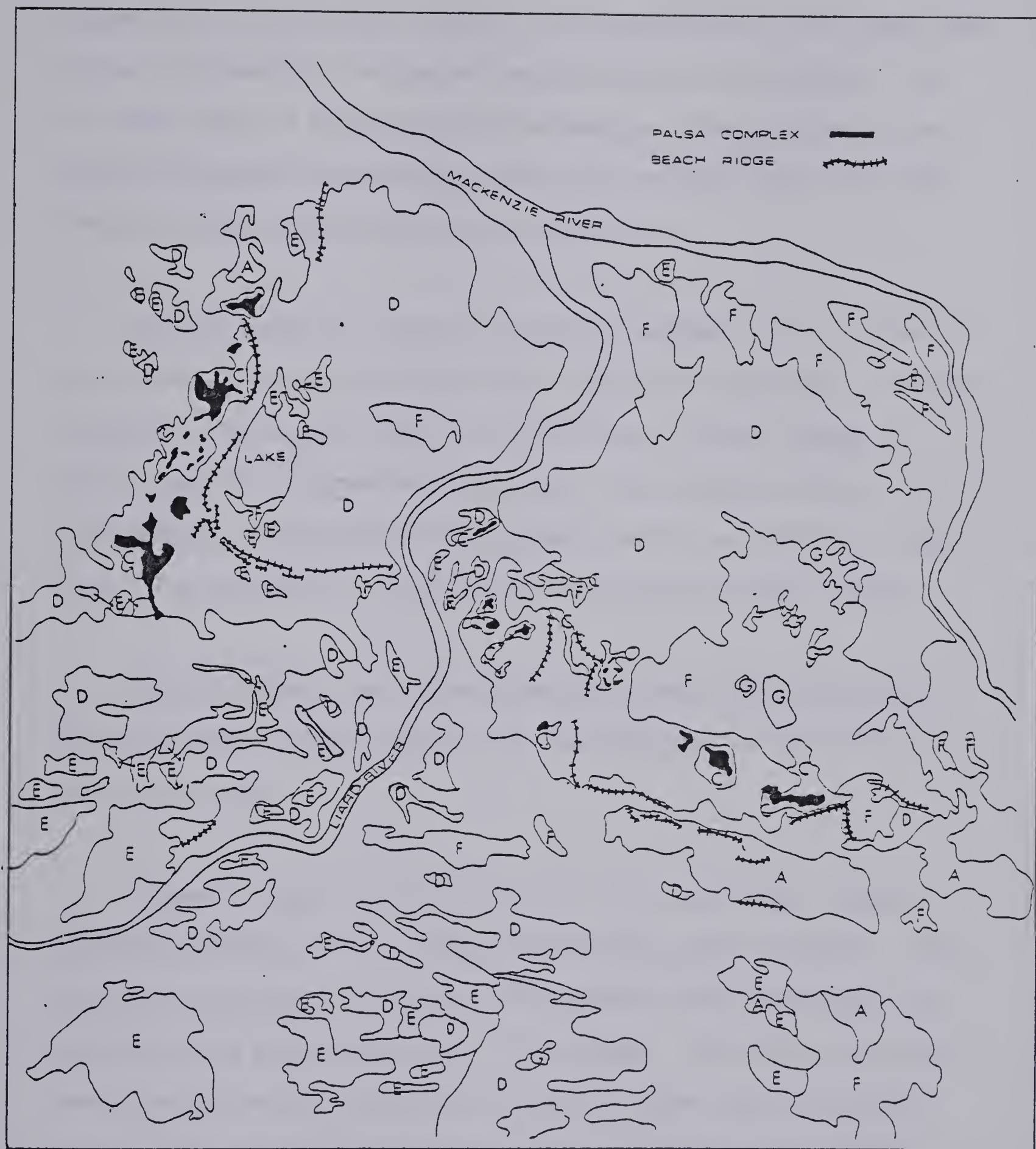
There are definite physiographic-peatland type relationships (see



LEGEND - FIGURE 3  
PEATLAND - PERMAFROST RELATIONSHIPS

| Map Symbol | Peatland Type                    | Surface Characteristics   | Permafrost Characteristics  |
|------------|----------------------------------|---|---|
| A          | Peat plateau                     | Relatively dry peat elevated approximately 1 meter above fen; Individual plateaux up to 1 km <sup>2</sup> . Flat topography with minor surface irregularities; may be surrounded by collapse scars; collapsing edges can form a moderately steep bank with outward leaning trees; Black Spruce - <u>Ledum</u> - <u>Cladonia</u> vegetation.   | Permafrost is usually restricted to the peat, but can extend into the mineral soil, especially near the center of the plateaux. Mostly pore ice and small segregated lenses.  |
| B          | 'Speckled bog' palsa complex     | Individual palsas cannot be recognized on air photos; palsas complexes can cover several square km.; highly vaulted, elevations up to 5.0 m above fen; moderate to heavy Black Spruce and White Birch; large unfrozen, sparsely treed bogs of <u>Sphagnum fuscum</u> occurs within the palsa complex; very steep to vertical and overhanging collapse banks; interior collapse 'sinkholes'; Black Spruce - <u>Cladonia</u> - <u>Ledum</u> - White Birch vegetation. | Permafrost extends into the mineral soil to approximately 8-12 meters in depth; large amounts of segregated ice; individual ice lenses up to 1.0 meters thick.  |
| C          | Collapse scars and ponds         | Intimately associated with 'B' and to a much lesser extent, with 'A' and 'E'; abundant, non-oriented ponds, surrounding permafrost feature, separated by floating sedge mats; vegetation is sedge, <u>carex</u> , cattail and duckweed.   | Mostly absent; can occur locally in small peat hummocks and occasional strings.   |
| D          | Fen with scattered peat plateaux | Fen is the same as in 'F'; peat plateaux are usually less than 100 m in diameter, circular to slightly elongate; elevated up to 1 m above surrounding fen; moderate to heavy cover of Black Spruce.   | Unfrozen in fens; ground ice in peat plateaux is restricted to the peat and rarely extends to the mineral soil substratum; typically less than 3 m thick.   |
| E          | 'Speckled bog' peat plateaux     | Large peat plateaux containing unfrozen <u>Sphagnum</u> bogs within the plateau; may cover areas in excess of 3 km <sup>2</sup> ; relief from 1-1.5 meters; Black Spruce - <u>Cladonia</u> - <u>Ledum</u> vegetation; does not have the relief, the steep collapse banks, and the surrounding open water fen of 'B'.  | Permafrost may be up to 15 m in depth; predominately developed in low permeability tills; ground ice is typically massive segregated silty clays with few segregated ice lenses; lenses usually less than 10-15 cm thick. |
| F          | Fen                              | Unpatterned or ribbed at right angles to drainage; saturated depressions; open water reaches; vegetation is sedges, <u>carex</u> , willow, dwarf birch and tamarack.  | Unfrozen; may contain lenses of seasonal ice in string hummocks.  |
| G          |                                  | Lakes   | Absent  |





Scale: 1:500000

Figure 3 : Distribution of peatland types and associated beach deposits in the Ft. Simpson area.





Figure 3). Of particular interest is the association of the palsa complexes, representing the greatest segregational ice development, with the inner edges of former glacial lake margins. The two areas of best palsa development are the study area at the southern edge of the lake basin and near Antoine Lake at the western edge.

Collapse scars and non-oriented lakes (peatland type C, Figure 3) are intimately associated with, often completely surrounding, the palsa complexes. The central areas of the lake basin contains lakes, unfrozen fens and scattered peat plateaus. The peripheral edges of the lake margins are covered in shallow peat deposits and modern day sedge fens. The permafrost in these areas is scattered and very shallow.

The till uplands are either permafrost free in the well drained sites or contain large 'speckled bog' peat plateaus in low lying depressional areas.

It must be emphasized that this is a very generalized zonation. Individual palsas cannot be identified at this scale of mapping; therefore they may occur under certain topographical and hydrological conditions in the more central parts of the basin. Individual palsas have been observed on the till plains, especially where there is abundant water. Palsa complexes greater than 100 m in diameter are, however, restricted to the margins of the former glacial lake.





## 2.4 Morphology

The study site was selected to represent all major geomorphic features of the permafrost body. Morphology, vegetation and ground ice descriptions are applicable to the entire palsa complex. The open fen surrounding the palsa is distinctly different however, and is described separately.

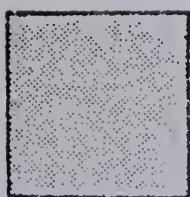
The palsa complex is approximately 2000 m long. Its width at the broadest point is about 300 m but narrows to 100 m at its eastern end. The total area is about 4 hectares.

Sharp collapsing edges with an average height of 2.5 meters, mark the edge of the palsa. The edges are discontinuous however; with more gently sloping peat banks common.

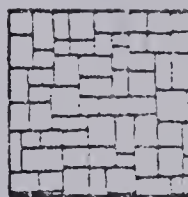
Three transects (Figure 2) were made to determine the surface morphology, the active layer depths, the depths of peat and total ground ice thickness. The transects are illustrated in three cross-sections (Figures 4, 5 and 6).

Surface elevations range from 2.5 to 4.7 meters above the surrounding fen, averaging 3.0 meters. There is considerable local relief however, created mainly by interior thawed Sphagnum bogs and by interior 'thermokarst' sinkholes. The sinkholes have near vertical banks and show signs of active collapse. The Sphagnum bogs have more gently sloping banks and are usually less than 1 meter below the sur-

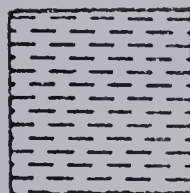




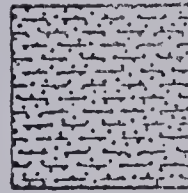
PEAT,  
UNFROZEN



PEAT,  
FROZEN



CLAY,  
UNFROZEN



CLAY,  
FROZEN

LEGEND FOR PROFILES.



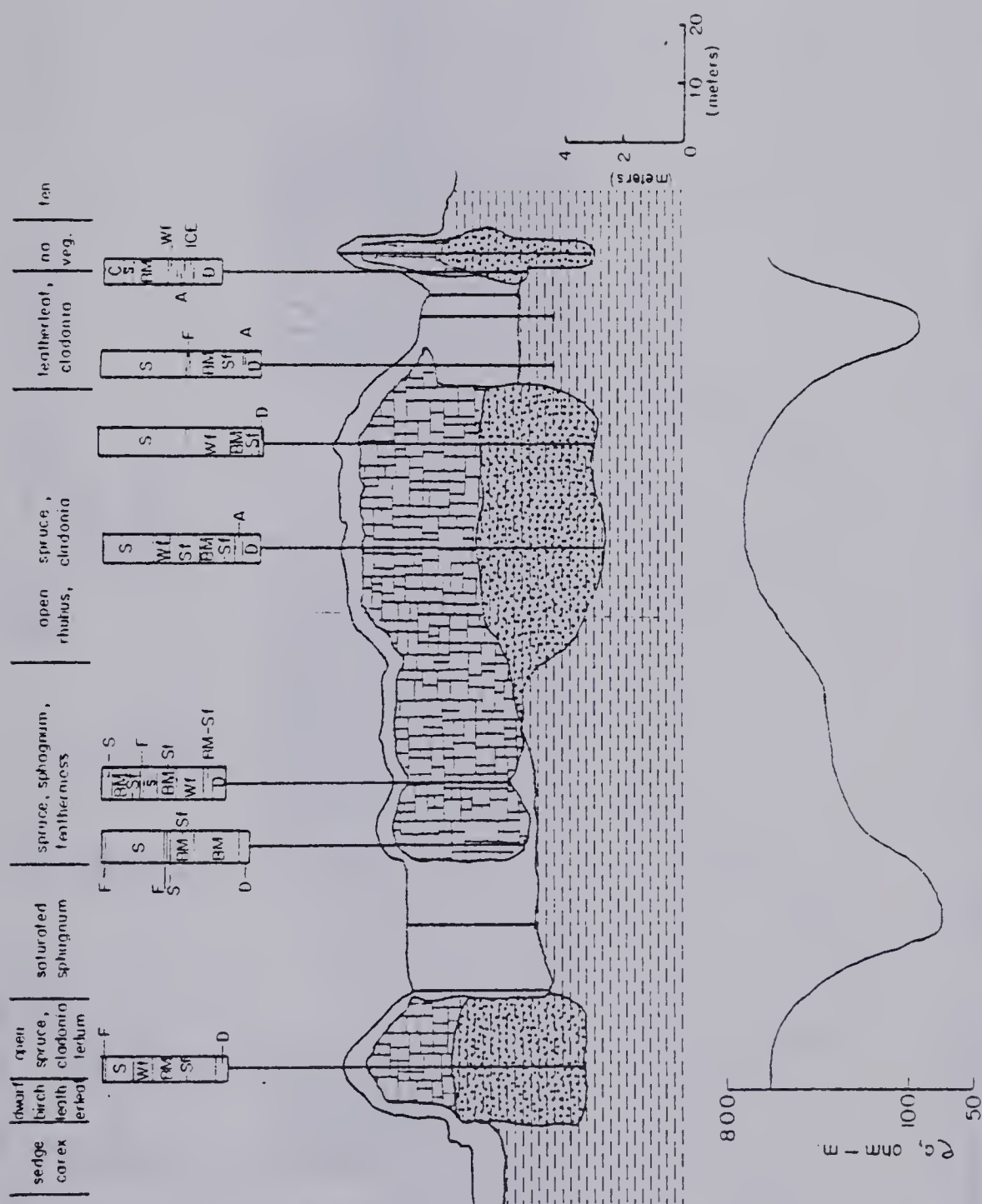


FIGURE 4 : TOPOGRAPHIC PROFILE , GROUND ICE CONFIGURATION , GEOPHYSICAL RESISTIVITY RESPONSE , PEAT STRATIGRAPHY AND VEGETATION DISTRIBUTION FOR TRANSECT E—E'.



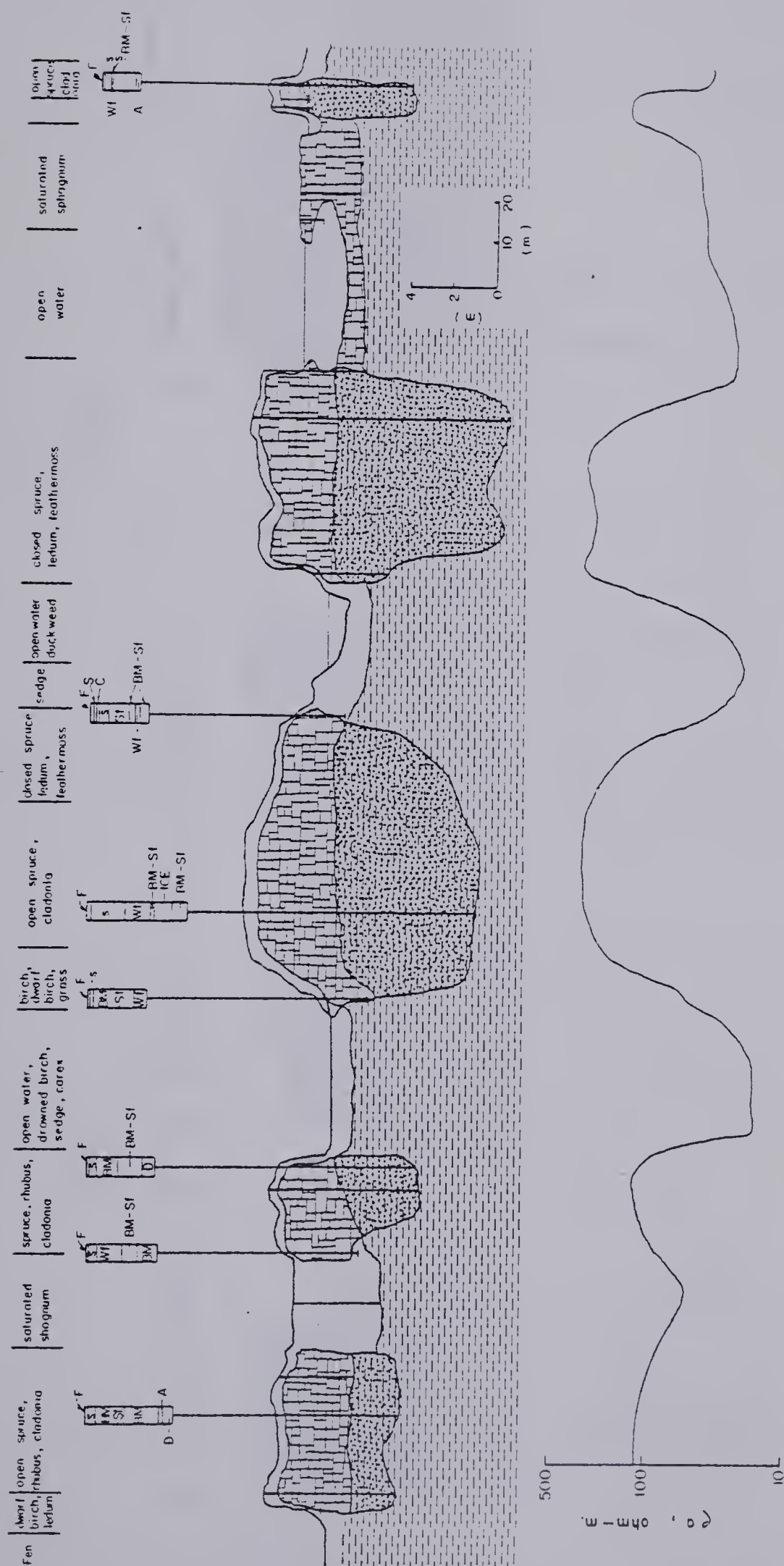


FIGURE 5 : TOPOGRAPHIC PROFILE, GROUND ICE CONFIGURATION, GEOPHYSICAL RESISTIVITY RESPONSE, PEAT STRATIGRAPHY AND VEGETATION DISTRIBUTION FOR TRANSECT S—S'









face of the frozen peat.

Palsa heights appear, from the cross-sections, to correlate with the total thickness of permafrost. Where permafrost is thicker, ground elevations are higher.

Distinct marginal ridges are elevated approximately 0.5 to 1.0 meters above the interior regions of the palsa complex. The ridges are discontinuous, usually associated with steep collapsing edges.

Section E-E' (Figure 4) contains an unfrozen unsaturated collapsed bog. The peat stratigraphy indicates a former saturated Sphagnum bog that has drained due to melting of the adjacent, damming permafrost. The surface elevation is locally depressed to nearly that of the surrounding fen. The feature is marked by sharp collapsed edges on 3 sides and a 'hinge-like' connection on the fourth side.

Active layer depths are strongly controlled by vegetation. Individual palsa summits, which are sparsely treed, have the greatest active layers, averaging 85 cm in late August. Active layers average 55-60 cm elsewhere, except in areas of dense Black Spruce- feathermoss communities where the mean depth is only 35 cm.

The surface of the palsa complex is extensively dissected by cracks extending the full thickness of the active layer. Crack densities and dimensions are greatest on palsa summits, especially near collapsing edges where a strong orientation parallel to the edge is observed. The moister regions of the palsa complex, especially in the dense Black



Spruce-feathermoss communities, are less dissected tending to have cracks less than 7 cm in width compared to widths of over 70 cm on palsa summits. The role of surface cracking on ground ice degradation is discussed in chapter four.

The unfrozen peatland surrounding the palsa complex is an open sedge fen. The fen consists of small randomly oriented ponds, often greater than 3 m in depth, separated by floating mats of sedges. The fen area on the beach ridge side (south side) of the palsa complex appears to have recently been much drier, probably a flat fen or horizontal fen (Tarnocai, 1970 classification). The area once supported a birch grove, however renewed paludification, probably due to beaver dams, has reestablished the open fen. Aerial photography shows the area has been flooded since at least 1946. The thickness of peat in the fen is less than on the palsa complex, averaging only 1.5 meters, compared to the 3.0 meter average on the palsas.

Peat plateaus are scattered throughout the fen. There is a great variation in size, from a maximum of 1 hectare to a minimum of only a few tens of square meters, but averaging approximately 400 square meters. The surface elevation of the peat plateaus is much less than the palsa complex, averaging 1 m above the surrounding fen. Bank edges lack a steep collapsing bank. Thermokarsting is evident however from the numerous dead trees leaning toward the fen.





## 2.5 Vegetation

Vegetation on the palsa complex and on surrounding fen was sampled using a random point sample technique. Percent cover of each species was visually estimated, then recorded on a five point scale modified from Braun-Blanquet (Kershaw, 1969). The main peatland types with their respective vegetative communities are detailed in Table 1.

## 2.6 Stratigraphy

The peat stratigraphy of the palsa complex was determined by macroscopic analysis of 46 cores. Depth profiles along two transects are illustrated in Figures 4 and 5. The classification of the peat materials is similar to that used by Zoltai and Tarnocai (1975). The peat types and their modern growth environments are summarized in Table 2.

The peat strata record a sequence of six broad vegetative communities in the following order from the bottom of the core to the top:

1. detrital organic in a silt matrix
2. aquatic
3. brown moss-sedge fens
4. sedge-shrub communities
5. Sphagnum bogs
6. Black Spruce-feathermoss-Cladonia communities.

Each of these communities implies a different wetland environment.





## PEATLAND TYPES AND VEGETATION COMMUNITIES

TABLE 1

| Peatland Type  | Main Species   | Common Species   | Minor Species   | Rare Species                      |
|--|--|--|---|-----------------------------------|
| 1. Raised palsas   | Picea mariana<br>Rubus chamaemorus<br>Cladonia rangiferina | Ledum groenlandicum<br>Ledum decumbens<br>Vaccinium vitis-idaea<br>Cladonia ssp. stris | Betula glandulosa<br>Cladonia mitis   | Sphagnum spp.<br>Cetraria nivalis |
| 2. Interior thawed bogs, no drainage                                     | Sphagnum spp.  | Chamaedaphne calyculata<br>Drepanocladus exannulatus                                   | Ledum groenlandicum<br>Picea mariana<br>Andromeda polifolia<br>Cladopodiella fluitans | Larix sp.                         |
| 3. Fens  | Betula glandulosa<br>Myrica gale<br>Carex aquatilis        | Drepanocladus sp.<br>Brachythecium sp.<br>Equisetum arvense                            | Salix spp.<br>Potentilla fruticosa<br>Potentilla palustris<br>Larix sp.               | Sphagnum spp.                     |
| 4. Transitional fen-bog complexes within palsa complex but with drainage | Carex aquatilis<br>Myrica gale<br>Drepanocladus sp.        | Chamaedaphne calyculata  | Sphagnum spp.<br>Andromeda polifolia<br>Betula glandulosa<br>Picea mariana            | Larix sp.                         |



TABLE 2  
PEAT TYPES AND MODERN GROWTH ENVIRONMENTS

| Peat Type                    | Main Species  | Growth Environment   |
|------------------------------|---|--|
| 1. Sphagnum                  | Sphagnum sp.  | Very wet to wet acidic bogs  |
| 2. Brown moss fen peat       | Drepanocladus sp.<br>Aulacomnium sp.  | Submerged in peaty ponds in open fens  |
| 3. Sedge fen peat            | Carex sp.   | Open fens and marshes  |
| 4. Brown moss-sedge fen peat | Carex sp.<br>Drepanocladus sp.<br>Aulacomnium sp.   | Open fens  |
| 5. Woody fen peat            | Brown mosses<br>Carex sp.<br>Shrubs: Andromeda<br>Chamaedaphne<br>Betula<br>Occasional Picea sp. and<br>Larix sp. | Shallow fens, closed fens and string fens  |
| 6. Aquatic peat              | Aquatic mosses<br>Algae<br>Duckweed   | Shallow lakes and ponds  |
| 7. Mixed peat                | Any of the above  | Transitional fen-bog environments; near actively collapsing areas at palsa complex margins |
| 8. Forest peat               | Picea mariana<br>Ledum spp.<br>Vaccinium spp.<br>Feather mosses<br>Cladonia sp.                                   | Upraised, treed, perennially frozen peatlands  |
| 9. Detrital                  | Detrital organic sediments in silt matrix   | Large lakes  |



Modern correlatives of the vegetation sequence implies an environmental transition through:

1. large deep lake
2. numerous shallow lakes and ponds
3. open sedge fen
4. sedge and shrub fen or paludificated shrub forest or fen ridge complex
5. ombrotrophic Sphagnum bogs
6. raised frozen peat plateau.

Variation is found between cores however, implying that local edaphic factors have played a part in determining the local stratigraphy. For example, in some cores, the woody fen layer is absent or is succeeded by a brown moss-sedge peat. The above scheme does, however, portray the average environmental sequence.

The mineral soil stratigraphy reflects the proximal position of the palsas in the former glaciolacustrine basin. The contact between peat and mineral soil is sharp. Typically, the underlying sediment is a silty sand for the uppermost .3 to 1.0 m, grading to a uniform, massive, blue-grey silty clay. The grain size distribution of a composite sample of the clay is 64% clay, 32% silt and 4% sand. Occasional lenses of fine to medium grained sand randomly intersect the silty clay. Large water yields were encountered when unfrozen sand lenses were drilled, indicating the lenses are fairly continuous. Glacial till was not encountered up to a depth of 11 meters. Nearby shot hole data indicate approximately 15-20 m of glaciolacustrine clays



overlie approximately 3 to 10 m of till.

## 2.7 Permafrost Configuration

The configuration of the permafrost body is illustrated in three cross-sections (Figures 4, 5 and 6). The permafrost boundaries were determined through interpretation of an electromagnetic resistivity survey completed with a Geonics EM 31 instrument. The predicted depth of permafrost correlates well with the depth measured in 44 boreholes. Boundaries between frozen and unfrozen zones are sharp and well defined.

## 2.8 Ground Thermal Regime

Permanent thermistor strings were installed to measure the thermal structure of the palsa and the adjacent fen and collapse bog. Random ground temperatures were also measured with a needle probe thermistor. The method of thermistor construction is detailed in Appendix 1.

The vertical temperature profiles of the frozen palsa, to a depth of 15 m, and the adjacent unfrozen bog, to a depth of 9 m, are illustrated in Figures 7 and 8 respectively. Temperatures were recorded in mid-March and late August, hence should reasonably represent the annual soil temperature variation (see Brown, 1966).





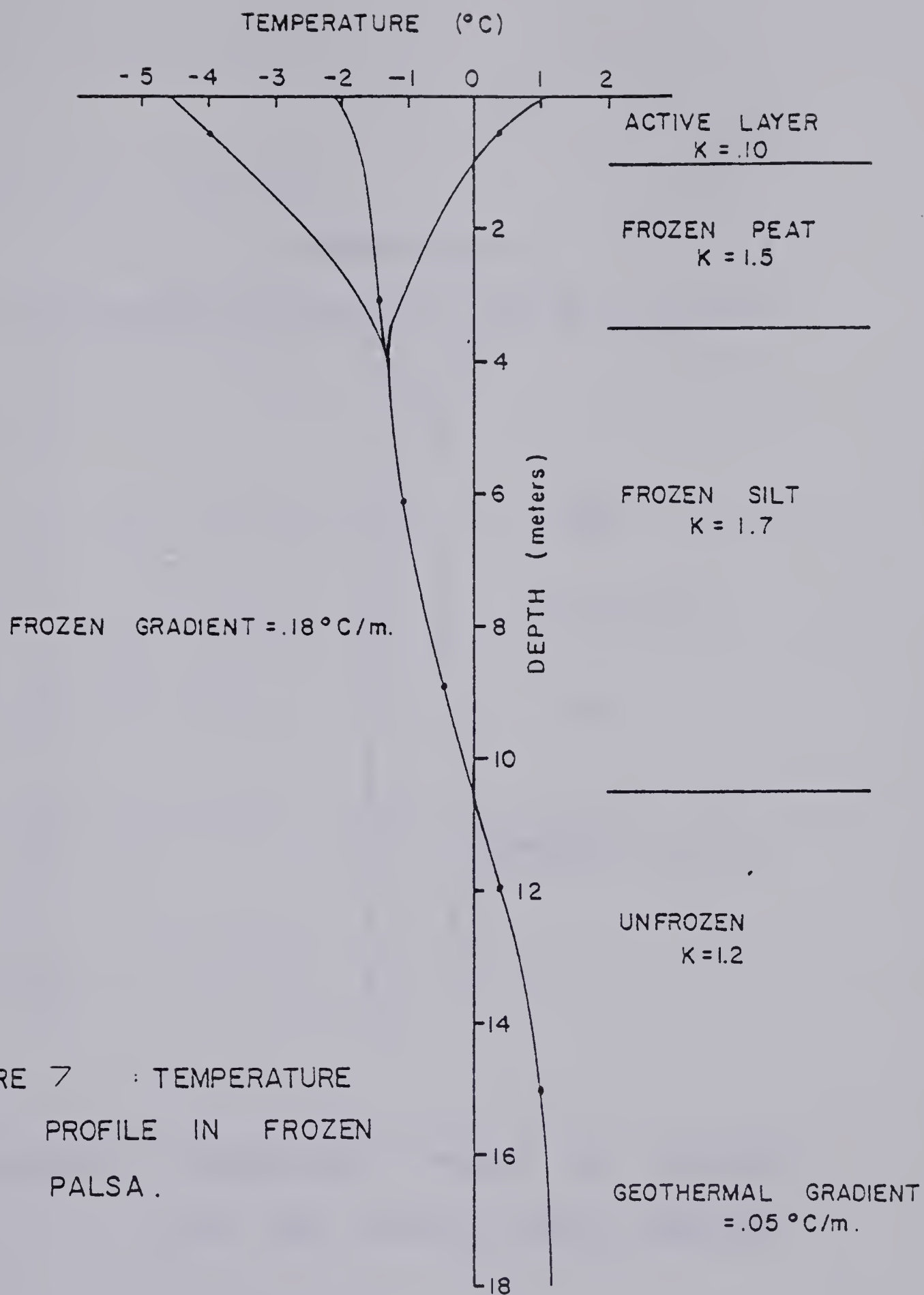


FIGURE 7 : TEMPERATURE  
PROFILE IN FROZEN  
PALSA.



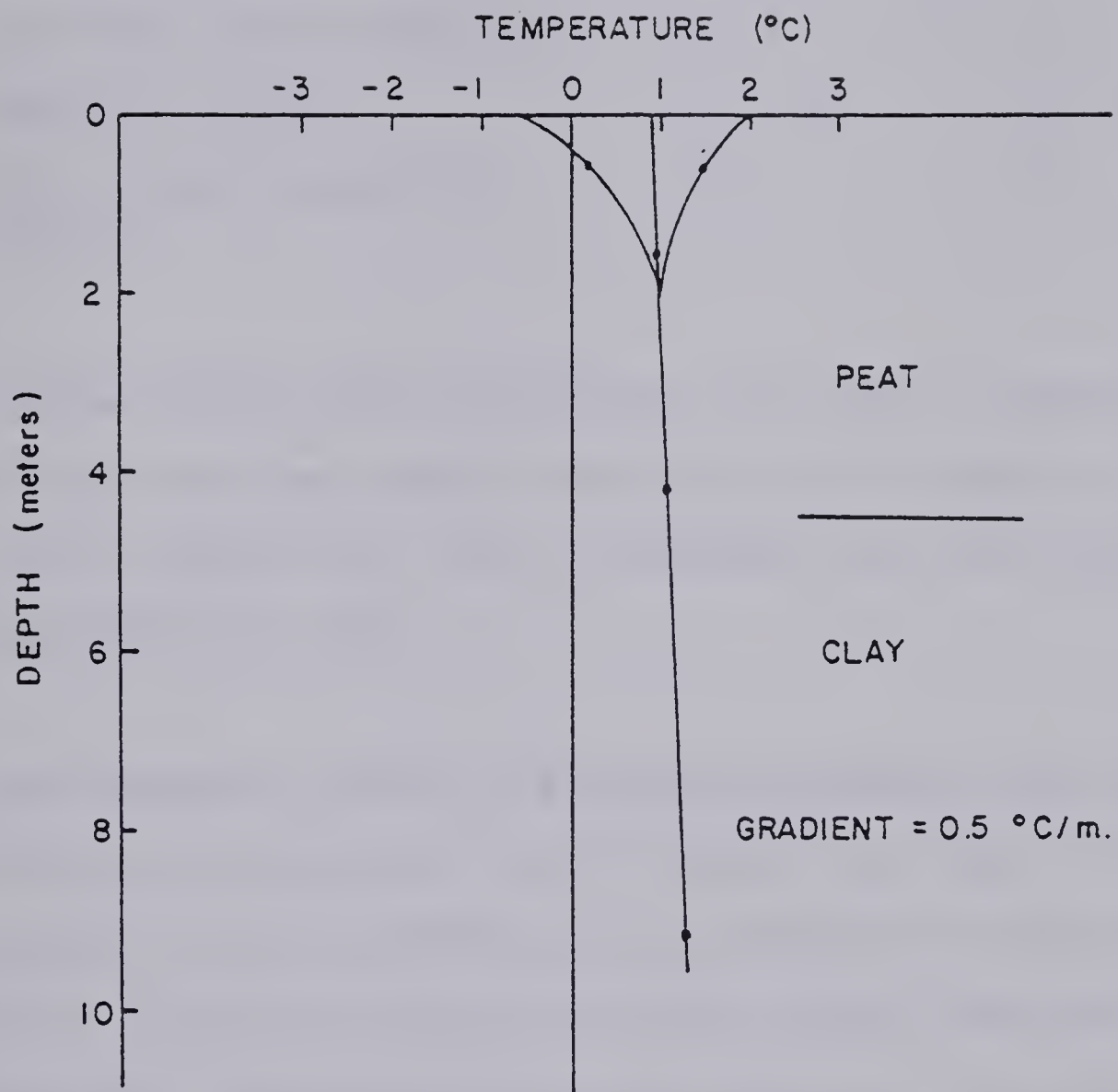


FIGURE 8 : TEMPERATURE PROFILE IN UNFROZEN  
PEAT BOG WITHIN PALSA COMPLEX.



Thermal characteristics of the palsa and unfrozen bog are:

|   | <u>Frozen Palsa</u> | <u>Unfrozen Bog</u> |
|---|---------------------|---------------------|
| 1. Mean annual air temperature<br>(obtained from Ft. Simpson) | - 4.1° C            | - 4.1° C            |
| 2. Mean annual surface temperature                            | - 2.1° C            | + .9° C             |
| 3. Temperature gradient                                       | + .18° C/m          | + .05° C/m          |
| 4. Depth of annual temperature<br>variation                   | 3.4 m               | 1.6 m               |

The mean annual surface temperature of the palsa is significantly colder than mineral soil surface temperatures at Ft. Simpson, of + 0.8 to + 1.6° C. (Burns, 1974). This is consistent with other studies in peatlands (Williams, 1968).

The temperature gradient in the palsa is unusually steep compared with other measurements made in the Ft. Simpson area (Judge, 1974). The gradient in shallow permafrost is very sensitive to changes in mean winter temperatures because of the high thermal conductivity and Sphagnum cover. Sphagnum promotes rapid outward heat flow during winter because its thermal conductivity when frozen is ten times that when dry and unfrozen (Jumikis, 1977). The recent decline in mean winter temperatures in the Ft. Simpson area over the past eight years (Burns, 1974; Atmospheric Environment Service Records 1974- 1977) has probably created the steep temperature gradient observed in the palsa.



## 2.9 Ground Ice Characteristics

### 2.91 Description

The frozen peat and mineral soil contain a variety of ground ice types. Fourteen cores, each 9 cm in diameter, were examined in the field, to determine ground ice variability across the palsa. The permafrost was classified as pore ice, vein ice, reticulate vein ice, or as ice lenses of a specified thickness (Figure 9). Lenses thicker than 8 cm are illustrated individually.

Pore ice is primarily restricted to the active layer. The active layer is usually within the unsaturated fibric Sphagnum horizon, with little moisture available for ice lens development. Crystal sizes, averaging  $1 \text{ mm}^2$  or less, were equidimensional throughout the entire active layer. In one core, slightly larger crystals with small spherical bubbles had developed within a forest peat layer. The small crystals and small spherical bubbles represent rapid freezing in an undersaturated medium (Gell, 1976).

Most of the peat column contains numerous, closely spaced, friable lenses less than 2 mm in thickness. The lenses are oriented parallel to the inferred heat flow direction. Bubbles are numerous and appear spherical. Water content averages 800% by weight and 46% by volume which is approximately the same as the adjacent unfrozen Sphagnum bogs.

The basal 0.5 m of peat often contains numerous ice lenses up to 10 cm in thickness. Crystals are only slightly elongate, averaging 15 to 20 mm in length and 15 mm in width. The basal peat is considerably







# LEGEND

PORE ICE



ICE VEINS AND LENSES,  
LESS THAN 1 CM. THICK.



ICE LENSE,  
1-3 CM. THICK.



ICE LENSES,  
3-8 CM. THICK.



ICE LENSES,  
>8 CM. THICK.



RETICULE ICE VEINS.



|         |         |
|---------|---------|
| P E A T | S I L T |
|---------|---------|

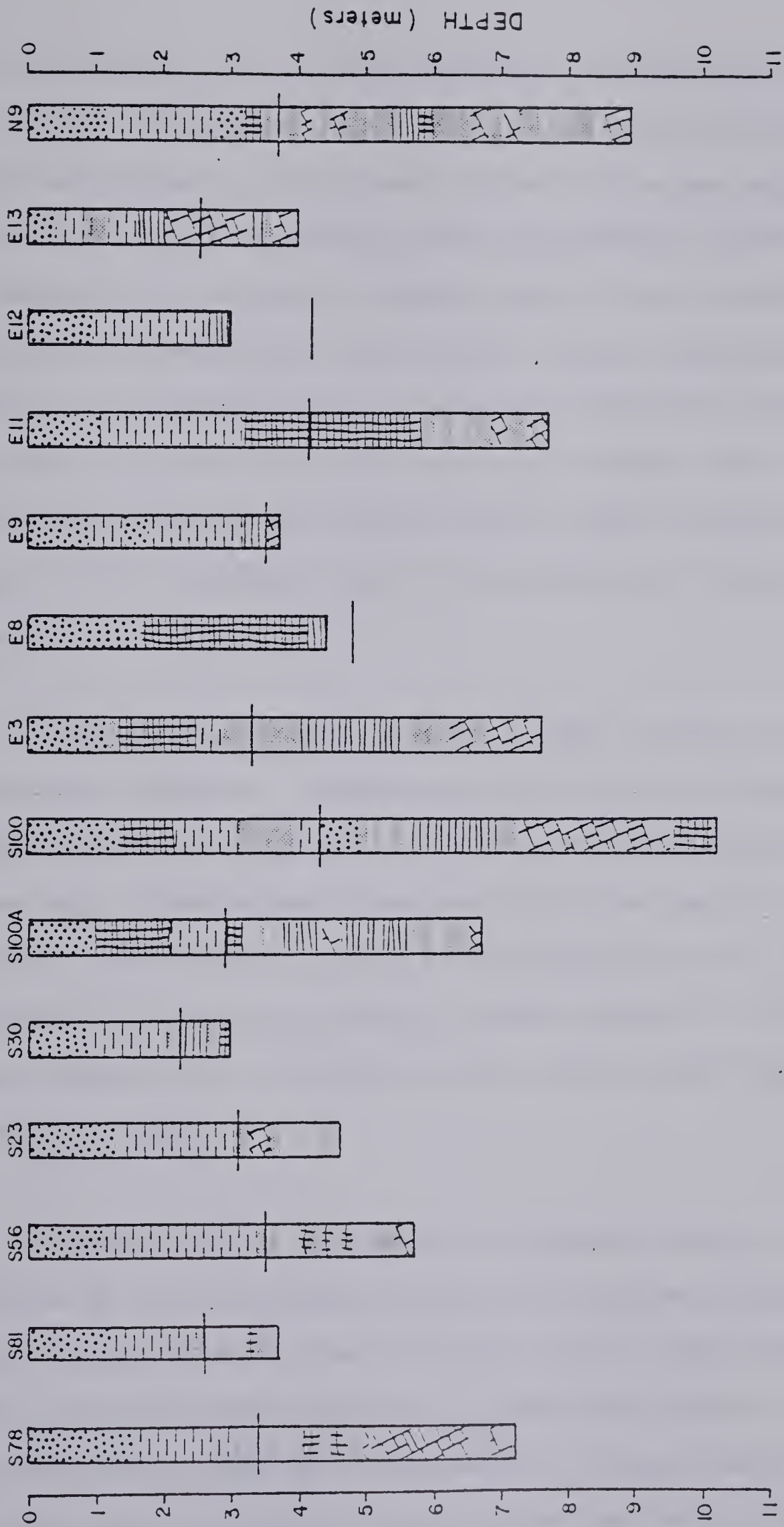


FIGURE 9 : GROUND ICE PROFILES FROM TWO TRANSECTS ACROSS THE PALSA COMPLEX .



more decomposed ( $H = 6$ , von Post Scale) than the upper portions of the peat column. The greater amounts of colloidal sized particles and slowly moving freezing fronts have combined to encourage segregational ice lensing. Ice lensing results from the nucleation, growth and coalescence of ice crystals in layers normal to the direction of heat extraction in freezing soil (Gell, 1976). Subtle variations of temperature at the freezing plane are believed to determine whether segregational ice grows in the field situation (Mackay, 1974). This may explain why lensing in the lowermost peat is highly variable, creating lenses up to 10 cm in some cores but not creating any lenses in other cores.

A characteristic of most cores was a large ice lens at the peat mineral soil interface. The lens was up to 85 cm in thickness, typically contained peat inclusions at the top but was clear for the bottom 75 per cent. Crystals were large, some up to 8 cm long and 2.5 cm wide, with the c-axis strongly oriented in the vertical direction. Although few were seen, bubbles were slightly elongate parallel to the c-axis. These characteristics are typical of slow crystal growth (Anderson and Morgenstern, 1973).

The mineral soil is characterized by numerous discrete ice lenses separated by overconsolidated mineral soil containing reticulate ice veins. In some cores, such as N9 and S56, the ice lenses are spaced nearly evenly throughout the core. In other cores however, such as S78, S100 and E3, lenses are concentrated in the upper portion of the core with reticulate vein ice dominating the lower half of the frozen



mineral soil. This is the exact opposite of what would be expected with a continually slowing freezing front with depth (Mackay, 1974). Similar profiles have been observed by Gell (1976), in pingo ice, who ascribed them to an increase of freezing rates due to pingo uplift and exposure of the surface to cold air temperatures. A similar mechanism would account for the basal reticulate vein ice in the palsa cores, as could a series of very cold winters with little snowfall.

Many of the cores (S78, S56, S100a, E11 and N9) have a large ice lens averaging .4m thick, but up to .75 m thick, just above the base of the permafrost. This lens, typically thicker than the other mineral soil lenses, is often bounded by long sections of reticulate vein ice.

Crystal structures in the segregational vein ice are well developed with an assortment of sizes. Maximum observed crystal dimensions were 70 mm in length and 15 mm in width; c-axis orientations were all parallel to the core. Macroscopic bubbles were rare and slightly elongate where observed.

## 2.92 Ionic Chemistry

The major ion chemistry of the palsa ground ice can aid in determining the hydrological history of the site. Vertical variability in conductivity of permafrost cores may represent periods of thaw and surface leaching (O'Sullivan, 1963; Pewe and Sellman, 1972); while horizontal variations may reflect differences in water sources (Brown,





1963; Allen, 1976).

The hydrochemistry of eight potential water sources for the ground ice was determined. In addition, six permafrost cores were analyzed for major ions, pH and conductivity. The major cations: calcium, magnesium, sodium and potassium were analyzed by atomic absorption spectroscopy. Chloride was determined by mercuric nitrate titration; and bicarbonate by potentiometric titration with sulphuric acid. Sulphate ion concentration was determined gravimetrically using a barium chlorate reagent for the mineral soil ice and by difference for the peat ice. As a check on the validity of the analysis, cation and anion balances were calculated for each sample. In general, the balance, expressed as  $\frac{\text{cations} - \text{anions}}{\text{cations} + \text{anions}}$  was less than 2% for 80% of the samples and less than 5% for the remainder. Analytical results are tabulated in Appendix Two.

The potential water sources for the ground ice have quite distinct chemistry (Table 3). Sphagnum bog water is very similar to that of precipitation; conductivity averages 40 mhos/cm and pH is approximately 5.0. Water from the fen has a conductivity of 250 mhos/cm, with a pH of 7.9; calcium and bicarbonate are the major ions. Deeper mineral soil groundwater has moderately high conductivities (350-550 mhos/cm, and a pH of 7.4. Calcium, magnesium, and sodium are the major cations; bicarbonate is the major anion.

Hydrochemistry of the permafrost cores reflects the various source



TABLE 3

MAJOR ION CHEMISTRY OF SURFACE WATERS AND  
GROUNDWATERS, IN EQUIVALENTS PER MOLE

| Environment                             | pH   | HCO <sub>3</sub> <sup>=</sup> | SO <sub>4</sub> <sup>=</sup> | Cl <sup>-</sup> | Na <sup>+</sup> | Ca <sup>+</sup> | K <sup>+</sup> | Mg <sup>++</sup> | Conductivity |
|---|------|-------------------------------|------------------------------|-----------------|-----------------|-----------------|----------------|------------------|--------------|
| 1. Groundwater beneath palsas           | 7.50 | 5.2                           | .5                           | .10             | 1.3             | 1.3             | .10            | 1.7              | 550          |
| 2. Groundwater beneath 'sinkhole' ponds | 7.30 | 4.0                           | 1.4                          | .10             | 1.3             | 3.3             | .08            | 1.5              | 550          |
| 3. Groundwater beneath collapsed palsas | 7.40 | 4.0                           | ---                          | .10             | 1.5             | 3.0             | .10            | .7               | 350          |
| 4. Sphagnum bog, surface                | 5.00 | 0.1                           | .02                          | .10             | 0.1             | 0.2             | .02            | .06              | 40           |
| 5. Fen, surface                         | 7.91 | 3.09                          | ---                          | ---             | .31             | 2.25            | .005           | .62              | 260          |
| 6. 'Sinkhole pond, surface              | 6.92 | 1.53                          | ----                         | .10             | ---             | .8              | .02            | .22              | 113          |
| 7. Pals lag, surface                    | 6.62 | 1.12                          | ---                          | ---             | .4              | .5              | .02            | .11              | 108          |
| 8. Collapse bog, at 2.0 m depth         | 5.30 | 0.3                           | 2.4                          | .10             | .2              | 2.0             | .03            | .5               | 250          |



waters in some instances, but is significantly enriched in other parts of the core. The upper frozen peat portions of the cores are very low in dissolved solids (Figures 10 to 13), similar to the modern Sphagnum bogs. This indicates that at the time of freezing, the bogs were probably ombrotrophic as their surfaces were raised above the regional water table, therefore receiving no mineralized groundwater.

The chemistry of the lower frozen peat cores is again similar to modern fen water, except for a marked increase in the  $\text{SO}_4$  ion. As modern peatland water and subpermafrost groundwater shows only trace amounts of  $\text{SO}_4$ , the origin of the  $\text{SO}_4$  ion is problematic. One possibility is the mineralization of sulphate which occurs during decomposition of organic matter (Barrow, 1960 and 1961). In non-decomposed plant material, sulphur is present as organically bound sulphate. With decomposition, available carbon is progressively utilized by soil microbes until the carbon/sulphur ratio is about 50, after which sulphur mineralization occurs. Barrow (1961) also found a large increase in inorganic sulphur with drying of the organic matter. Freezing has been shown to be a similar physicochemical process to drying; while experimental evidence is lacking, it would seem reasonable to predict an inorganic  $\text{SO}_4$  increase during freeze-thaw cycles. Tarnocai (1974) has found such an increase in  $\text{Ca}^{++}$  content of frozen organic soils which he attributes to the freezing process. The origin of the sulphate ion in the decomposed peat is further supported by comparison of the groundwater chemistry beneath a frozen palsa with that beneath a recently collapsed palsa: beneath the frozen palsa, sulphates average 0.5 epm, while beneath the collapsed palsa, sulphates average 1.4 epm.



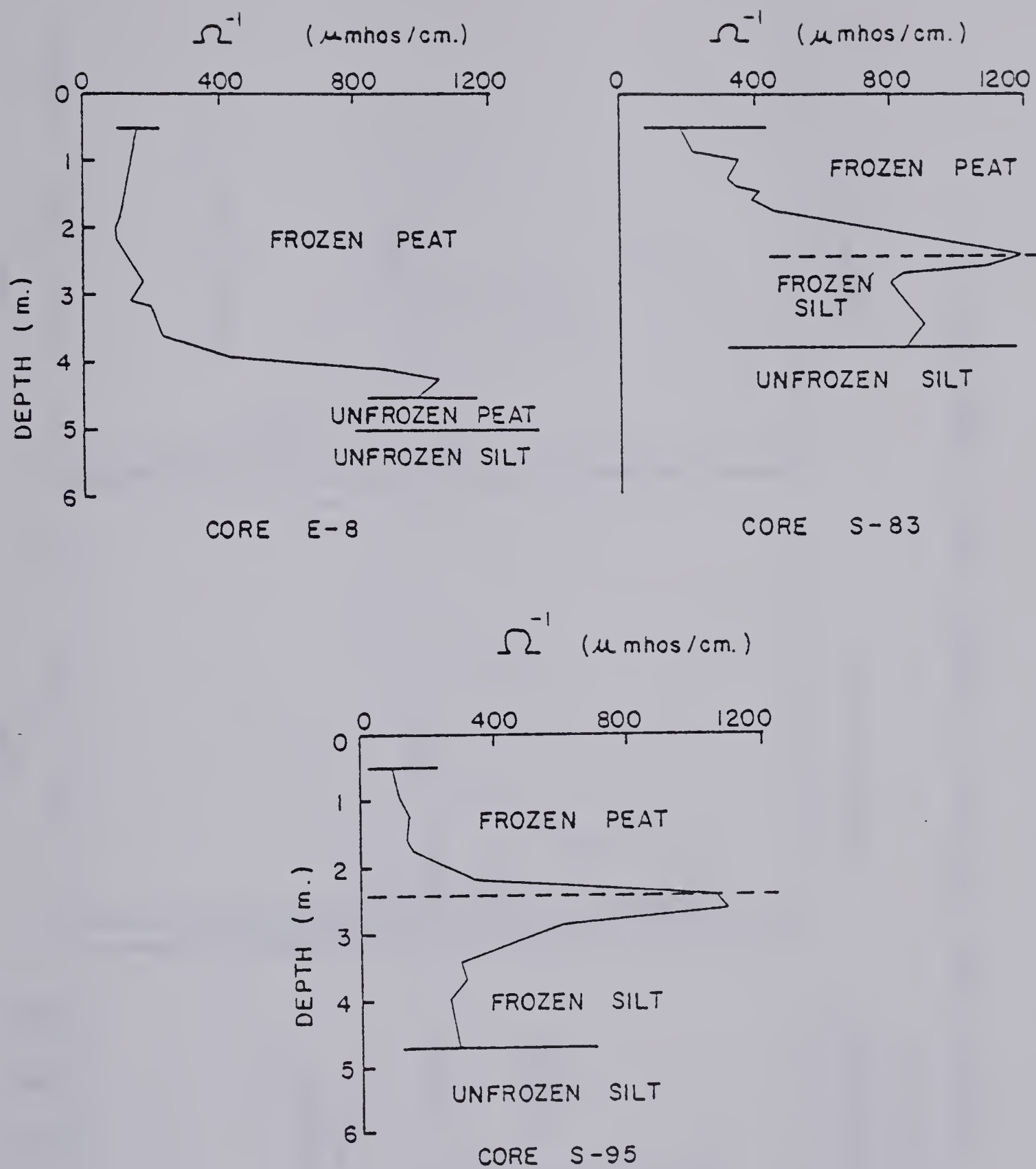


FIGURE 10 : GROUND ICE CONDUCTIVITY PROFILES.





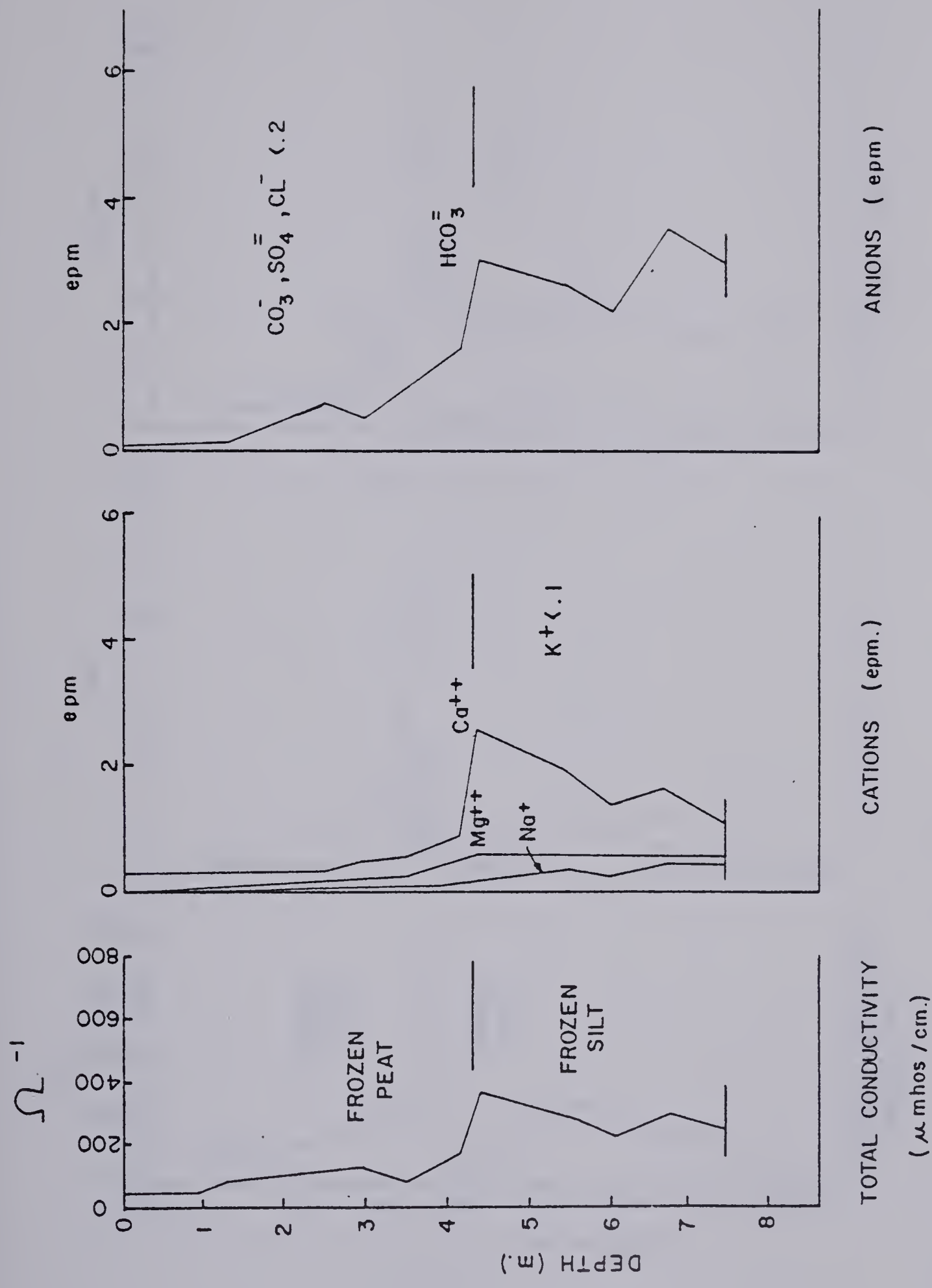


FIGURE 11 : MAJOR ION CHEMISTRY PROFILE FOR CORE E-11 .



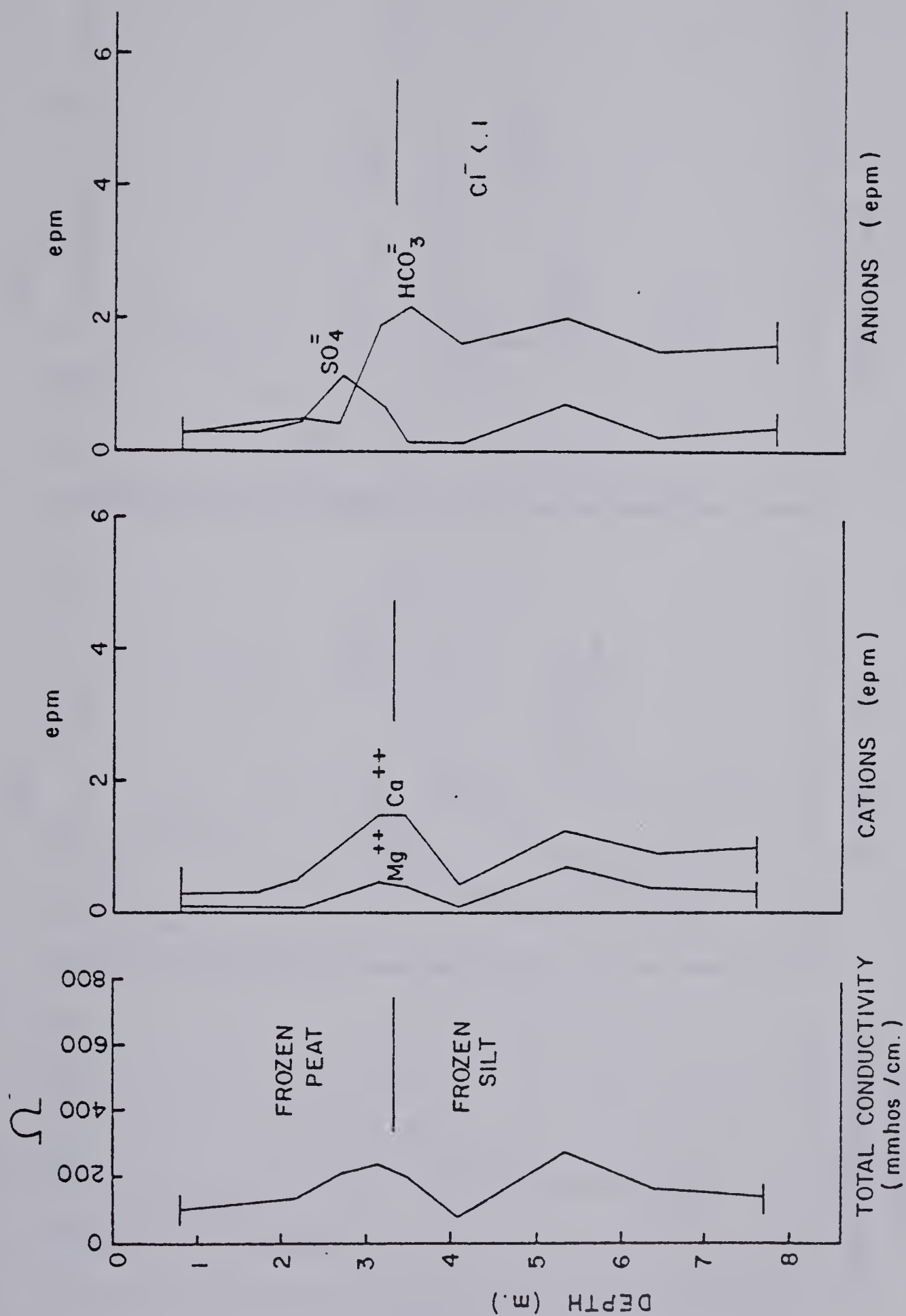


FIGURE 12 : MAJOR ION CHEMISTRY PROFILE FOR CORE E-3 .



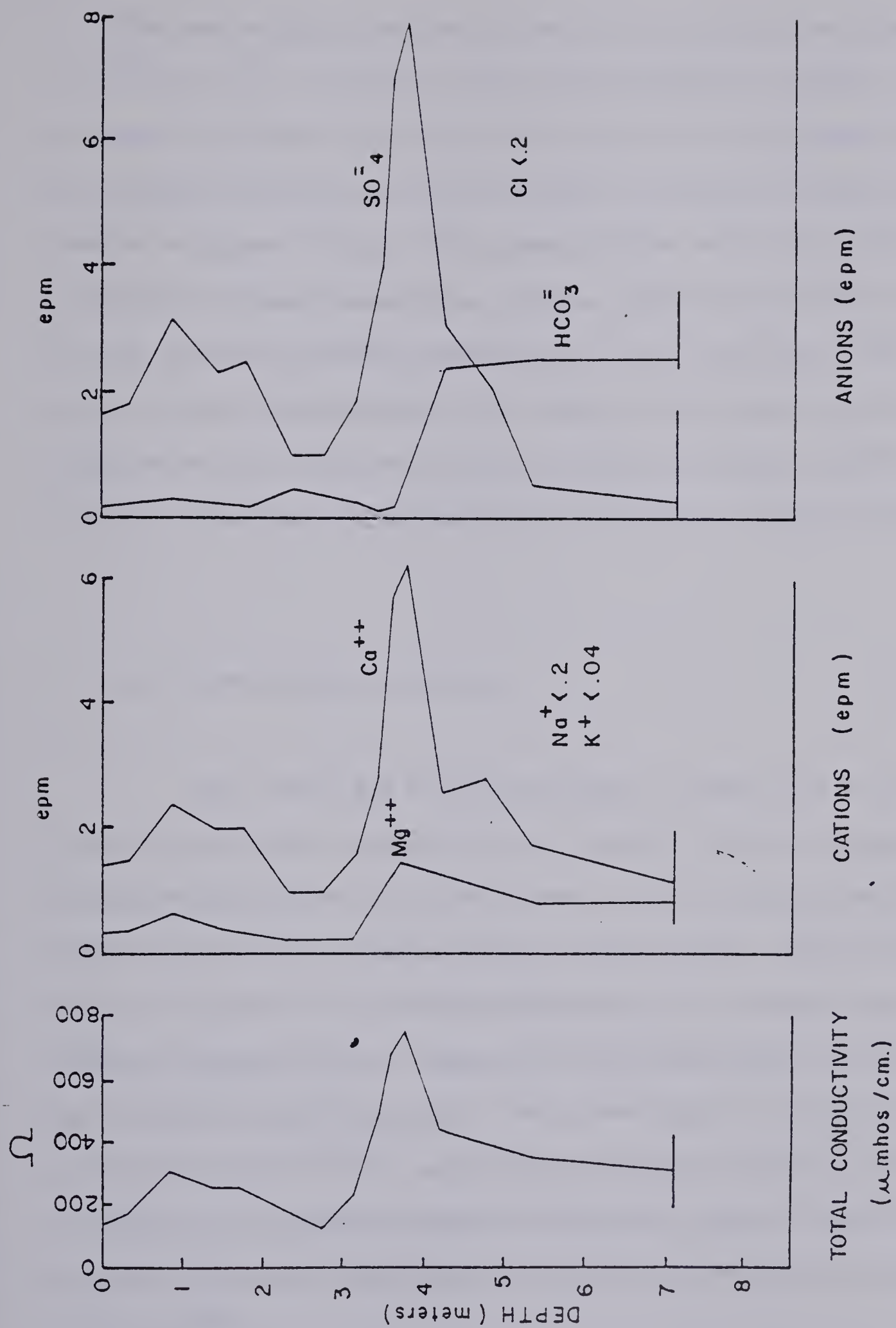


FIGURE 13: MAJOR ION CHEMISTRY PROFILE FOR CORE S-78.



The most striking feature of four of the cores is the strong peak in  $\text{Ca}^{+2}$  and  $\text{SO}_4^{=}$  displayed at the peat-mineral soil boundary. Part of this peak is probably due to the above freeze-thaw mechanism, however the extreme concentration is most likely the result of solute precipitation as gypsum ( $\text{CaSO}_4$ ). This precipitation would only occur during a period of intense dessication. Gypsum crystals have been so observed by F.W. Schwartz (personal communication) while drilling in dry lake beds in central Saskatchewan. The timing of the dessication period, based on evidence from central Alberta (May and Thomson, 1977), was probably immediately post-glacial preceeding the build-up of peat.

### 2.93 Environmental Isotopes

Both stable and natural radiogenic isotopes are well established as hydrologic research tools. Recently, stable isotopes have also provided information on the thermal history (Michels and Fritz, 1978) and freezing mechanisms (Mackay and Lavkulich, 1974) of permafrost. In spite of only recent application, the potential use of isotopes in determining past temperatures was established over 20 years ago by Weston (1955) and others. Water was found to undergo a maximum 2 % shift in its  $\text{O}^{18}/\text{O}^{16}$  ratio during freezing, thereby maintaining a record of its original isotopic composition, which in turn is a function of the air temperature at the time of precipitation (see O'Neil, 1968 ).

Natural radiogenic isotopes have also seen very limited use in





permafrost research, being used in a tritium study by Forsgren (1964) in Northern Sweden. Because of the relatively short half-life of tritium (12.26 years) its use as a dating isotope is restricted. It can, however, be employed as an indicator of recent or old permafrost. This is because of the enormous increase in the natural tritium content of meteoric water that has occurred since the detonation of nuclear devices in the early 1950's. For example, precipitation at Ft. Smith, N.W.T. reached a post-bomb maximum of 3616 TU in 1963, which has since decreased to about 200 TU. According to Simard (1977), groundwater with concentrations greater than 20 TU has been contaminated by thermonuclear tritium hence are of recent origin; water with concentrations less than 3 TU are said to be free tritium water introduced into the flow system prior to the bomb testing period; tritium concentrations between 3 TU and 20 TU indicate mixing of post bomb and pre-bomb precipitation.

Oxygen, deuterium, and tritium isotopic analyses were made on a permafrost core from the palsas, as well as on several groundwater samples collected through piezometer. Condensation of tritium-rich vapor onto the ice cores was minimized by coring at temperatures less than the temperature of the permafrost, then quickly wrapping the frozen core in air-tight polyvinyl and heavy plastic. Such precautions were not necessary for the stable isotopes. Samples were taken from both ice lenses and fine reticulate vein ice. This necessitated separation of soil and water by high speed centrifugation; fractionation effects due to centrifugation are unknown, but are most probably negligible.



## 2.931 Tritium

All tritium measurements were made at the Weizmann Institute, using internal gas counting preceded by electrolytic enrichment. The analytical results are listed in Table Four. Tritium values for the sub-permafrost groundwater and the ice lenses in the mineral soil are essentially equal. The groundwater value of 7.9 TU indicates that the water is a mixture of pre-1950 and post-1950 water. This supports the theory that the mineral soil groundwater receives minimal recharge from fen surface waters (see previous section). The high tritium values for the uppermost frozen peat sample indicates infiltration by modern precipitation. The depth of the infiltration appears to be limited to the upper 0.5 m of frozen peat on the basis of oxygen -18 analysis.

The magnitude of the tritium value of the ground ice in the mineral soil as well as the fact that it is nearly the same as the value for the sub-permafrost groundwater presents a paradox. Carbon-14 dating of the palsa indicates an approximate age of 1500 years (see Chapter 3). Tritium values for uncontaminated ground ice of this age should be less than 2 TU. The magnitude of the ground ice value exceeds the likely amount of contamination, but this possibility certainly cannot be excluded. Recent ground ice melting followed by rapid reheaving so that no additional peat is added to the palsa, may also cause anomalous tritium values. Melting is not supported by peat stratigraphic or thaw consolidation analysis, however (see Chapter 5). A third explanation, and one that also accounts for the similarity of tritium values in the



TABLE 4  
ENVIRONMENTAL TRITIUM ANALYSIS

| Sample Number | Depth (meters) | Tritium Value      | Location                    |
|---------------|----------------|--------------------|-----------------------------|
| FC-1          | 1.20           | $23 \pm 0.3$ T.U.  | Peat                        |
| FC-2          | 3.5            | $7.9 \pm 0.3$ T.U. | Peat-mineral soil interface |
| FC-3          | 6.5            | $6.4 \pm 0.4$ T.U. | Mineral soil ice lenses     |
| FC-4          | 10.0           | $6.4 \pm 0.4$ T.U. | Sub-permafrost groundwater  |





ice and groundwater, is for some water exchange to have occurred between the frozen core and the groundwater. This explanation is supported by the stable isotope data which is elaborated upon in the following section.

## 2.932 Stable Isotopes

Oxygen isotope ratios were determined by the carbon dioxide equilibration technique of Epstein and Mayeda (1953). Deuterium measurements were made by reacting the samples with uranium metal at 600 degrees Celsius to produce hydrogen gas (Bigeleisen, 1952). The analytical results are listed in Table 5, as well as plotted as a depth profile in Figure 14.

Prior to analyzing the stable isotope profiles, it is necessary to determine whether any isotopic enrichment had occurred prior to freezing. Such enrichment can be caused by partial evaporation of the water. The previous occurrence of evaporation can be detected by measuring both oxygen and deuterium isotope values for the same samples, then comparing a plot of these values with the Meteoric Water Line (Craig, 1961). A plot of  $\delta D$  vs.  $\delta^{18}O$  values from the samples falls on the regression line:  $\delta D = 8 \delta^{18}O + 5$  (Figure 15). This equation is the same as that found by Hage et al (1975) for weighted mean precipitation from high latitude continental areas. The slight deviation from the meteoric water line is believed due to near equilibrium evaporation of North Pacific sea water during the summer (Hage et al, 1975). The ground ice samples are therefore representative of





TABLE 5

| Sample | $\delta^{18}\text{O}$ (SMOW)* | $\delta\text{D}$ (SMOW) | Depth   | Description                         |
|--------|-------------------------------|-------------------------|---------|-------------------------------------|
| 1-A    | -13.90                        |                         | Surface | Surface sample from fen (July)      |
| 1-B    | -15.19                        |                         | Surface | Surface sample from bog (July)      |
| 2-A    | -22.79                        | -176.22                 | .8 m    | frozen peat                         |
| 2-B    | -22.29                        | -176.69                 | 1.2 m   | frozen peat                         |
| 2-C    | -22.25                        |                         | 1.8 m   | frozen peat                         |
| 2-D    | -21.95                        |                         | 2.5 m   | frozen peat                         |
| 2-E    | -22.28                        |                         | 3.2 m   | frozen peat                         |
| 3-A    | -21.42                        | -165.68                 | 3.5 m   | lens at peat-mineral soil interface |
| 3-B    | -21.40                        | -165.52                 | 4.3 m   | reticulate vein ice                 |
| 3-C    | -21.68                        |                         | 5.4 m   | ice lens                            |
| 3-D    | -21.36                        |                         | 6.1 m   | reticulate vein ice                 |
| 3-E    | -21.70                        | -170.51                 | 6.9 m   | ice lens                            |
| 4-A    | -22.81                        | -187.26                 | 7.5 m   | groundwater                         |
| 4-B    | -23.18                        | -185.01                 | 8.5 m   | groundwater                         |

\* SMOW: Standard Mean Ocean Water

Table 5: Oxygen and Hydrogen Isotope Ratios in Ground Ice, Surface Water, and Groundwater



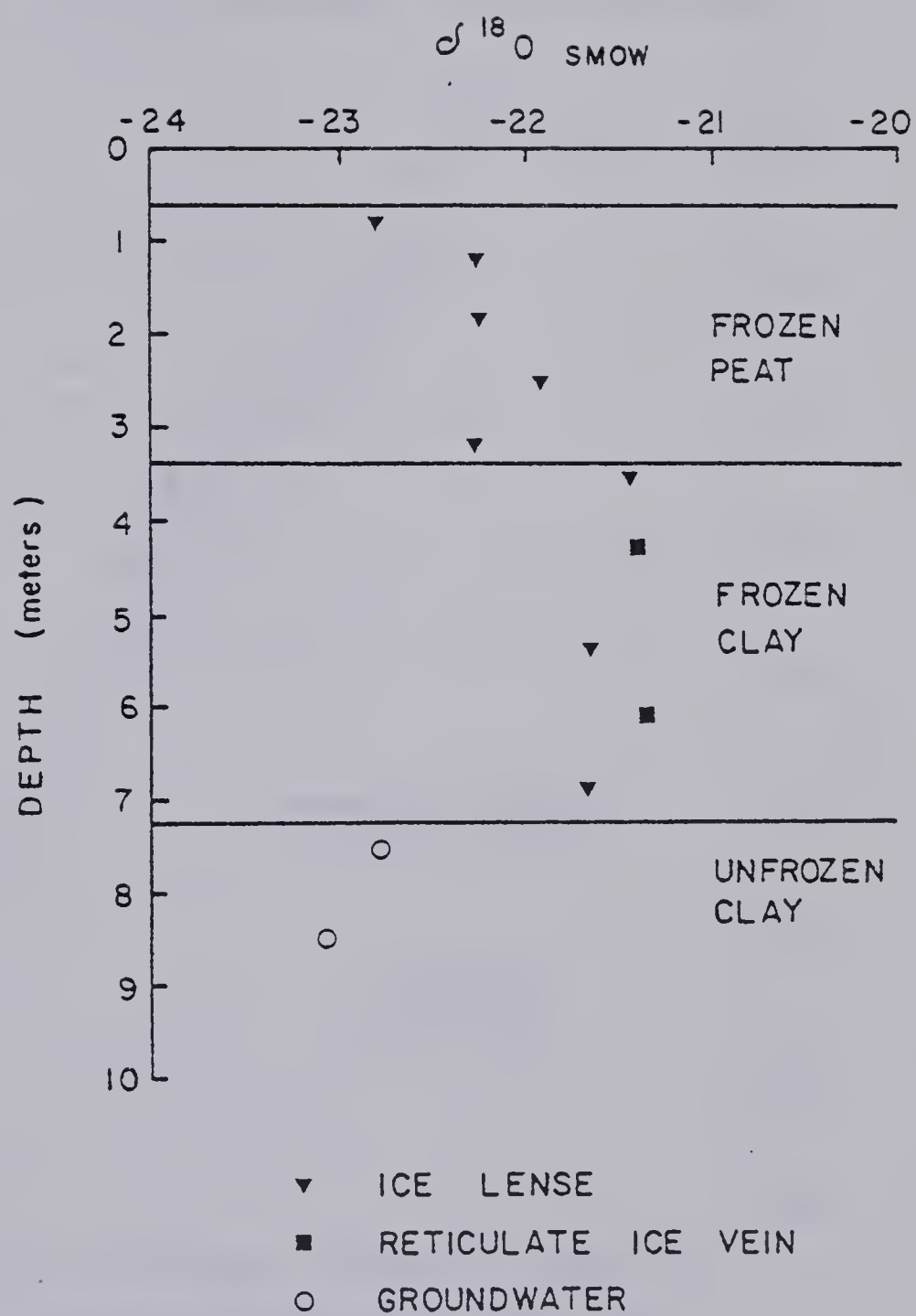


FIGURE 14 : OXYGEN - 18 PROFILE WITH DEPTH  
FOR CORE E-11 .



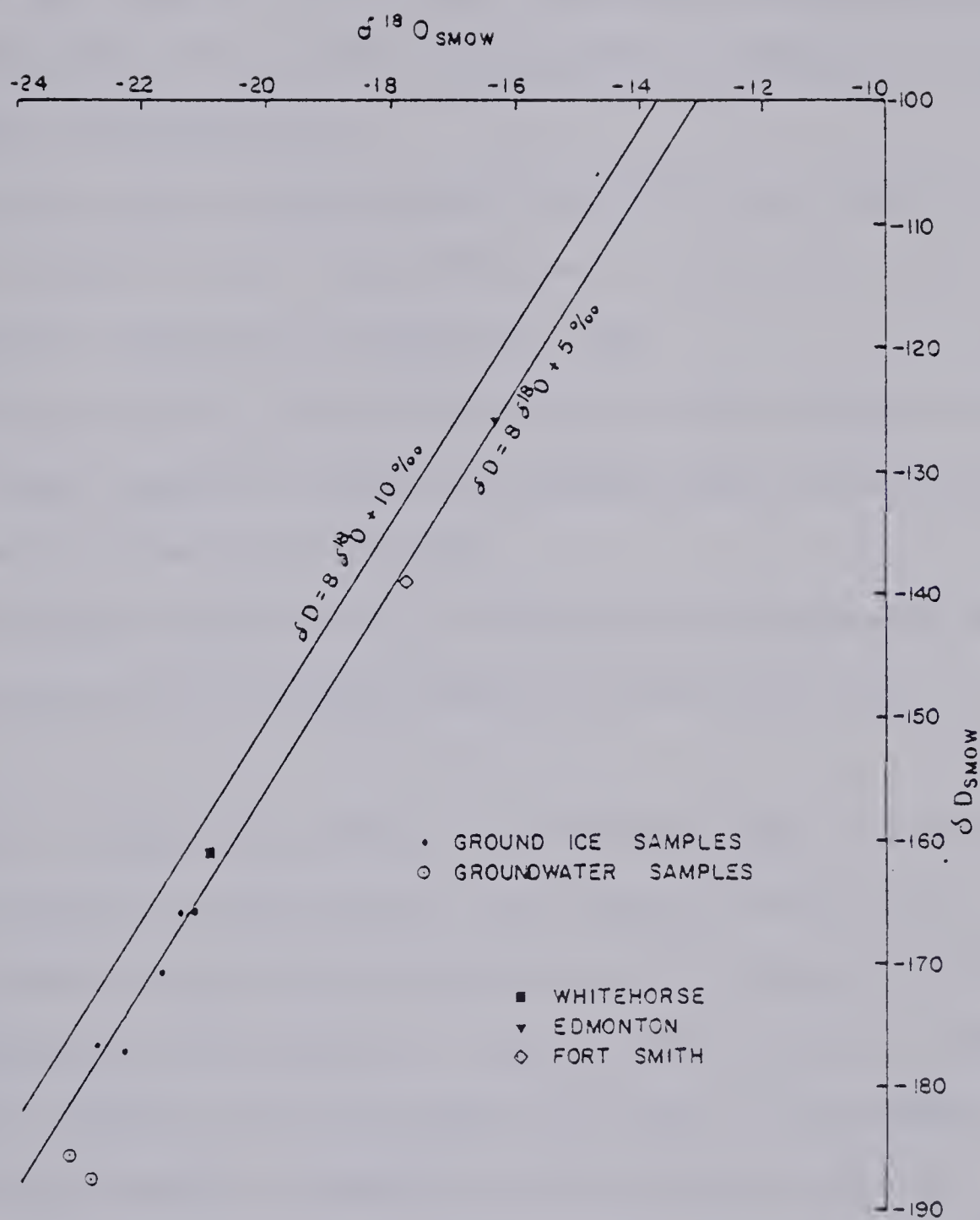


FIGURE 15 : RELATIONSHIP BETWEEN OXYGEN 18  
AND DEUTERIUM FOR CORE S-78 .



the weighted local mean precipitation, and have not undergone isotopic enrichment due to evaporation. The relatively high  $^{18}\text{O}$  values for the surface waters suggest, however, that high summer evaporation rates occur.

Examination of the stable isotope profile in Figure 14 reveals three unique characteristics:

1. the frozen peat and frozen mineral soil  $^{18}\text{O}$  values differ by approximately 1.0‰; this difference is significant as the analytical technique is accurate to 0.2‰.
2. within each group: peat and mineral soil; stable isotope values are nearly constant; values for reticulate vein ice and ice lenses are essentially the same.
3. the isotopic composition of the sub-permafrost groundwater is approximately 1.5‰ lighter than the frozen mineral soil.

It is unlikely that ground ice of different ages is accounting for the different isotopic ratios in the peat and mineral soil. A previous period of permafrost degradation is not indicated by the paleo-temperature determinations. Oxygen isotope analysis of peat cellulose, indicates that the present day climate is the warmest since the development of permafrost in this region (chapter 3). Further, results from thaw consolidation tests of the frozen peat (chapter 5) do not suggest a previous thaw period.

The difference in isotope ratios between the groundwater and ice may be due to fractionation effects. Fractionation occurs during the freezing of water under equilibrium conditions



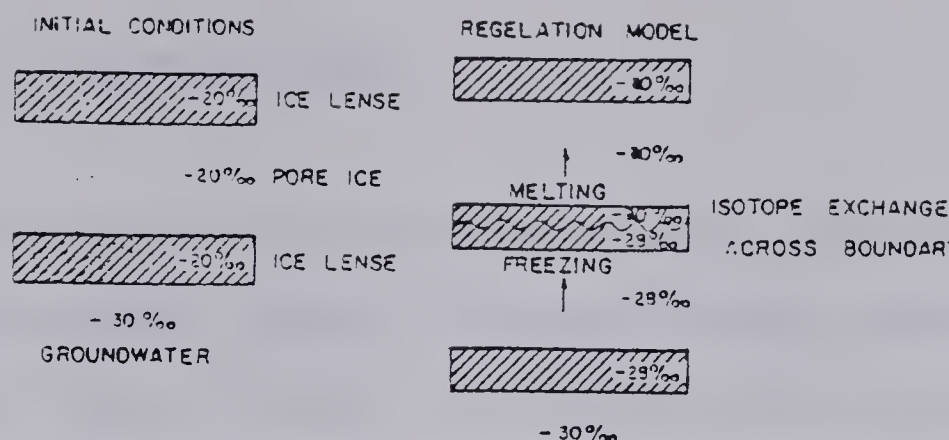


(ie. from an infinitely large source of well mixed water); the ice containing about 2 % more  $^{18}\text{O}$  than the water from which it has frozen (Weston, 1955; Arnason, 1969). Mackay and Lavkulich (1974) and Michels and Fritz (1978) have interpreted isotope differences between surface, subsurface and frozen waters for an aggrading permafrost site as due to fractionation effects.

There is some evidence however that fractionation may not have occurred during initial freezing of the palsa soil, but rather is the result of post freezing modification of the ice core. The identical isotopic values for reticulate vein ice and the large ice lenses suggests that freezing of incoming water at the frost interface occurred very rapidly (Mackay, 1974; McRoberts and Nixon, 1975) with little chance for isotopic selection to occur. Neither is a Rayleigh fractionation model (Freidman et al, 1964) supported due to the homogeneous isotopic values throughout a single ice lens. A second possibility is for post - freezing, "steady state", isotopic exchange to have occurred in the palsa. Consider an ice lens system with unfrozen pore water beneath the lowest ice lens (figure 16). The isotope values of the frozen soil and the unfrozen water are significantly different, say -30 % for the water and -20% for the ice. As the water freezes onto the bottom of the ice lens, water will also melt off the top of the lens due to temperature induced pressure gradients (Ershov, 1976; Mageau, 1978). This process, called regelation, is exactly that outlined by Miller (1972, 1978) for pore ice movement in frozen soils.



FIGURE 16



CONCEPTUAL MODELS FOR ISOTOPE EXCHANGE IN  
GROUND ICE UNDER A TEMPERATURE GRADIENT.

In the above example, the water freezing at the bottom of the lens will become isotopically enriched by 2 ‰ to become  $-28\text{‰}$ . Ice melting at the top of the lens will be  $-20\text{‰}$ . The  $-28\text{‰}$  ice will slowly be moved up the ice lens. A similar process involving pore ice regelation and an unfrozen water flux through films and ice-free pores (Miller, 1975) will occur in the frozen soil above the lens. The net result is a frozen soil with near homogeneous isotope profiles in the ice, underlain by unfrozen water which is depleted 2‰ in  $^{18}\text{O}$ .

In summary, stable isotopic analysis of the palsa cores has shown that there was minimal evaporation of the soil water prior to its being permafrozen. This supports the conclusion, made in a later chapter, that paleotemperatures were significantly cooler than present day temperatures. Separate groundwater flow systems for the peat and mineral soils were earlier deduced from the water chemistry. This conclusion was supported by the isotope analysis. Tritium dating revealed an anomalously young age for the ground ice as compared to the palsa itself, suggesting some water exchange has taken place. This conclusion was supported by analysis of the stable isotope profiles, where a model was proposed for regelation flow, with accompanying isotope exchange, as water moves upward in response to thermal gradients.



## 2.10 Hydrogeology of the Palsa Complex

An investigation was made of the groundwater regime within the palsa complex for two reasons. First, to document the pore pressures immediately beneath a palsa. Secondly, to determine whether the collapse bogs and thermokarst sinkholes are underlain by permafrost at depth or are local sources of groundwater recharge. Recharge may be expected as water levels in the bogs are higher than the surrounding fen (see Figure 4) with no apparent surface drainage.

For each collapse feature studied, piezometers were installed by driving well points in the deepest part of the bog or pond in order to eliminate two-dimensional effects. Piezometers that pierced the permafrost were installed during the winter drilling program. The saturated bogs acted as a body of standing water with no head loss with depth. Piezometer installations were completed in the usual manner then charged with a mixture of kerosene and methyl alcohol (unit weight equal to water) in order to prevent freezing. Hydraulic conductivities were determined by the Hvorslev (1949) water level response technique, using the 'University of Alberta transducer piezometer' (see McRoberts and Morgenstern, 1974 for full description). Head measurements are reported relative to the level of the water surface of the surrounding fen.

As would be expected in a discontinuously frozen area, no excess hydrostatic heads were recorded. All piezometric measurements were consistent in showing a decrease in fluid potential with depth. The





head measurements and approximate isopotentials for one of the collapse bogs is illustrated in Figure 17 . The decrease with depth indicates that the collapse features are not underlain by permafrost; that water is moving from the raised bog, beneath the palsa, and discharging into the surrounding fen.

Estimates of the volume of groundwater supplied by the raised bogs can be determined from Darcy's equation:

$$Q = k i A$$

where Q is the volume of flow

k is the permeability, which ranged from  $2.9 \times 10^{-7}$  cm/sec to  $6.8 \times 10^{-7}$  cm/sec; averaging  $5.5 \times 10^{-7}$  cm/sec

i is the hydraulic gradient; averaging .08

A is the bog area;  $300 \text{ m}^2$

The calculated recharge of  $4 \text{ m}^3/\text{year}$  corresponds to a water thickness of 1.3 cm over the bog surface or roughly 5 % of the mean annual precipitation. Assuming a steady water table, evaporation must nearly equal precipitation for the closed bogs. Oxygen isotope analysis of bog surface waters (Chapter 4 ) confirms the high evaporation rates.





PIEZOMETER, HEAD MEASUREMENTS IN CM., RELATIVE TO FEN SURFACE.

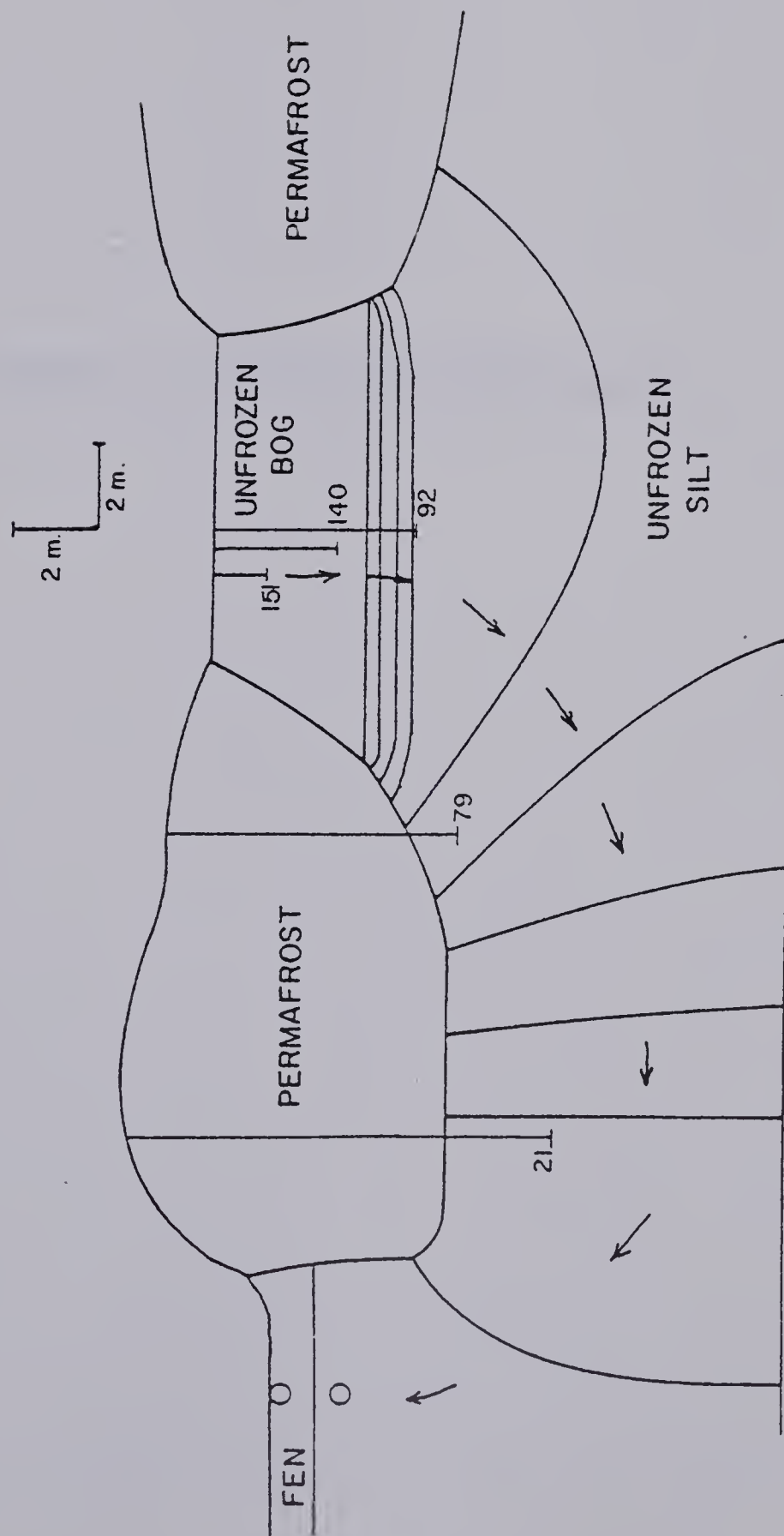


FIGURE 17 : ISOPOTENTIALS AND LOCAL GROUNDWATER FLOW DUE TO A PERCHED SATURATED COLLAPSE BOG; SITE E-3.



### CHAPTER 3: PALEOCLIMATIC DETERMINATION



### 3.1 Introduction

Paleoclimatic information is vital in the determination of the history of permafrost aggradation and degradation. While other elements of a regional climate play a role in permafrost development, temperature is acknowledged as the most important component (Brown, 1966). In the Arctic and Sub-Arctic regions of North America, paleotemperatures have been estimated from palynological studies, peat stratigraphy, and freshwater paleontology. All of these studies have relied on biological response to inferred climatic change. The dependence of biological systems on many local edaphic factors apart from climate is well documented (Iverson, 1953) the result being that many of these studies have been contradictory and yielded little quantitative data.

The determination of oxygen and deuterium isotope ratios in non-exchangeable plant cellulose has been recently shown to reflect the isotope ratio of the water used by the plant in its synthesis of cellulose (Epstein et al, 1976; Thompson and Gray, 1977). Numerous studies (Epstein and Mayeda, 1953; Dansgaard, 1964; Friedman, 1964) have shown that D/H and  $^{18}\text{O}/^{16}\text{O}$  ratios in meteoric waters reflect the temperatures at the sites of precipitation; the lower the temperature, the smaller the isotopic ratio. The climatic significance of D/H ratios (Epstein and Yapp, 1976) and  $^{18}\text{O}/^{16}\text{O}$  ratios (Gray and Thompson, 1977) have subsequently been demonstrated for tree-ring sequences from different climatic regimes. It follows that the isotopic variations in plant cellulose may reflect the temperature of



precipitation at the growth site.

In this chapter, oxygen isotope ratios of peat cellulose are used to estimate paleotemperatures at the study site over the last 10,000 years. This information will be used in later discussion of the history of permafrost in Upper Mackenzie Valley peatlands.

### 3.2 Previous Investigations of Holocene Paleoclimate in N. W. North America

A comprehensive review of paleoclimatic investigations in the Arctic and Sub-Arctic regions of North America has been compiled by Ritchie and Hare (1971). The reviewers found many of the results, especially that based on pollen evidence, to be contradictory. While some workers supported a mid-Holocene warm period (Livingstone, 1957; Heusser, 1960); others have concluded that "the climate has never been significantly warmer than it is at the present" (Colinvaux, 1967). Megafossil evidence was more definitive. Definite evidence of the tundra-taiga boundary being significantly further north than at present, suggesting greater mean summer temperatures, has been found in the form of buried wood and fossil beaver artifacts in the following areas: Seward Peninsula (McCulloch and Hopkins, 1966); Kendal Island (Mackay, 1971); Tuktoyaktuk Peninsula (Ritchie and Hare, 1971); and in buried forest paleosols at Keewatin (Bryson et al, 1965). Notable studies carried out in recent years include new results by Ritchie and Hare (1971); Matthews (1974); Rampton (1971); Zoltai and Tarnocai (1975);





and Delorme et al (1977).

The pollen stratigraphy of Kettle Lakes near Tuktoyaktuk is interpreted by Ritchie and Hare (1971) as indicative of mean summer temperatures approximately  $5^{\circ}$  C. higher than at present, with the growing season about 30 days longer, during the time interval 8500 years to 5500 years Before Present. J.R. Mackay (personal communication) feels that the large summer temperature increase at their site, may be more apparent than real. During this time interval sea level was at least 15 m below present day levels (Mackay, 1963). Bathymetric contours off the Tuktoyaktuk peninsula indicate that a relative sea level lowering of 15 m would result in a coast line displaced 50 km to the north. By assuming temperature gradients similar to those existing today, much of the mean summer temperature increase postulated by Ritchie and Hare could be accounted for by the increased distance from the Arctic Ocean.

Matthews (1974), in a palynological study of colluviated silts near Fairbanks, Alaska found evidence for arid steppe-tundra conditions from approximately 12,000 years B.P. until sometime between 9200 and 7800 years B.P. He postulated that Central Alaska possessed an arctic climate similar to present day Northern Alaska during this time interval. Alder fluctuations in the pollen record suggest that climatic warming followed, leading to a taiga vegetation.

Rampton (1971), has attempted to quantify his pollen record from the Snag-Klutlan area, Yukon Territory. The former vegetative



community suggests both mean July temperatures and mean annual temperatures approximately  $7^{\circ}$  to  $8^{\circ}$  cooler than present values during the time interval 13,500 to 10,000 years B.P. Mean July temperatures and mean annual temperatures of approximately  $4.5^{\circ}$  C. to  $5.5^{\circ}$  C. cooler than present values were proposed for the time interval 10,000 years to 8700 years B.P. The pollen evidence indicates similar vegetation to the present day since 8700 years B.P. The presence of fossil logs above tree line suggest that temperatures may have fluctuated up to  $1^{\circ}$  C. above present day values between 6000 years and 1220 years B.P. Tree ring studies indicate temperatures during the last 200 years were at least  $1^{\circ}$  cooler than present.

Zoltai and Tarnocai (1975) and Zoltai and Pettapiece (1978) have used peat-permafrost relationships and dated organic horizons in cryoturbated soils to suggest that during the time interval 8000 years to 4000 years B.P., permafrost was much less widespread throughout the Mackenzie Valley. They believe that a climatic cooling some 3000 to 4000 years B.P. initiated permafrost conditions, restricting peat accumulation to unfrozen fens.

Most recently, Delorme et al (1977) have used ostracod assemblages to infer climatic conditions in the Mackenzie Delta - Northwestern Arctic Coast area during the time interval 14,410 to 6820 years B.P. Mean annual temperatures of up to  $+1.2^{\circ}$  C., approximately  $10^{\circ}$  C. higher than present day values, and annual precipitation from 55 to 234 mm greater than the present day, were postulated.



Mackay (1978), in response to the paper by Delorme et al, has cited both the preservation of icy Pleistocene sediments and the lower portions of relic ice wedges beneath a widespread thaw unconformity along the Arctic Coast as evidence that maximum postglacial thaw was only a few meters. The depth of thaw indicates some post-glacial climatic warming, however, mean annual temperature must have remained several degrees below  $0^{\circ}\text{C}$ . during this time interval.

In summary, there is reasonably strong evidence for a post-glacial period in North Western Arctic Canada when tree lines were further north and the active layer was thicker than at the present time. These changes were no doubt due to an increase in mean summer temperatures. Temperature increases of the magnitude suggested by Ritchie and Hare, as well as Delorme et al are not substantiated. Evidence for mean summer temperatures substantially greater than those of the present day is not as compelling for inland sites as it is for arctic coastal sites.

### 3.3 Methods of Analysis

Frozen peat samples were collected with a CRREL (Cold Regions Research and Engineering Laboratory - U.S. Army) barrel coring device from site E 11 within the frozen palsa complex.

Cellulose was extracted from the peat samples using a modification of a method described by Theander (1954), which is illustrated by a





flow chart in Figure 18 . The method yields a greyish-white to light grey substance. An X-ray diffraction pattern of the substance reveals strong peaks in the range characteristic of alpha-cellulose. Following extraction, approximately 25 mg of vacuum dried sample is weighed into a nickel boat, placed under vacuum, then combusted in a reaction vessel at  $1150^{\circ}\text{C}$ . for 1 hour (see Thompson and Gray, 1976). The reaction produces a mixture of  $\text{CO}$ ,  $\text{CO}_2$  and  $\text{H}_2$  gasses. The  $\text{H}_2$  gas diffuses through the walls of the reaction vessels, forcing the reaction to completion. After combustion, the gasses are trapped in a silica gel trap maintained at liquid nitrogen temperature. The  $\text{CO}$  fraction is converted to  $\text{CO}_2$  and  $\text{C}$  by sparking between platinum electrodes. The  $\text{CO}_2$  fractions are combined and the yields measured manometrically. The peat samples averaged 90 to 95% of the theoretical predictions, indicating trace amount of contaminant. All peat samples were run as replicates; if replicate results did not agree, a third sample was run. The precision of the replicate analysis was better than  $\pm .4\%$ . Isotope measurements were made on a  $90^{\circ}$  sector, 25 cm double collecting isotope ratio mass spectrometer.

### 3.4 Results

Isotope measurements are expressed as a  $\delta$  value ( $^{\circ}/\text{oo}$ ) with respect to Standard Mean Ocean Water (SMOW). The results are listed in Table 6 .

The isotopic results are plotted with respect to depth in Figure





FIGURE 18  
FLOW CHART FOR PEAT CELLULOSE EXTRACTION

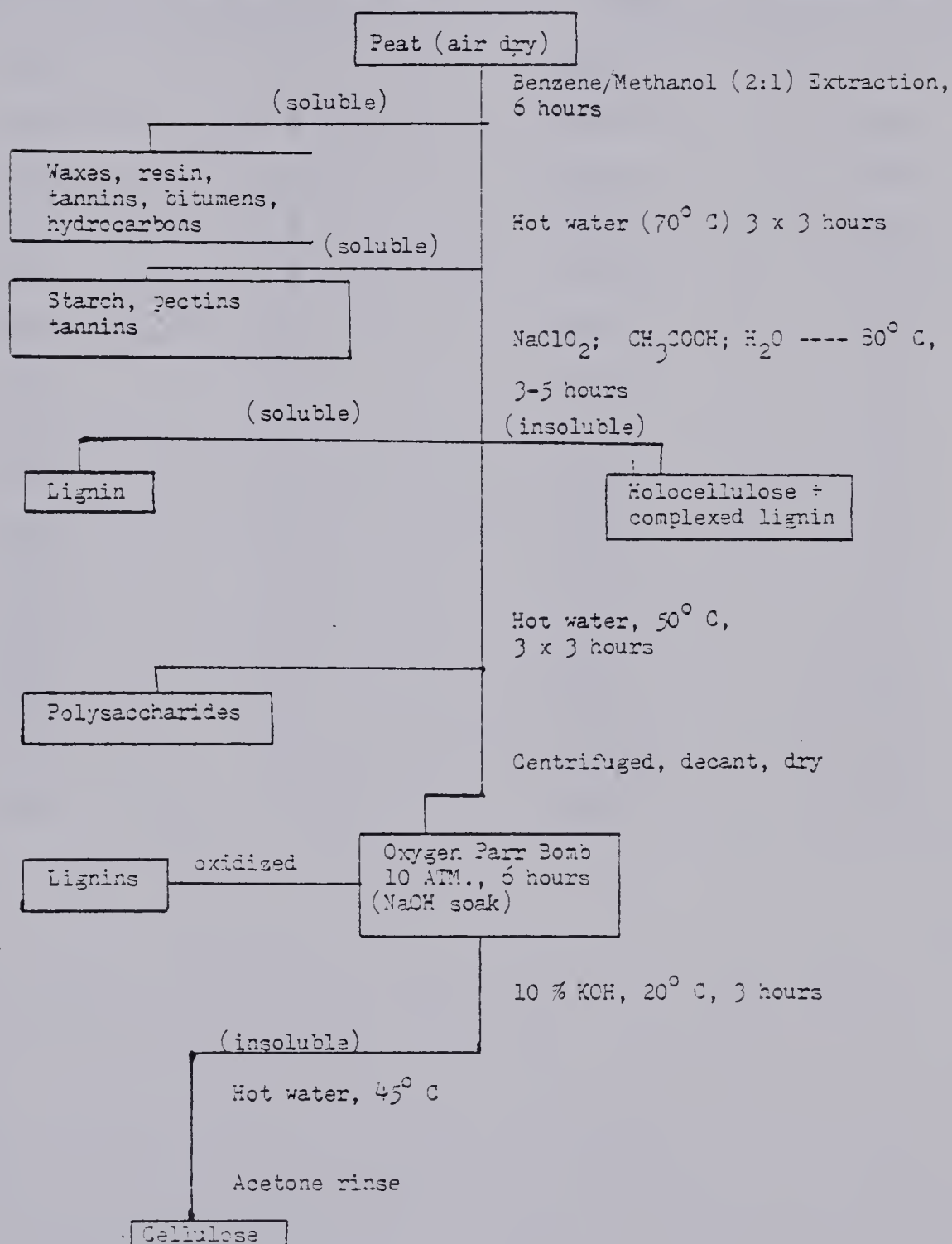




TABLE 6  
 PEAT OXYGEN ISOTOPE RESULTS  
 - Core E 3

| Sample | Depth (m) | Analysis number | $^{18}\text{O}_{\text{SMOW}}$ | Standard deviation |
|--------|-----------|-----------------|-------------------------------|--------------------|
| E 3-1  | .05       | 3               | 16.80                         | .40                |
| E 3-2  | .20       | 2               | 17.02                         | .14                |
| E 3-3  | .51       | 2               | 16.58                         | .39                |
| E 3-4  | .77       | 2               | 16.17                         | .10                |
| E 3-5  | 1.00      | 2               | 16.66                         | .33                |
| E 3-6  | 1.25      | 2               | 16.44                         | .32                |
| E 3-7  | 1.42      | 2               | 16.05                         | .19                |
| E 3-8  | 1.63      | 2               | 15.38                         | .40                |
| E 3-9  | 1.82      | 3               | 15.85                         | .15                |
| E 3-10 | 2.12      | 2               | 16.36                         | .35                |
| E 3-11 | 2.30      | 3               | 16.84                         | .20                |
| E 3-12 | 2.50      | 2               | 16.45                         | .31                |
| E 3-13 | 2.75      | 4               | 15.55                         | .27                |
| E 3-14 | 3.15      | 2               | 15.70                         | .15                |
| E 3-15 | 3.45      | 3               | 15.50                         | .41                |



19 , together with a radio-carbon age depth profile and an illustration of the peat stratigraphy. A description of the peat characteristics and phytological components can be found in chapter 1. The radiocarbon plot depicts corrected C-14 ages as determined by the University of Waterloo Isotope Lab (Wat 400 to 405). In constructing the age-depth profile, rates of peat accumulation were assumed linear between dated samples. Peat accumulation began 10,380 years B.P., terminating approximately 400 years B.P. Analysis of modern peat forming plants at the study site has allowed extrapolation of the isotope curve to the present day.

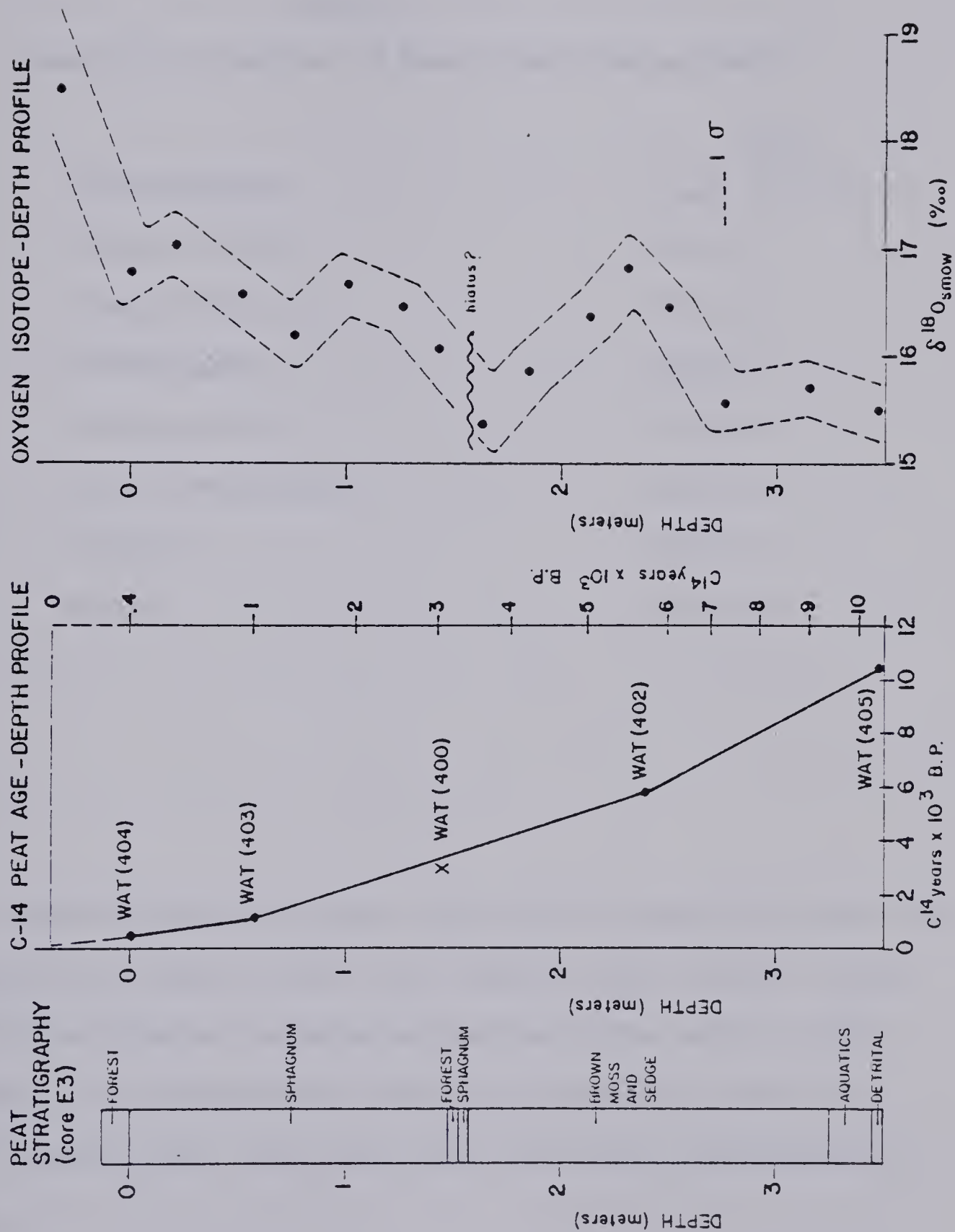
A possible hiatus due to a period of freezing then uplift or to drying of the peatland is found at a depth of 1.6 m. This level is marked by a 2 cm layer of woody nanolignid peat, similar to the forest peat layer found on the surface of modern palsas. The interval was apparently short lived; a plot of the C-14 age of the woody peat lies only slightly off the line connecting peat ages on either side of the layer (Figure 19 ).

### 3.41 Effect of Different Plant Species

Prior to analysing the isotopic composition of bulk peat samples, it was necessary to determine whether individual peat-forming plant species have similar oxygen isotope ratios. Samples of living plants, representing all the major peat forming species, were collected from the study site during the summer field season. The oxygen isotopic composition of each of the species was determined; the



FIGURE 19 : Showing the relationship between peat stratigraphy, carbon-14 age of the peat, and oxygen isotopic value of the peat cellulose with depth, core E-3.







results are listed in Table 7 .

TABLE 7

Isotopic Composition of Modern Peat Forming Plants

| <u>Plant Species</u> | $\frac{^{18}\text{O}}{^{16}\text{O}}$ SMOW<br>± 0.2 ‰ |
|----------------------|---|
| Sphagnum fuscum      | 18.65 ‰   |
| Sphagnum recurvum    | 18.51 ‰   |
| Drepanocladus        | 18.37 ‰   |
| Carex aquatilis      | 18.40 ‰   |
| Carex (various spp.) | 18.47 ‰   |
| Duckweed             | 18.39 ‰   |
| Mixture              | 18.48 ‰   |

The results show that, within the limits of analytical error, all the analyzed plant species have very similar oxygen isotopic values, reflecting the constant isotopic composition of the water in which they grew. It is therefore not necessary to separate individual species from the peat; bulk peat samples will give representative results.



### 3.42 Effect of Humification on Isotope Values

There is a possibility of oxygen exchange between the C-O bonds in the peat cellulose and percolating bog waters or with bacteria during decomposition. If such exchange did occur, the result would be to produce an homogenization of isotope values in the peat. Evidence suggests, however, that such isotope exchange is very unlikely; the C-O molecular bond in cellulose being very strong.

No oxygen exchange was detected in cellulose samples that were subjected to harsh oxidizing conditions (Gray and Thompson, 1976; Epstein, Yapp, and Hall, 1976; this thesis) or to high partial pressures of oxygen (this thesis). Further, Yapp and Epstein (1977) found no evidence for isotope exchange having occurred in wood that had been buried in wet soils for 11,800 years. In conclusion, the evidence to date, does not support the probability of isotope exchange occurring in the peat during humification.

### 3.43 Temperature Effects

The effect of temperature on the ultimate isotope values of plant cellulose is very complex. The temperature of air mass vapor condensation largely determines the isotopic composition at a specific site, but the degree of proportionality is a function of the history of the air mass (Dansgaard, 1964; Friedman et al, 1964). The effect of evaporation and evapotranspiration, both temperature dependent, on increasing  $^{18}\text{O}$  values in plant cellulose has been discussed by Epstein



et al (1977). When comparing localities that have widely different humidities, this effect will be of importance. Gray and Thompson (1976) however have shown that at a specific locality, where large humidity changes over time are not usually encountered, excellent agreement can be found between Mean Annual Temperature and  $^{18}\text{O}$  (cellulose). In peat bogs, humidity is always high, and effects due to changes of evapotranspiration rates can probably be neglected, especially when examining variations at a specific site. If enrichment due to evapotranspiration has occurred, the effect will be to overestimate Mean Annual Temperatures. Fractionation occurring during cellulose synthesis may also be temperature dependent (Epstein et al, 1977; Gray and Thompson, 1976). In all previous site specific studies, the temperature coefficient for cellulose was positive, ranging between 1 and 3 ‰  $^{18}\text{O}/^{\circ}\text{C}$ . (Libby and Pandolfi, 1974; Epstein and Yapp, 1977; Gray and Thompson, 1976).

### 3.5 Paleoclimatic Interpretations

The preceding discussion documented that Mean Annual Air Temperatures are strongly correlated with oxygen isotope ratios in plant cellulose. Before paleo-temperature interpretations can be made of the isotope fluctuations however, a temperature coefficient must be found for peat cellulose. Unfortunately, peat cannot be calibrated in the same way as tree rings because it is impossible to separate yearly accumulations. The temperature coefficient for Edmonton Spruce, 1.3‰  $^{18}\text{O}/^{\circ}\text{C}$ . (Thompson and Gray, 1976), might be applicable; however





Sphagnum cellulose may fractionate differently than spruce.

A method of comparing Sphagnum and tree ring temperature coefficients is to plot  $^{18}\text{O}_{(\text{cellulose})}$  of plants from various locations versus the Mean Annual Temperature at that site. Sphagnum moss from a wide variety of climatic zones was analyzed, then results plotted against Mean Annual Temperature (average of last 5 years) in Figure 20. For some of the locations, Sphagnum samples were available from more than one bog; the range of results at these locations is plotted as a bar. On the same graph, oxygen isotope values of modern tree ring cellulose from various sites are plotted (unpublished data, P. Thompson). This data set includes the previously mentioned Edmonton spruce analyzed by Gray and Thompson (1976). The isotopic values from northern continental North America (Edmonton, Alberta; North Bay, Ontario; Fort Simpson, N.W.T.; Old Crow, Yukon; and Coppermine, N.W.T.) are reasonably defined by the linear relationship:

$$\delta^{18}\text{O} = 0.5 T + 19.90$$

The values for subtropical and tropical localities (Houston, Texas; Campinas, Brazil) fall significantly below this line, while values from a Pacific maritime area (Queen Charlotte Islands, B.C.) fall above the line.

The tree ring isotope values respond in a similar manner; the regression line is parallel to the peat line but displaced 2 ‰ higher (Figure 20). The reason for the displacement is not apparent but may be due to a degree of isotopic equilibration of atmospheric  $\text{CO}_2$  with the tree water prior to photosynthesis and the fixation of





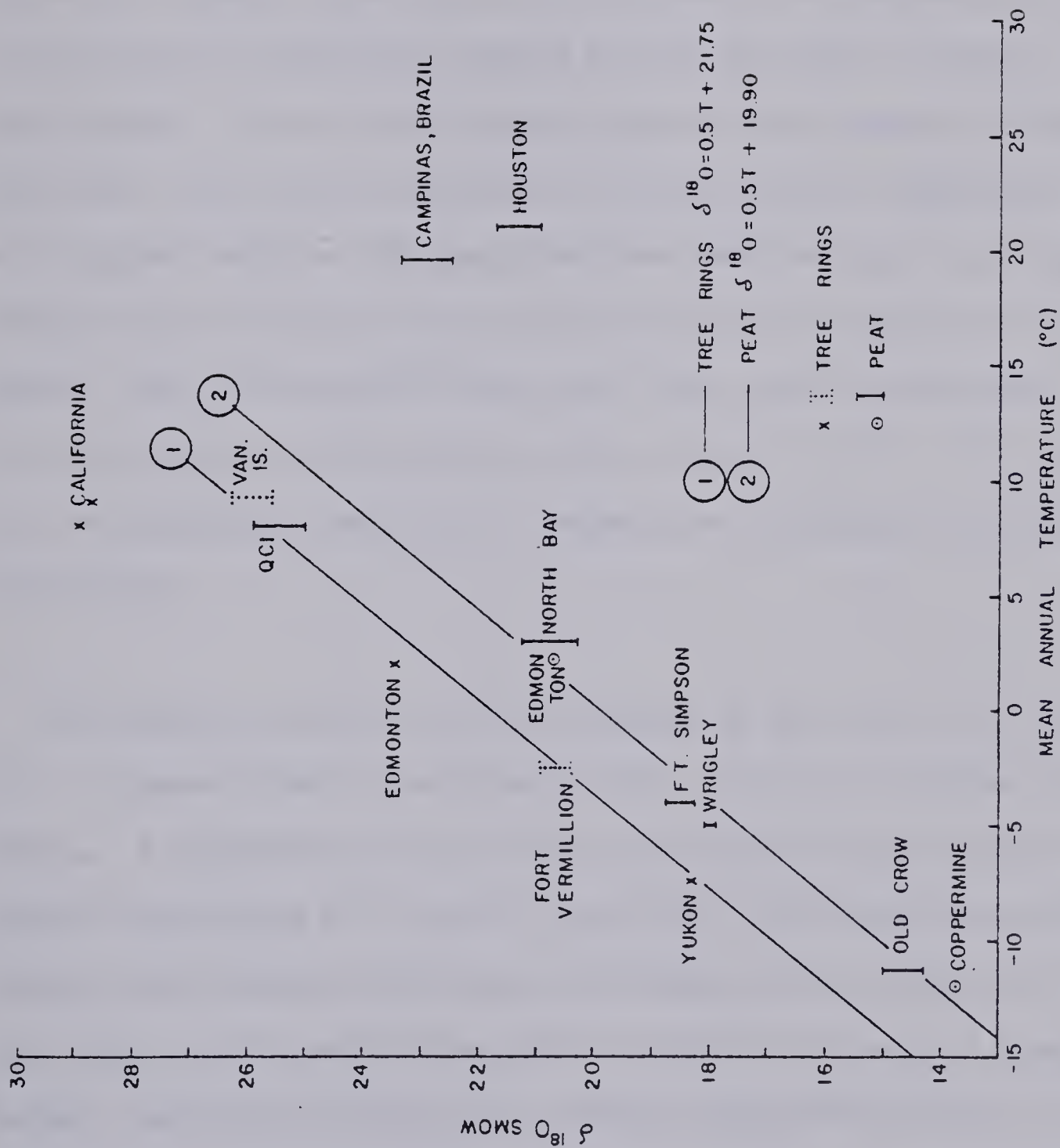


Figure 20 : Change in oxygen isotope content of modern *Sphagnum* moss with the mean annual temperature of their place of growth.



CO<sub>2</sub> into cellulose (Gray and Thompson, 1976).

In theory, this method should lead to a temperature coefficient for plant cellulose. Comparison of Gray and Thompsons' tree ring coefficient of 1.3 ‰/°C. with the value of 0.5 ‰/°C. from Figure 20, clearly shows this is not the case. As previously discussed, many non-temperature related factors can effect isotopic fractionation. These effects become apparent when comparing different localities, hence also the scatter of the data points, especially for more tropical samples. The graph does show that peat and tree ring isotope ratios increase in parallel as Mean Annual Temperatures increase. While the need for a great deal more work is acknowledged, use of the temperature coefficient for White Spruce (1.3 ‰/°C.) should give the approximate magnitude of temperature fluctuations during peat accumulation.

The oxygen isotope curve, from analysis of peat core E 11 (Figure 19), is characterized by relatively little variation throughout the profile. A comparatively cool climate is indicated between approximately 10,000 years B.P. and 7000 years B.P. This was followed by a warming trend between approximately 6000 years B.P. and 5000 years B.P. While this time interval corresponds to that of the classical Hypsithermal, the isotope values do not indicate exceptional warming. A cooling trend followed, reaching a minimum value between approximately 4000 and 3000 years B.P.; this was the lowest isotope value measured in the entire peat column. Interestingly, a change in peat type is



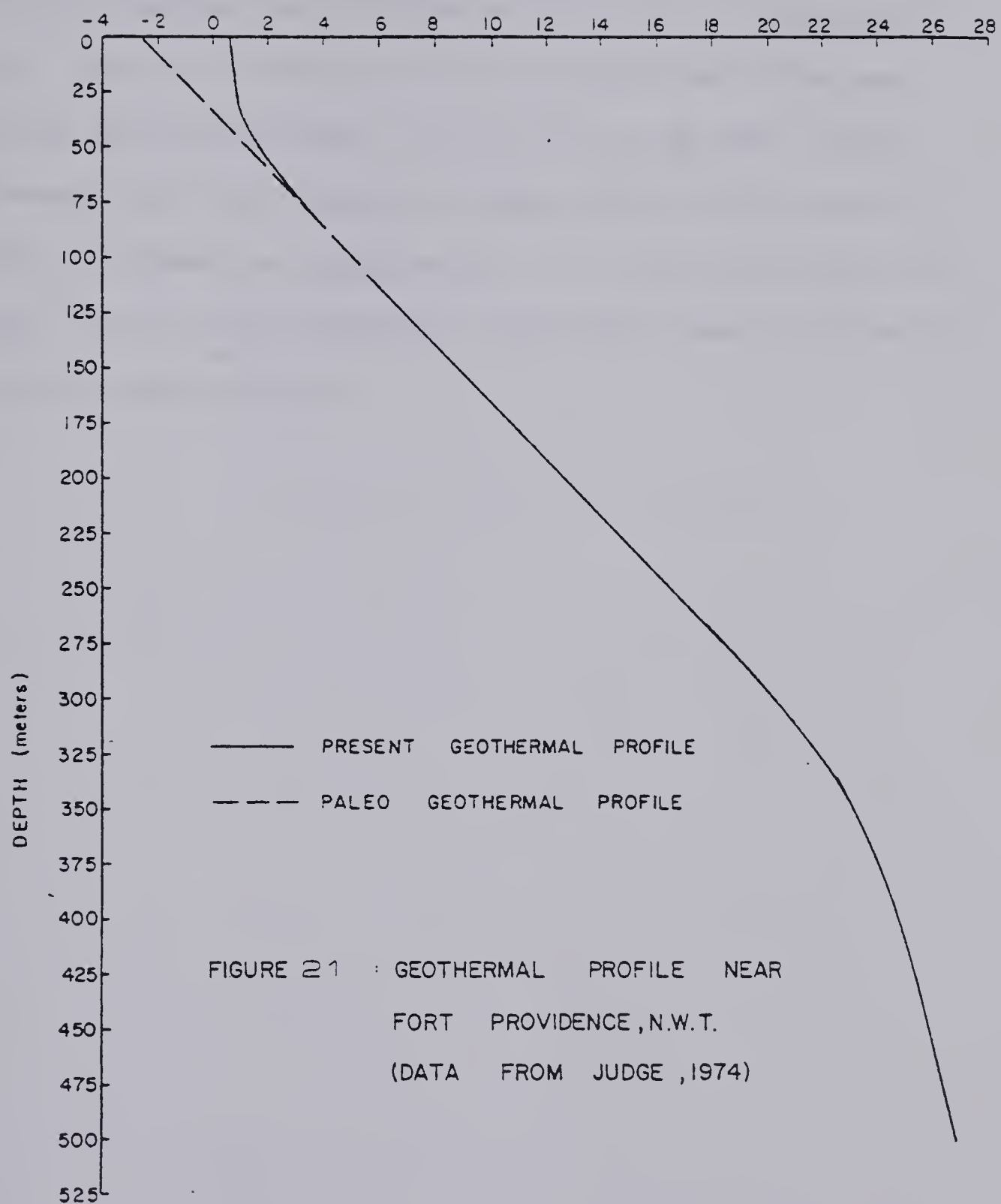
encountered immediately above this layer, from a Sphagnum peat to a forest peat, suggesting a brief period of permafrost invasion then colonization by Black Spruce. Isotope variations are small in the upper 1.5 meters of core; a gradual warming trend is indicated, especially over the past 400 years.

Modern peat producing plants in the Fort Simpson area have higher isotope ratios than any of the peat samples. This suggests current Mean Annual Temperatures are the warmest that have occurred in the past 10,000 years. Using the above temperature coefficient of  $1.3^{\circ}/\text{oo}/^{\circ}\text{C}.$ , a minimum Mean Annual Temperature approximately  $3^{\circ}\text{C}.$  colder than present, or  $-7^{\circ}\text{C}.$ , is indicated.

An independent method of checking these temperature approximations is to examine nearby deep temperature profiles. At depth, the geothermal gradient is slow to respond to surface temperature changes; hence perturbations in the gradient can be used to calculate previous ground surface temperatures (Judge, 1974). A deep temperature profile from an oil exploratory well, 200 km east of Fort Simpson, is plotted in Figure 21 (data from Judge, 1974). The well penetrates 33.5 m of unfrozen unconsolidated material, underlain by 300 m of shale and 113 m of carbonates. The temperature gradient is abnormally low to a depth of 66 m, which does not correspond to any change in lithology, hence is indicative of recent climatic warming.

Extrapolation of the lower unaffected part of the curve to the surface indicates a Paleo-Mean Annual Surface Temperature (M.A.S.T.) of









-2.8 °C. Compared to the present day M.A.S.T. of + 0.4 °C., this represents a warming of +3.2 °C. Prior to the onset of surface warming, at least 30 m of permafrost was present (Figure 21). Degradation of the permafrost was by bottom melting due to the geothermal heat flux. The rate of melting of the permafrost due to the geothermal heat flux is calculated to be 1.0 to 1.5 cm/ year, hence surface warming must have commenced roughly 2000 to 3000 years B.P. A Mean Annual Temperature approximately 3 °C. cooler, 2500 years B.P., agrees well with the paleotemperature predictions based on oxygen isotopes from the peat cellulose.



## CHAPTER 4: EVOLUTION OF THE PEATLAND LANDSCAPE



## 4.1 Introduction

The evolution of a peatland is recorded in the peat stratigraphy. The interrelationships of mineral soil topography, hydrologic regimes, vegetational sequences, bog processes and climate create distinct peatland types; therefore, the peat is more than just a record of past plant communities. The work of Kulczynski (1949) and Heinselman (1963) is unique in examining past environmental conditions, as deduced from the peat stratigraphy, for their role in creating the modern peatland landscape. This type of integrated study has not been carried out in discontinuously frozen peatlands.

In this chapter, the change in physical environmental conditions in the Fort Simpson peatland over the past 10,000 years is inferred from the peat stratigraphy. The stratigraphy across the palsa complex records six vegetative communities:

1. organic detritus in silt
2. aquatic plants
3. brown moss-sedge
4. sedge-shrub-Black Spruce
5. Sphagnum bog
6. Black Spruce-Cladonia-feathermoss

Each of these communities implies a different wetland environment. Modern analogues of these communities allow reconstruction of environmental conditions at the time of deposition. Six radiocarbon dates permit a chronological sequence to be outlined for the vegetative and environmental successions.



## 4.2 Environmental Sequences

Immediately after the retreat of the Laurentide Ice Sheet, Glacial Lake McConnell occupied large areas of the Mackenzie Valley (Rutter, 1974). While the lake was subject to numerous fluctuations creating complex beach ridges around its margins, deep water conditions persisted until approximately 11,000 years B.P. Pollen profiles indicate that during the approximately 1000 year existence of the lake, boreal forest vegetation occupied the poorly drained, possibly discontinuously frozen, glacial soils bordering the lake (T. Habgood, personal communication). Black Spruce was the dominant tree species, being probably the first to re-colonize the area as it is best adapted to poorly drained soils. Organic deposition in the turbid waters was very slow but created a relatively thick layer of organic detritus in a silt matrix.

Drainage and evaporation of Lake McConnell was not sudden but involved a progressive lowering of base levels. Eventually, a level plain with many shallow lakes and ponds remained. This phase was relatively short lived and resulted in the discontinuous deposition of shallow organic gyttja and aquatic peat.

It is uncertain whether the lake plain completely dried up. A dessication period has been reported in northern Alberta (May and Thomson, 1977) for this time interval. Further, near surface lacustrine sediments are overconsolidated (see section 3A), a characteristic of dessicated soils (Wu, 1977). Also, calcium sulphate concen-





trations were recorded at the top of the mineral soil (Chapter 1), a characteristic of evaporated lake waters. Conflicting evidence is the lack of a phyto response in the pollen diagrams from the area. If an arid interval coincided with the drainage of Lake McConnell, it was probably of short duration.

Fens quickly overspread the nutrient rich lacustrine plain and paludification of the landscape began. Fen communities can form peat capable of holding back water hence causing significant rises in the water table (Heinselman, 1970). This event is dated by the basal layer of brown moss and sedge fen peats that nearly uniformly cover the former glacial lake basin, dated at approximately 8500 years B.P. Radio-carbon dated horizons and the uniform thickness of the brown moss-sedge peat layer suggests that this community lasted for several thousand years. The area around the large lakes to the north of the palsa complex is a modern analogue of the treeless, very gently sloping, mineratrophic fens that occupied the site.

As the peat accumulated, drier sites became available. Shrubs such as Sweet Gale, dwarf birch, willow and to a lesser extent trees like Black Spruce and Tamarack invaded the fens; in some localities a shrub fen or carr resulted. The vegetative community was floristically rich: the peat contains sedges, brown mosses, shrubs, wood, mosses and possibly grasses. Spruce is much more abundant in the woody fen peat than that described by Zoltai and Tarnocai (1975) from peat plateaus in the central Mackenzie Valley.



The thick Sphagnum peat layer found in all cores is testimony to a change from nutrient rich mineratrophic fens to nutrient poor ombrotrophic bogs. Prior to the Sphagnum bloom, the fen surface had a very gentle uniform slope; the continual accumulation of peat tending to level out the peatland surface. Ombrotrophic conditions developed when the peatland surface rose above the level of percolating, mineral rich, groundwater; hence creating a local water table divide. The divide may have been partly present in the original physiography, or was developed entirely by peat accumulation, or was created by stream capture (Heinselman, 1970). The importance of local water table divides in the development of large Sphagnum bogs is also stressed by Kulczynski (1949).

The lowering of regional water tables, possibly related to the more integrated drainage system that was developing, initiated peatland drainage in more than one direction. Areas of elevated mineral soil beneath the peat provided the first areas to develop local water table divides. The lake marginal area was particularly favored, having an irregular substratum topography (Chapter 1). Sphagnum quickly invaded these ombrotrophic sites creating extensive bogs along the margins of the former glacial lake. Peat accumulation continued until approximately 1500 years B.P. Wood remains in the Sphagnum peat are very scarce, indicating a bog with only scattered trees.

The change from Sphagnum peat to a nanolignid forest peat marks the raising of the bog surface with the aggradation of permafrost. The lack of permafrost development in this area prior to approximately



4000 years B.P. (Zoltai and Tarnocai, 1975; Zoltai and Pettapiece, 1978), in spite of sufficiently cool mean annual temperatures (see Chapter 3), was because of the lack of suitable sites. Permafrost will not develop in ponded fens due to the vast reservoir of latent heat and high thermal transfer rates. By contrast, Sphagnum sites are very conducive to permafrost aggradation because of their unique thermal qualities (Brown, 1966). The Picea-Ledum-Rubus-Cladonia community that followed permafrost development has remained to the present day.

The unfrozen Sphagnum bogs contained within the palsa complex are the result of permafrost degradation. Stratigraphically, two Sphagnum layers are divided by a thin horizon of forest peat (Figure 4); radio-carbon dating of the forest peat from core E 11, at a depth of 1.5 m, indicates initial freezing took place approximately 3500 years B.P. (WAT 400). The areas around the fringes of the bogs have recently re-frozen, permafrost being re-established approximately 400 years B.P. The marginal areas of the thaw bogs appear to be comparatively dynamic; continued climatic warming may result in another collapse, alternatively cooling may re-establish permafrost along the bog edges.

The 'thermokarst' sinkholes by contrast, do not appear to be a result of permafrost degradation. Sinkholes differ from the unfrozen bogs in that they are contained ponds with virtually no Sphagnum and very little aquatic vegetation (see Chapter 1 and Figure 4). The peat stratigraphy of the sinkholes is greatly different from the rest of the palsa complex, consisting of 25 cm of moderately decomposed duckweed, 15 cm of gyttja, 25 cm of ponded fine grained detrital sands, and





glaciolacustrine clay. There is no evidence of collapsed peat in the center of the hole. Around the edges of the sinkhole however, large lobes of semi-submerged Sphagnum peat are evident, as are actively collapsing walls. It is unlikely that decomposition rates have been sufficient to totally digest the collapsed peat. The stratigraphy suggests that some holes are primary features and have been present since the initial aggradation of ground ice. Recent permafrost degradation in the form of wall collapse has enlarged the area of the ponds.

In summary, the following sequence of landscapes have developed in peatlands near Ft. Simpson:

1. a large deep glacial lake
2. a partially dessicated lake plain with numerous shallow ponds
3. a paludificated fenland
4. ombrotrophic bogs, and
5. extensive permafrozen peatlands.





## CHAPTER 5: PERMAFROST AGGRADATION AND DEGRADATION



## 5.1 Introduction

The development of ground ice in peatlands is a complex process. While cold air temperatures are a necessary criteria for permafrost aggradation, paleotemperature analysis has shown that it is not a solely sufficient control. The role of different vegetation communities in creating various soil temperatures has been emphasized by numerous researchers (Williams, 1968; Brown, 1970). Similarly, the role of surface water in modifying ground thermal regimes is well acknowledged (Mackay, 1972; Brown, 1970). A less discussed aspect of the role of vegetation and water, however, is the evolution of the vegetative communities and the hydrological regimes with their subsequent effect on ground ice development. This evolution is discussed in this chapter. An examination will also be made of the role of the mineral soil morphology and stratigraphy in determining where in a watershed permafrost will develop.

The melting or degradation of permafrost is equally complex as its aggradation. Three components of the melt process: lateral melting, surface warming, and melting from the bottom contribute to ground ice degradation. The relative roles of each of these components is examined in the second section of this chapter. The rate of lateral melting is determined quantitatively from historical records. By extrapolation of the rate of lateral degradation, the former extent of permafrost in the peatland is estimated.

Both ground ice aggradation and degradation have created the



present day palsa relief. This fact has not been acknowledged in the literature. Only the role of segregated ground ice development in the mineral soil has been cited as a contributor to palsa height. The last section of this chapter shows that degradational processes are equally important in creating the present day landscape.

## 5.2 Ground Ice Aggradation

### 5.21 Processes and Controls

#### 5.211 Climatic Controls

Two climatic requirements for the presence of palsas are a Mean Annual Temperature colder than  $-1^{\circ}\text{C}$ . to  $-3^{\circ}\text{C}$ . (Ruuhijarvi, 1960) and a winter precipitation less than 30 cm (Lundqvist, 1962). The present day climate at Fort Simpson is within these bounds, with a Mean Annual Temperature of  $-4^{\circ}\text{C}$ . and a winter precipitation averaging 15 cm. Holocene Mean Annual Temperatures at Fort Simpson were also below these limits, varying between  $-7^{\circ}\text{C}$ . and  $-3^{\circ}\text{C}$ . (see Chapter 3).

While it is problematic whether palsas are only being maintained at the above temperatures or whether new permafrost is actually aggrading, it is still unlikely that climate has been an impediment to permafrost development over the past 8000 years. The question remains therefore, of why extensive permafrost did not develop until approximately 4000 years B.P. in spite of a sufficiently cold climate? Clearly ed-



aphic factors such as peatland vegetation and hydrology have played a key role.

#### 5.212 Vegetational And Hydrological Controls

The influence of vegetation, in particular Sphagnum moss, in creating ground thermal conditions suitable for permafrost aggradation has been well documented (Brown, 1963; Williams, 1968; Zoltai and Tarnocai, 1975). The thermal conductivity of Sphagnum changes sufficiently with moisture content or when frozen that the outward transfer of heat in the winter exceeds the inward heat transfer in the summer, hence creating a negative heat budget. Because of this unique thermal characteristic, permafrost will develop beneath Sphagnum at a higher Mean Annual Temperature than beneath mineral soil.

Nearly all palsas have a Sphagnum cover at the time of formation; this is not the only prerequisite for permafrost aggradation however. Palsas from the study area typically have a .8 meter cap of Sphagnum, representing approximately 1000 years of accumulation, before permafrost developed. Also, modern collapse bogs contained within the palsa complex have a Sphagnum cover up to 1.5 meters in thickness, yet are unfrozen. This dilemma may be due to the changing hydrology of the bogs. If the bogs have very high water tables, the moss will be continually saturated. The thermal properties of the Sphagnum will not seasonally change; a negative heat budget will not develop. A domed or raised bog surface, that allows partial drying of the upper peat layers, is essential to permafrost development in the present climate.







Black Spruce may also play an important role in permafrost aggradation in peatlands. Small permafrost lenses have been observed beneath spruce seedlings that were growing on isolated Sphagnum hummocks in an otherwise unfrozen bog (Zoltai and Tarnocai, 1975). Shading from the spruce creates a cooler micro-climate suitable for ground ice development. Zoltai and Tarnocai maintain that the small frozen hummocks eventually coalesce to create a peat plateau. Further, the presence of these frozen hummocks indicates that palsas are presently forming (Zoltai and Tarnocai, 1975).

While a number of 'embryonic' palsas of the type described were observed near the study site, they appear to be temporary features. One frost mound, first observed in August, 1976, was about 35 cm high, had a basal diameter of 1.1m with ground ice to a depth of 50 cm. Two 8 year old Black Spruce trees grew on the frost mounds. In September of the following year the mound was only 20 cm high, had a basal diameter of 0.6 m with ground ice at a depth of 35 cm. Two other frost mounds, only 20 to 25 cm high, with a basal diameter of 30 cm, in the summer of 1976, had completely disappeared by September, 1977. In addition, a ground ice lens had developed beneath a nearby seedling covered hummock where the previous year there had been no permafrost.

Previous discussion on the observed thermal structure of the palsa (Chapter 1) has demonstrated the sensitivity of the permafrost to small changes in surface temperatures. Ruuhijarvi (1960), Wramner (1967, 1973) and Sollid and Sorbel (1974) have also noted the temporary nature of small frost mounds in peatlands.



The strongest argument against the role of spruce in palsa development is the lack of spruce on palsas in Scandinavia and Ungava. Here, palsas develop readily above the tree line.

In summary, the presence of large ombrotrophic Sphagnum bogs that have sufficiently raised and drained surfaces are necessary for extensive permafrost development in peatlands in the Ft. Simpson area. The ombrotrophic conditions are created by a reorganization of the surface drainage, as was detailed in the previous chapter. The role of Black Spruce is important in maintaining permafrost, but probably has little to do with regional permafrost aggradation.

#### 5.213 Influence of Mineral Soil Topography

The possible role of the mineral soil topography in determining preferential zones of permafrost aggradation was first suggested by Thie (1974). In the Ft. Simpson area, the close association between beach ridges and palsa complexes (see Chapter 1) suggests that the initial mineral soil topography may affect the sites of segregated ground ice development in the peatlands. The topography of the mineral soil beneath a palsa can be re-created by thawing a palsa core in increments under in situ overburden stresses. Any 'residual height' following thaw consolidation will theoretically equal the relief of the mineral soil prior to freezing.

Methods for such tests have recently been proven for a variety of soil types (Watson et al, 1973; Luscher and Afifi, 1973; Smith and Morgenstern, 1972) and a comprehensive theory for thaw consolidation



established (Morgenstern and Nixon, 1971; Nixon and Morgenstern, 1973).

The total thaw consolidation,  $E^0$ , of a thawing soil is made up of three separate processes:

1. settlement due to volume reduction associated with a phase change of ice to water
2. consolidation during the period of thaw
3. consolidation subsequent to thaw

The total thaw strain can be expressed:

$$E^0 = A_0 X + a_0 \int_0^X (P + \gamma' X) dX$$

where  $E^0$  = total settlement

$A_0$  = initial thaw settlement parameter

$a_0$  = coefficient of compressibility

$P$  = surcharge load

$X$  = depth to the thaw front

$\gamma'$  = submerged unit weight of thawed soil

(Lusher and Afifi, 1973)

Total thaw settlement can also be correlated with some of the bulk properties of the frozen soil. Speer et al (1973), in a study of ground ice variability near Norman Wells, found an excellent correlation between frozen bulk density and total thaw strain at a stress equal to the average stress encountered in situ. Following this methodology, 31 thaw consolidation tests were made on the frozen mineral soil from core E 3 of the palsa. The results of the testing are tabulated in Appendix 3. The testing methods were similar to those described by Roggensack (1978); a brief summary of which can be found in Appendix 4.





Following consolidation, linear and logarithmic relationships were derived between settlement parameters such as  $E^0$ ,  $a_0$ , and  $A_0$ ; and core physical parameters such as water content ( $w$ ), volumetric ice content ( $v$ ), and frozen bulk density ( $\gamma_f$ ), (Figures 22 to 26). The most significant of these correlations are listed in Table 8. The  $E^0:\gamma_f$  relationship and  $E^0: A_0 + a_0$  relationship gave the most accurate results; both predicted settlements within 1.5 % of that measured.

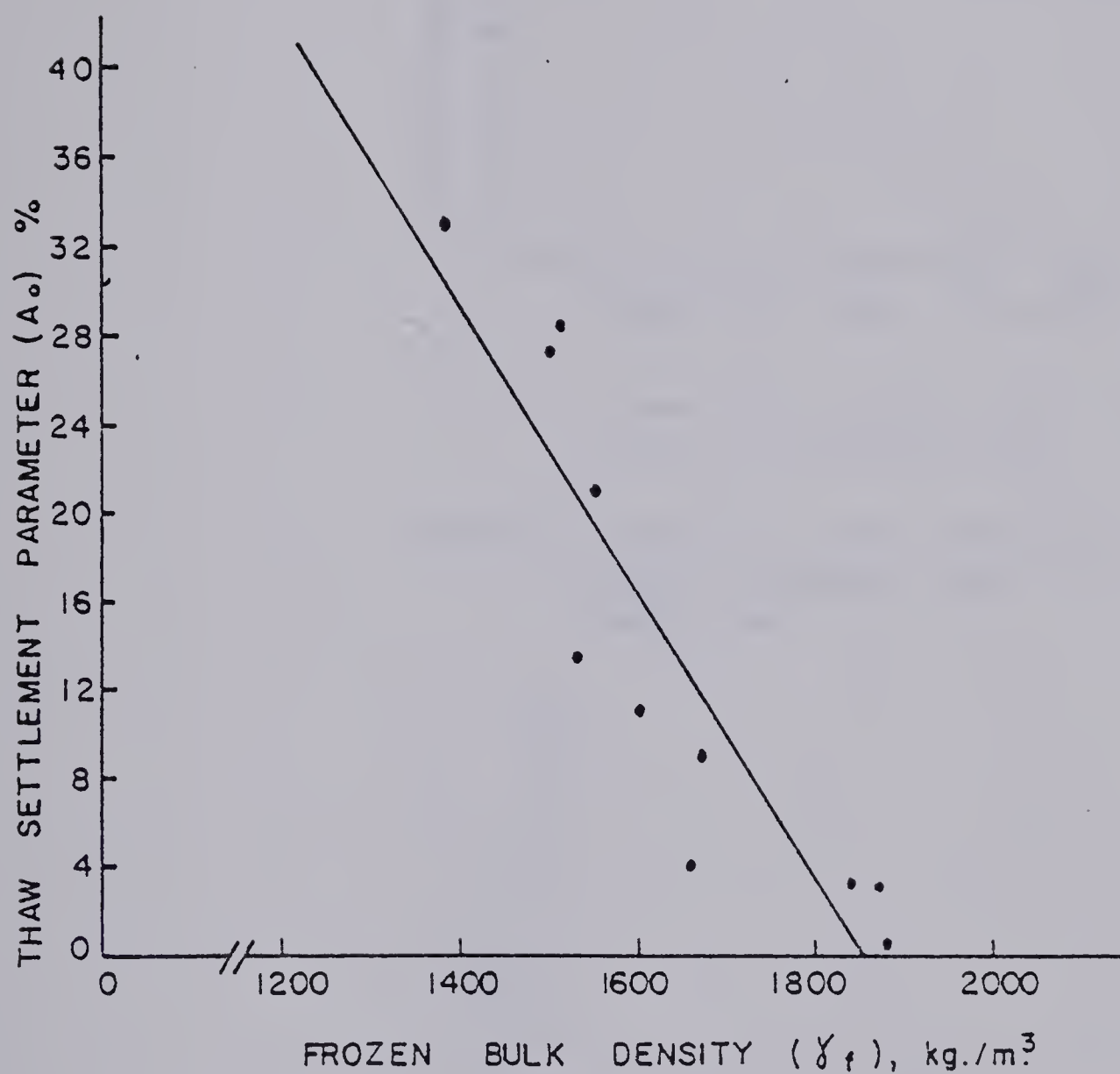
The bulk density relationship was used to predict settlement in six other cores from the palsa (Appendix 3). Total thaw settlements for each core are listed in Table 9, as are the respective differences in elevation between the peat-mineral soil interface in the palsa and that in the fen.

In each of the cores, a positive residual mineral soil relief was detected. The magnitude of the relief, from .23 to .65 m represents from 9% to 46% of the total frozen mineral soil relief, well in excess of the methodological error. The residual relief is approximately equal to the thickness of the sand layer usually encountered immediately beneath the peat. Freezing of the sand layer will produce insignificant heave compared to freezing of a silty clay layer. If the initial soil relief beneath the palsa is largely provided by a sand hummock, then the total heave in the mineral soil will decrease with the relative thickness of sand layer that is present. A plot of total heave in the mineral soil vs. initial mineral soil relief shows this to be the case (Figure 27), with a very strong negative correlation between the two parameters.





FIGURE 22



—————  $A_o = -6.32 \times 10^4 \gamma_f + 117.2$

-----  $A_o = -658.6 - 104.74 \ln \gamma_f$

THAW SETTLEMENT PARAMETER,  $A_o$ , FOR MINERAL SOIL RELATED TO FROZEN BULK DENSITY.



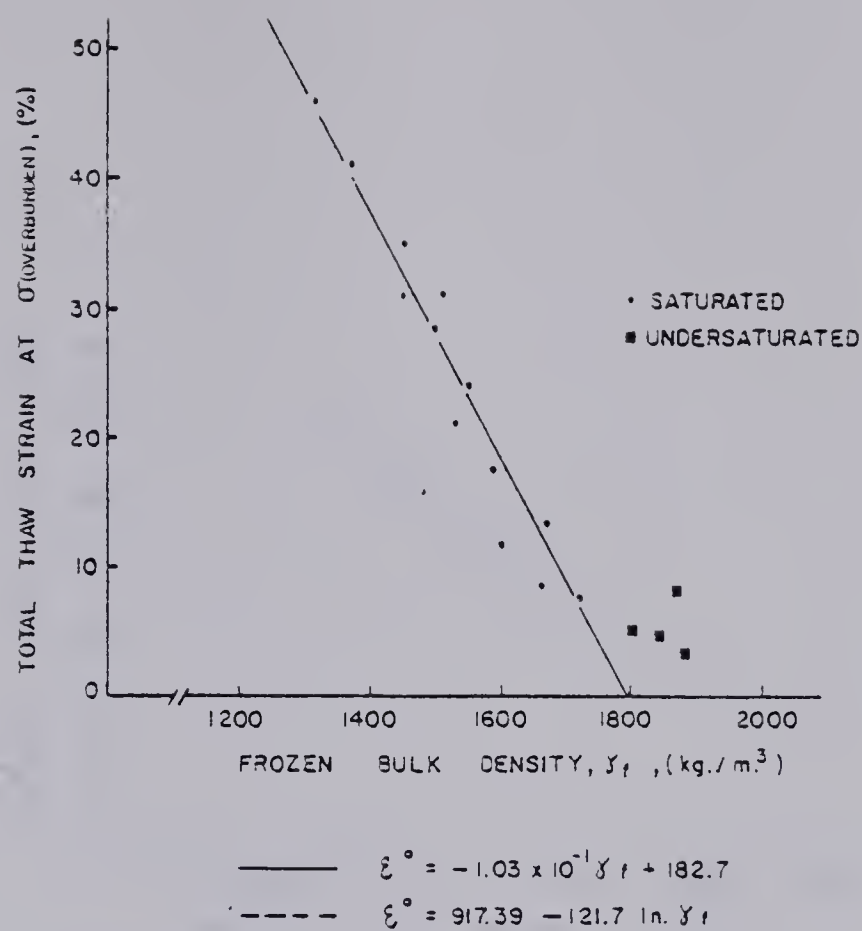


FIGURE 23 : TOTAL THAW STRAIN — FROZEN BULK DENSITY RELATIONSHIP FOR MINERAL SOILS.

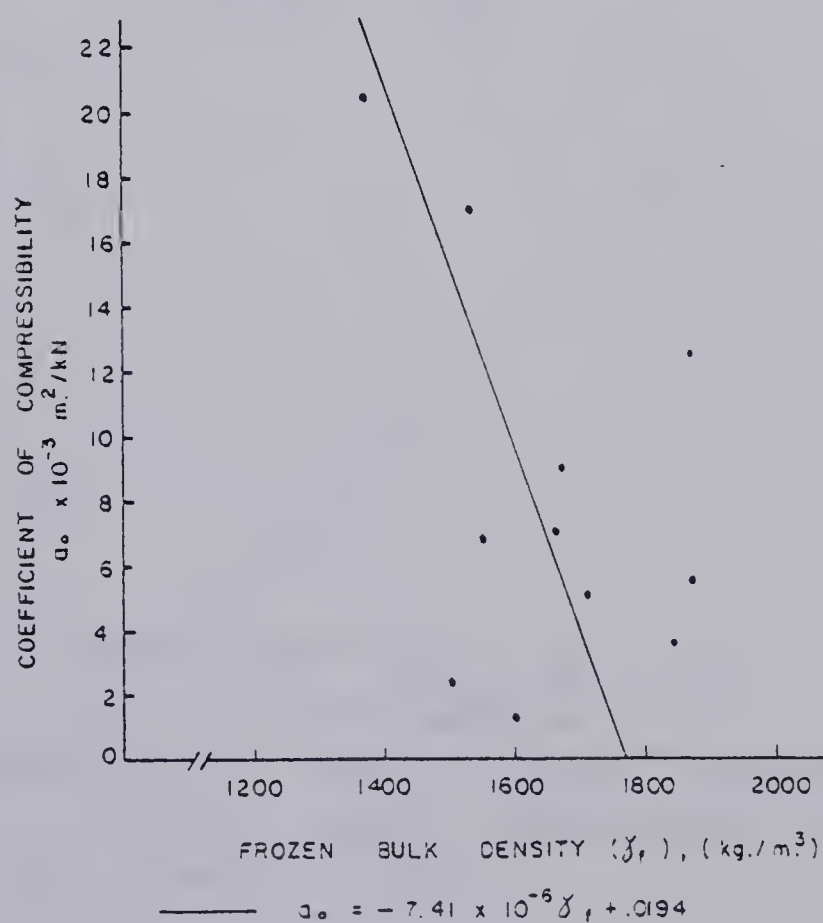


FIGURE 24 : COEFFICIENT OF COMPRESSIBILITY — FROZEN BULK DENSITY RELATIONSHIP FOR MINERAL SOILS.



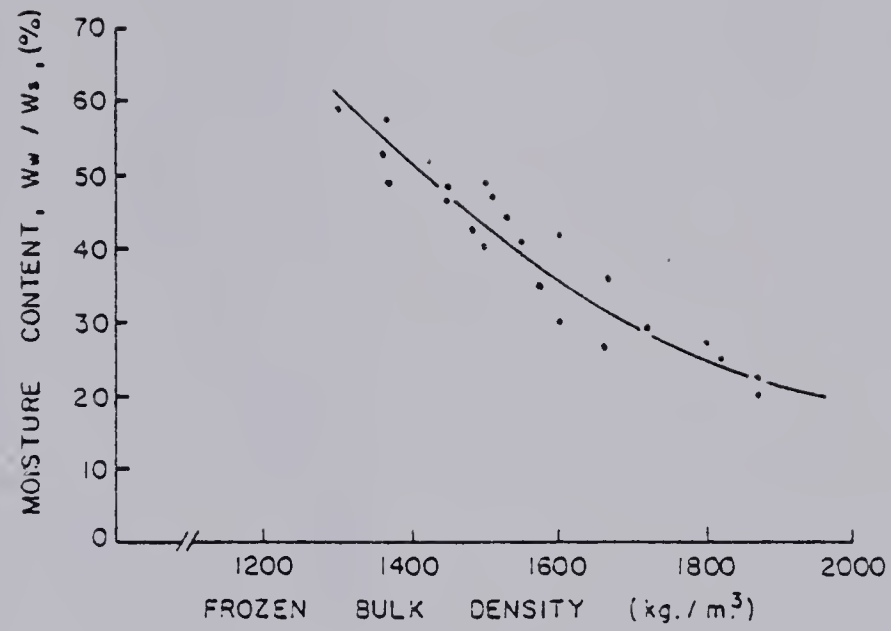


FIGURE 25 : MOISTURE CONTENT — FROZEN BULK DENSITY RELATIONSHIP FOR MINERAL SOILS.

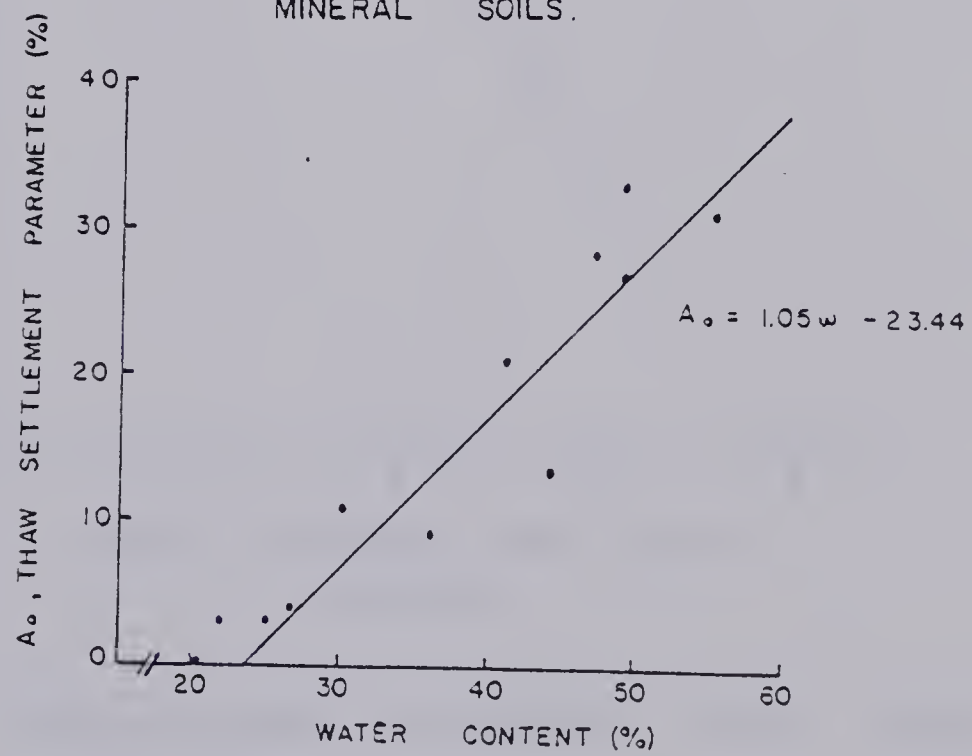


FIGURE 26 : INITIAL THAW SETTLEMENT PARAMETER — WATER CONTENT RELATIONSHIP FOR MINERAL SOILS



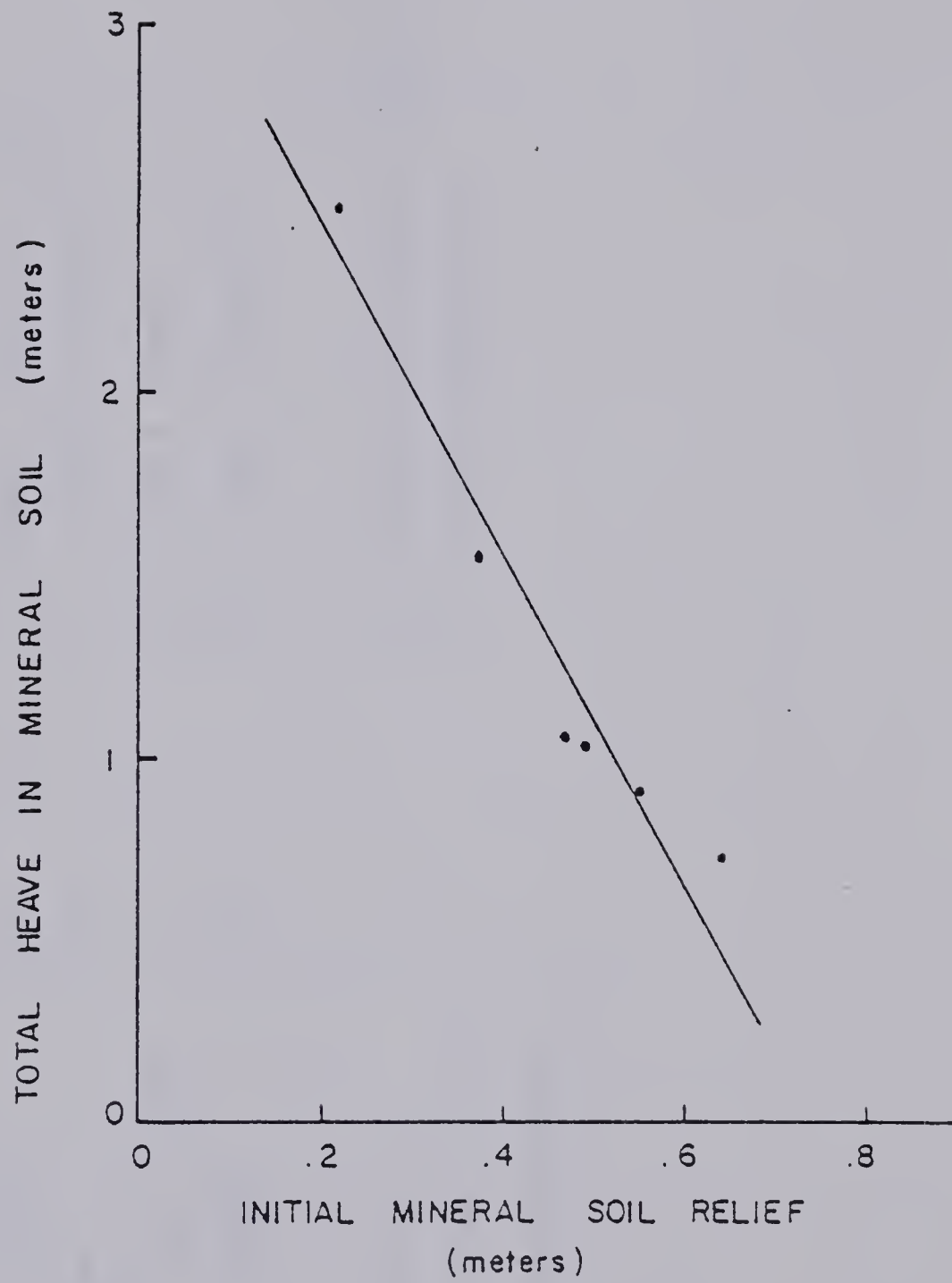


FIGURE 27: RELATIONSHIP BETWEEN TOTAL HEAVE IN MINERAL SOIL AND INITIAL MINERAL SOIL RELIEF.





SUMMARY OF THAW CONSOLIDATION RELATIONSHIPS  
-for mineral soils

|    | Linear  | Correlation (r) | Logarithmic                          | Correlation (r) |
|----|---|-----------------|--------------------------------------|-----------------|
| 1. | $E^o = -.1036 \gamma_f + 182.7$               | .97             | $E^o = 917.39 - 121.7 \ln \gamma_f$  | .98             |
| 2. | $A_o = -.0632 \gamma_f + 117.2$               | .90             | $A_o = 788.44 - 104.74 \ln \gamma_f$ | .91             |
| 3. | $A_o = 1.05 w - 23.44$                        | .82             | $A_o = -105.94 + 34.03 \ln w$        | .94             |
| 4. | $a_o = -7.41 \times 10^{-6} \gamma_f + .0194$ | .34             | $a_o = .1596 - .0205 \ln \gamma_f$   | .34             |
| 5. | $a_o = 2 \times 10^{-4} w + .0023$            | .30             | $a_o = -.010 + .0052 \ln w$          | .33             |

$E^o$  = vertical thaw strain in %

$A_o$  = thaw settlement parameter in %

$a_o$  = coefficient of compressibility  
in  $m^2/kN$

$\gamma_f$  = frozen bulk density in  $Kg/m^3$

$w$  = water content in %



TABLE 9  
TOTAL THAW SETTLEMENT OF THE MINERAL SOIL AND  
OBSERVED FROZEN MINERAL SOIL RELIEF IN THE PALSA COMPLEX

| Core    | Thaw settlement<br>(m) | Observed frozen soil<br>relief (m) | Residual mineral<br>soil relief after<br>thaw (m) |
|---------|------------------------|------------------------------------|---|
| S 100 * | 1.55                   | 1.95                               | + .40   |
| S 101   | 1.58                   | 1.93                               | + .35   |
| S 78    | 1.05                   | 1.52                               | + .47   |
| S 110   | 0.93                   | 1.49                               | + .56   |
| E 3     | 2.54                   | 2.76                               | + .23   |
| E 11    | 0.77                   | 1.42                               | + .65   |

Thaw settlements based on:  $E^0 = - .1036 \gamma_f + 182.7$

\* Thaw settlement directly measured in Permode



Further evidence of the hummocky mineral soil interface that underlies the palsa complex is the irregular mineral soil elevations measured in the collapse bogs and sinkholes (Table 10). Differences of up to 4 m exist between sites, but the average differential relief is approximately .5 to 1.0 meters.

Changes in the soil consolidation properties due to freezing will not significantly affect the above results. Local overconsolidation of the mineral soil can occur during freeze-thaw cycles due to negative pore pressures generated during freezing (Smith, 1972; Nixon and Morgenstern, 1973). Indeed, residual stress determinations (Table 2, Appendix 3) on the thawed permafrost core show significant residual stress in the massive silts, indicating local overconsolidation. Because of soil discontinuities due to lensing however, the bulk soil porosity of a soil after freezing and thawing often increases over the original (Tsytovich, 1976) especially under low effective stresses. These two processes, local ped overconsolidation and an overall bulk dilatancy due to lensing, work in opposite directions in determining the final thaw settlement; but the most characteristic phenomenon will be an increase in the bulk void ratio of the thawed soil (Tsytovich, 1976). Rates of settlement and pore pressures in the thawing soil will consequently be affected, however changes in the total thaw settlement due to these processes will be minimal.

In conclusion, the palsa complex has preferentially developed over an area with a slightly raised, irregular, mineral soil surface. This mineral soil relief contributes from 10 to 25 per cent of the observed height.



TABLE 10

THE ELEVATIONS OF THE MINERAL SOIL SURFACE BENEATH UNFROZEN BOGS AND  
SINKHOLES, RELATIVE TO THE FEN WATER LEVEL

| Site    | Bottom sediment | Elevation of<br>+bog surface | Depth to<br>mineral soil | Elevation of mineral<br>soil interface |
|---------|-----------------|------------------------------|--------------------------|--|
| S 110-0 | sand            | 2.39 m                       | .89 m                    | + 1.50 m                               |
| E 12    | clay            | .81                          | 2.74                     | - 2.30                                 |
| N 30    | silt            | .50                          | 2.89                     | - 2.39                                 |
| E 4     | clay            | 1.55                         | 4.17                     | -2.62                                  |
| E 0     | sand            | 0.00                         | 2.29                     | -2.29                                  |
| S 65    | clay            | 1.59                         | 3.96                     | -2.37                                  |
| S 134   | silt            | .39                          | 1.73                     | -1.34                                  |
| S 170   | sand            | 1.66                         | 3.05                     | -1.39                                  |
| S 181   | sand            | 2.02                         | 2.74                     | -0.72                                  |
| S 192   | silt            | 1.72                         | 3.35                     | -1.63                                  |





### 5.3 Ground Ice Degradation

Restricted to the discontinuous permafrost zone, a palsa is in a delicate thermal balance with its physical environment. A shift in this balance can produce ground ice degradation. Many degradational processes can be attributed to climatic change, but others are caused by changes in edaphic factors. This section examines ground ice degradational processes operating on the palsa complex, determines rates of permafrost degradation and attempts to determine the former extent of permafrost in the area.

#### 5.31 Processes and Controls

##### 5.311 Surface Processes

Surface cracking has been considered by some authors to be the most important degradational process (Ruuhijarvi, 1960; Svensson, 1962). The surface peat layer of the study palsa is very heavily cracked. Crack dimensions run up to 6 m in length, varying from a few millimeters to 80 cm in width. Cracking is most extreme on the palsa summits, on the steeper slopes, and particularly near the collapsing edges where there is a strong crack orientation parallel to the edges.

The cracks are the result of a number of possible causes:

1. surface rupture due to differential heaving during ground ice aggradation



Partial infilling of the cracks with semi-decomposed vegetation, in particular Ledum leaves, may partially offset their thermal influence. Only in heavy rainstorms does convective heat increase the depth of the crack relative to the active layer. This increase was always observed to disappear within a few days of cessation of the rain. There is no evidence to suggest that the present day active layer is increasing.

#### 5.312 Bottom Melting

Bottom melting of a palsa has been discussed in detail in Chapter One. It was shown that a mean annual surface temperature at the study site greater than  $-0.75^{\circ}\text{C}$ . would result in melting at the base of the permafrost at a rate of approximately 1 cm/year. This melting rate is entirely governed by the geothermal heat flux, but can vary depending on the local ice stratigraphy.

#### 5.313 Lateral Erosion

Lateral erosion of the palsa complex occurs mainly through thermal degradation of the palsa perimeter by ponded water. The process is facilitated by the high thermal conductivity of saturated peat as compared to the dry peat on the palsa summit as well as by the high convective heat capacity of water.

Where the palsa sides are in direct contact with water, the



permafrost core is undermined, creating a steep erosional edge. Undercutting of the peat bank is greatest at a depth of approximately 30 to 50 cm beneath the pond surface, corresponding to the thickness of the winter ice layer. The ice seasonally protects part of the palsa sides; below this layer the submerged permafrost is being continuously eroded. The result is a permafrost 'nose' near and just above the water table (Figure 4 ). Zoltai and Tarnocai (1971) have also noted such features but have considered them proof of ground ice aggradation instead of degradation.

Numerous surface cracks form parallel to the collapsing edge of the palsa. The cracking results in discrete peat blocks that slide along the permafrost surface when sufficient undercutting has occurred. Progressive widening of the cracks toward the collapsing edge indicates an accelerating creep rate towards the margin (Plate 2 ).

Lateral erosion may be accompanied by concurrent frost heave along the palsa perimeter. Most palsa complexes and peat plateaus have distinct but discontinuous marginal ridges, usually from .5 m to 1.0 m above the interior regions of the plateau. As ponded water is available along most of the collapsing perimeter, water may be migrating into the frozen soils along thermal gradients, producing 'secondary heave' in the palsa soils. Further evidence for, and discussion of, secondary heave is in Chapter Six.

The palsa complex also erodes laterally from interior sinkholes





2. thermal contraction of the surface layers, and
3. dessication cracking.

Cracks up to several meters in length, but only a few millimeters wide were observed, suggesting that cracking starts while the peat is frozen. Clearing of the snow from a palsa summit during the winter revealed that some of the thin cracks were infilled with ice. Thermal gradients due to cold penetration in the cracks may induce moisture migration towards the crack from the adjacent peat. Crack enlargement due to subsequent ice wedging is considered a minor process however, and limited to the narrowest cracks.

Dessication cracking may be a relatively more important process on the steeper sloping palsa sides. Rainfall and snowmelt quickly run off the steep slopes with little water infiltration, producing a locally dessicated environment. The only vegetation growing on the slopes is Ledum, which grows within the wider cracks, presumably due to the higher moisture availability.

Overall, surface melting is not considered to be a major degradational process at the study site. Dry Sphagnum peat has a thermal conductivity as low as  $.05 \text{ Cal/m-hr.}^{\circ}\text{C}$  (Jumikis, 1977), providing excellent insulation from surface warming. Surface cracks, while extensive, do not have a strong effect on the overall surface insulation. The average depth to permafrost beneath the cracks does not exceed the average active layer depth on other parts of the palsa.





and collapse bogs. The mechanism of erosion is similar to erosion along the outside perimeter, but involves much slower degradation of the ground ice without a significant collapsing edge. The bogs are filled with Sphagnum, greatly reducing rates of water filtration and hence heat transfer. Further, the near surface summer water temperatures in the bog areas average only  $1.5^{\circ}$  C. compared to 5 to  $7^{\circ}$  C. in the surrounding fens; the lower temperatures being due to a combination of the high evapotranspiration, high albedo, and low thermal conductivity of the Sphagnum moss.

Of the three degradational processes, lateral erosion is by far the most effective. This is borne out by the extraordinary rates of lateral melting that have occurred over the past 30 years, as is discussed in the following sections.

### 5.32 Former Extent of Permafrost

The former extent of permafrost near the study site can be inferred from the present day distribution of peatland types. As previously discussed (Chapter 1), the peatland type described as "open sedge fen with abundant non-oriented ponds" preferentially occurs in areas known to have been formerly permafrozen. Cores taken from this peatland type should therefore stratigraphically indicate the former presence of a thick Sphagnum layer and possibly a Black Spruce forest cover. These characteristics were indeed found in a core obtained from a sedge fen 1.2 km north of the palsa complex.



Chemical analysis was used to detect the Sphagnum because the plants were too decomposed to identify macroscopically. Major cation differences occur in the vegetation from each peatland type because of their distinctive aquatic nutrient regimes (Stanek et al, 1977). While decomposition processes will modify the peat chemistry, changing particularly the carbon and nitrogen contents, cation differences are still evident, hence providing a stratigraphic tool for peat differentiation.

Results from the chemical analysis are presented in Table 11. Samples from modern peat-forming plants indicate that Ca is the most sensitive indicator for distinguishing peat types. Sphagnum mosses and forest peat typically have Ca contents of 2 to 6 mg/gm while fens average 10 to 22 mg/gm. The chemical differences are maintained in spite of moderate decomposition; proof of which is seen in the results from the analysis of the frozen palsa core. The peat in this core is identifiable macroscopically; the stratigraphy of which correlates well with Ca differences between the ombrotrophic and minerotrophic peats (Table 11). The peat core from the fenland shows a shift from a high Ca surface peat to a low Ca peat at a depth of 40 to 70 cm, then a very high Ca lower peat. This is interpreted as a basal fen peat, a middle Sphagnum peat followed by a return to minerotrophic fen conditions. A significant period of ombrotrophic conditions once existed at this site.

The presence of Black Spruce fragments in the peat also suggests



TABLE 11

## CHEMICAL ANALYSIS OF PEAT AND PEAT-FORMING VEGETATION

(Values are in mg/gm of dry peat)

| Sample type                                    | Sample number | Depth (cm) | Na <sup>+</sup> | Mg <sup>+</sup> | Ca <sup>+2</sup> | K <sup>+</sup> | Ca <sup>+2</sup> / Mg <sup>+2</sup> |
|--|---------------|------------|-----------------|-----------------|------------------|----------------|-------------------------------------|
| Present Day:                                   |               |            |                 |                 |                  |                |                                     |
| Dry fen  | 104           |            | .28             | 1.12            | 9.82             | .37            | 8.78                                |
| Sedge fen                                      | 102           |            | .70             | 2.90            | 21.07            | .11            | 7.27                                |
| Duckweed<br>(thaw ponds)                       | 100           |            | 1.51            | .92             | 6.27             | 2.50           | 6.82                                |
| Sphagnum bog                                   | 105           |            | .52             | .70             | 4.02             | .11            | 6.70                                |
| Sphagnum bog                                   | 106           |            | .17             | .79             | 3.34             | .13            | 4.12                                |
| Fen core<br>(from formerly<br>frozen peatland) |               |            |                 |                 |                  |                |                                     |
|  | 16-1          | 0          | .43             | 1.94            | 11.12            | .89            | 5.73                                |
|  | 16-2          | 15         | .40             | 1.71            | 10.59            | .60            | 6.19                                |
|  | 16-3          | 40         | .18             | .75             | 5.91             | .05            | 7.88                                |
|  | 16-4          | 55         | .19             | .72             | 6.67             | .04            | 9.26                                |
|  | 16-5          | 70         | .20             | .64             | 7.46             | .04            | 11.66                               |
|  | 16-6          | 85         | .28             | 2.11            | 16.68            | .05            | 7.91                                |
|  | 16-7          | 100        | .42             | 2.91            | 21.90            | .06            | 7.53                                |
|  | 16-8          | 120        | 1.53            | 2.75            | 19.22            | .56            | 6.99                                |
|  | 16-9          | 145        | .65             | 3.00            | 18.26            | .07            | 6.09                                |
| Palsa Core:                                    |               |            |                 |                 |                  |                |                                     |
| Forest peat                                    | 78-1          | 2          | .13             | .45             | 2.68             | .31            | 5.96                                |
| Sphagnum                                       | 78-2          | 12         | .02             | .62             | 4.02             | .10            | 6.48                                |
| Sphagnum                                       | 78-3          | 33         | .17             | .79             | 3.22             | .13            | 4.08                                |
| Woody sedge fen                                | 78-4          | 94         | .07             | 1.55            | 6.70             | .06            | 4.32                                |
| Sedge fen                                      | 78-5          | 100        | .13             | .90             | 10.71            | .07            | 11.68                               |
| Sedge fen                                      | 78-6          | 225        | .07             | 1.29            | 16.08            | .06            | 12.47                               |
| Aquatic  | 78-7          | 345        | .13             | 1.29            | 10.05            | .10            | 8.14                                |

Na<sup>+</sup> and K<sup>+</sup> analysis by flame emission spectroscopyCa<sup>+2</sup> and Mg<sup>+2</sup> analysis by atomic absorption spectroscopy





a previously frozen peatland, as modern spruce are nearly always confined to permafrozen areas in the peatland. Abundant pieces of wood charcoal, less than 2 mm in size, were observed along a horizon at a depth of 43 cm in the peat core. This horizon is near the top of the Sphagnum zone as defined by chemical analysis, suggesting that a former Black Spruce forest may have been the source. D. Rennie (personal communication) has also found identifiable pieces of Black Spruce in a number of cores taken from the fen in this vicinity.

The former presence of Sphagnum and Black Spruce communities in the "disoriented pond-sedge fen" peatland supports the hypothesis that this peatland type is an indicator of previously permafrozen terrain. As such, the study site was once part of a large permafrost body covering approximately 600 hectares. The present day palsa and peat plateau are erosional remnants of the once more extensive landform. Permafrost is not thought, however, to have been continuous. Most of the mineratrophic fens near the large lakes in the middle of the lake basin, to the north of the study site, do not display the characteristic peatland type of previously frozen areas.





### 5.33 Rates of Ground Ice Degradation

Rates of permafrost degradation can be measured by comparing recent and older aerial photography. This approach has been used by Thie (1974) in northern Manitoba, and by Reid (1977) in northern Alberta. Aerial photography for the study site was available from 1948 (1:40,000 RCAF) and 1976 (1:25,000, Burnett Resources). Both the linear rate of retreat of the palsa complex margin and the rate of areal degradation were measured.

To measure changes in the areal extent of the permafrost, individual peat plateaus were traced onto 'Mylar' film, carefully cut out with a dissecting scalpel, then weighed to an accuracy of  $1 \times 10^{-4}$  gm. Mylar film has extremely consistent density and thickness, permitting conversion from weight to area. Palsas and peat plateaus greater than 200 m in diameter have degraded by 15 to 20% over the last 28 years. Medium sized plateaus with a 1948 diameter of 50 to 150 meters experienced considerably faster decay, losing an average of 44% of their 1948 area. Most permafrost islands having a diameter of less than 50 m in 1948 were no longer discernible in 1976 photography.

Rates of margin retreat were measured relative to a line perpendicular to the 1976 palsa edge. A magnifying stereoscope, containing a built in scale with gradations of 0.1 mm, was used for taking measurements. The rate of edge retreat varied considerably around the palsa: from 8 to 38 meters for palsas in excess of 200 meters; from 21 to 43 meters for palsas of 50 to 150 meter diameter. No



particular aspect showed preferential melting. The size of thermo-karst holes and collapse bogs in the middle of the palsa complex was relatively unchanged from 1948 to 1976. These rates of edge collapse are approximately 50% less than that measured by Reid (1977) near Zama Lake, Alberta and are approximately the same as that reported by Thie (1974) in northern Manitoba.

On the basis of the former extent of the permafrost, it appears that rates of degradation have been greater than aggradation for a considerable number of years. If the former size of the palsa complex has degraded at present day melting rates, then all the degradation may have occurred in the past 250 years.

#### 5.4 The Effect on Palsa Relief

Palsas have been traditionally viewed as ground ice aggradational features; their height measured, using the surrounding fen as the local base level. The relief is considered a result of segregational ice development in the mineral soil. As segregated ice lenses are rarely observed in frozen peat, the peat thickness in the unfrozen fen



and on the frozen palsa are assumed identical, hence contribute little to the palsa relief.

This section presents evidence that contradicts this aggradational theory of palsa development. The relative roles that degradational and aggradational processes play in the resultant relief of the palsa complex is examined.

Various lines of evidence have shown that the area surrounding the study site has recently thawed. A nearly continuous band of frozen peatland may have once existed along the margins of the former glacial lake, as late as 400 years Before Present. With recent climatic warming, ground ice degradation has occurred at an extremely rapid rate; the modern palsa complex is a remnant of the former permafrost landform. The surrounding unfrozen peatland is composed of both the thaw consolidated peat and the thaw consolidated mineral soil.

Thaw consolidation tests, as detailed above, recorded an average settlement of 1.3 meters in the mineral soil of the palsas following thaw. This settlement accounts for less than fifty percent of the average 3.0 meter palsa height above the fen. As there is no evidence for wildly fluctuating fen levels, this conclusion clearly shows that segregational ice in the mineral soil is not solely responsible for palsa relief.

To determine what was responsible for the remaining height, thaw





consolidation tests were made on the frozen peat portion of cores S 100 and E 3. The consolidation methods were identical to that used on the frozen mineral soil. A total of 18 samples were tested; the results are listed in Appendix 3. Empirical relationships between the thaw settlement and physical parameters such as moisture content and bulk density were not as precise as those for the mineral soils (Figures 28 to 29); however, the simple relationship of total strain equal to the volumetric ice content of the frozen peat had a significantly high correlation (Figure 29). This relationship predicted the total settlement of the thawed peat cores to within 6.0 % of that measured (Table 12).

Application of the thaw settlement equation:  $E^0 = V + 4.5$ , to the five other frozen peat cores shows that the total thaw settlement of the peat is slightly greater than the thaw settlement of the mineral soils (Table 13). Further, it is interesting to note that the moisture contents of the frozen peat are approximately equal to the unfrozen peat in nearby bogs (Appendix 3 ); a finding consistent with other researchers results (Zoltai and Tarnocai, 1975; Reid et al, 1977). As there is no excess water, the main component of the thaw consolidation equation (see Section 5.213) is that due to the normal consolidation of the peat as it settles under its own weight. The large amount of observed settlement is due to the fact that the peat must have frozen while still in the unconsolidated state. When melting finally occurs, the peat has been uplifted above the fen surface, hence is free to drain and consolidate. A combination of the thaw of





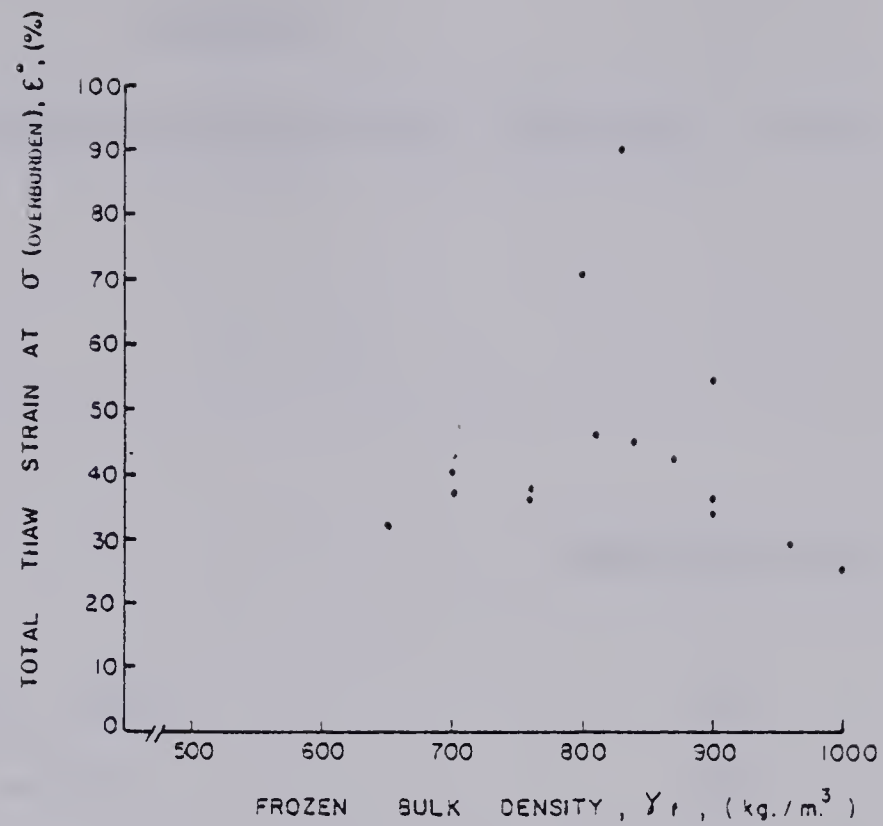


FIGURE 28 : TOTAL THAW STRAIN — FROZEN BULK DENSITY RELATIONSHIP FOR ORGANIC SOILS.

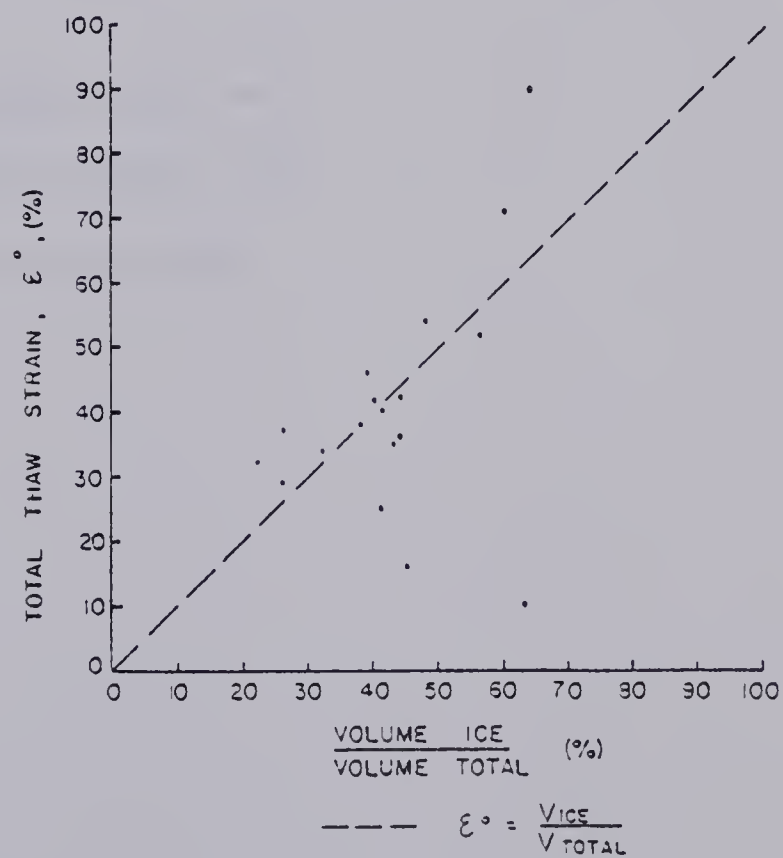


FIGURE 29: TOTAL THAW STRAIN — VOLUMETRIC ICE CONTENT RELATIONSHIP FOR ORGANIC SOILS.



TABLE 12

## EMPIRICAL RELATIONSHIPS PREDICTING THAW SETTLEMENT IN PEAT

CORRELATION (r)

|    |  |     |
|----|--|-----|
| 1. | $E^{\circ} = - .0162 \gamma_f + 56.93$ | .02 |
| 2. | $E^{\circ} = 97 - 7.97 \ln \gamma_f$   | .05 |
| 3. | $E^{\circ} = 1.09 w_v + 4.36$          | .81 |
|    | OR                                     |     |
|    | $E^{\circ} = V + 4.36$                 | .81 |

---

$\gamma_f$  = frozen bulk density (Kg/ m<sup>3</sup>)

$w_v$  = volumetric water content (%)

$V$  = volumetric ice content (%)



TABLE 13  
THAW SETTLEMENT OF THE FROZEN PEAT CORES,  
AND COMPARISON WITH MINERAL SOIL SETTLEMENT

| Core  | Frozen peat<br>thickness (m) | Peat thaw<br>settlement (m) | Mineral soil thaw<br>settlement (m) |
|-------|------------------------------|-----------------------------|-------------------------------------|
| S 100 | 3.35                         | 1.79                        | 1.55                                |
| S 101 | 3.37                         | 1.89                        | 1.58                                |
| S 78  | 3.26                         | 2.46                        | 1.05                                |
| S 110 | 3.10                         | 2.51                        | .93                                 |
| E 3   | 3.20                         | 1.71                        | 2.54                                |
| E 11  | 4.30                         | 2.74                        | .77                                 |

Thaw settlements of the peat based on:  $E^0 = V + 4.5$

\* Measured in Permode



segregated ice lenses in the mineral soil plus the normal consolidation of the peat, is approximately equal to the amount that the land surface, now covered by the fen, has dropped below the former permafrost surface. The permafrost that remains forms the palsa complex.





## CHAPTER 6: CONCLUDING REMARKS



## 6.1 Regional Permafrost Development in the Fort Simpson Peatlands

Permafrost distribution in the Fort Simpson area is very discontinuous. It is found sporadically, to various depths, in treed till uplands; however, the largest areal extent is within the large glacial lacustrine basins. Any conceptual model of permafrost development in this area must include the following facts:

1. The most extensive zones of segregated ground ice accumulation in the Fort Simpson area, occur parallel to the margins of the former glacial lakes (Chapter 2).
2. These areas are underlain by a hummocky, stratified mineral soil, slightly elevated above the surrounding lacustrine plain (Chapter 5).
3. Permafrost has developed relatively recently, approximately 2000 years Before Present (Chapter 4).
4. This late development was in spite of relatively cold temperatures throughout the Holocene (Chapter 3).
5. There is evidence for only one period of regional permafrost formation; it does not appear to have been forming over the past few hundred years (Chapter 5).
6. Permafrost development was always preceded by an accumulation of Sphagnum moss; however, as much as 1000 years of Sphagnum could accumulate before permafrost formed (Chapter 4).
7. There is evidence for a period of aridity sometime during the Holocene (Chapter 2).



While somewhat conjectural, the following scenario best fits the findings of this thesis. During the waning stages of Glacial Lake McConnell, lake levels fluctuated greatly, creating extensive hummocky beach deposits and interfingered sandy and silty pro-lacustrine sediments along its margins. When the lake finally drained, an extensive fenland developed over the lacustrine basin. With the progressive development of an integrated drainage system, fen water levels slowly dropped. Local water table divides developed over the more elevated parts of the lake basin, especially near the beach ridges. The water divides soon became ombrotrophic, leading to the subsequent development of extensive Sphagnum bogs.

Permafrost does not develop in saturated Sphagnum; it is only dry Sphagnum that has the unique insulative properties that maintain cold soil temperatures. A period of aridity approximately 2000 years B.P. may have caused sufficient drying of the Sphagnum to initiate permafrost growth; alternatively water levels could have continued to drop, eventually exposing the pro-lacustrine zone. The temperature does not appear to have been a factor, remaining relatively cold throughout the Holocene. Eventually extensive permafrost development occurred over the bogs. Evidence suggests that permafrost covered an area of at least 600 hectares around the study site. Permafrost was not continuous however, as there is evidence that the deeper parts of the lacustrine basin have never been permafrozen.

While permafrost in the till uplands may be as deep as in the



palsa complex, by comparison there is very little segregated ground ice. The unique stratigraphy of the pro-lacustrine environment, with interfingering layers of sand and silt, provides an adequate supply of moisture to the freezing front, ensuring the growth of large ice lenses. Chemical and isotopic analysis of the ground ice has shown that mineral soil groundwater, not the ponded fens, is the water source for ice lens development, hence demonstrating the importance of groundwater flow in the sand lenses.

The ground ice stratigraphy has also been influenced by the evolution of the peatland. A characteristic feature of nearly all cores is a large ice lens, up to 1.0 m thick at the peat-mineral soil interface. This thick lens may be partially the result of high concentrations of  $\text{CaSO}_4$  at the top of the mineral soil, which was probably deposited during a prior dessication period (Chapter 2). It is well known that solutes will depress the freezing point of a liquid, the magnitude of which is proportional to the solute concentration (Hallet, 1978). Experiments by R.D. Miller (personal communication, 1978) have shown that while  $\text{CaSO}_4$  concentrations of 100% by dry weight are very effective in reducing frost heave, concentrations of 50% by dry weight have virtually no effect on water intake rate. The net effect of the solute then is to stall the advance of the freezing front by depressing the freezing point but without reducing the suction potential. High suction potentials are ensured by the very decomposed gyttja, with a large internal surface area, found immediately above the mineral soil. The combined effect produced the very thick ice lens at the interface.







In summary, the location of permafrost development, its ice content, and ice stratigraphy, have all been influenced by prior geologic, climatic, and hydrologic events within the glacial lacustrine basins of the Fort Simpson area. The pro-lacustrine zone is particularly suitable for segregated ground ice development.

## 6.2 The Palsa Complex: A Relic Thermo-erosional Landform

Historical air photo evidence has proven that rapid areal permafrost degradation is occurring around the study site. Stratigraphic chemical results indicate that large areas of the fenland presently surrounding the modern palsa complex were once permafrozen. The evidence is strong therefore that the present palsa complex - fenland environment is the degrading remnant of a once extensive permafrost landscape.

Previous experimental results and discussion have demonstrated that segregated ice development in the mineral soil does not account for the total palsa relief (Chapter 5). Segregated ice development in the mineral soil is therefore not the sole cause of palsa development. Rather, the thaw consolidation of the frozen peat accounts for a major part of the observed height of a frozen palsa complex above the surrounding unfrozen fen. Significantly, the main component of the thaw consolidation of the peat is that due to normal consolidation. The peat had frozen in a buoyant, unconsolidated state but has thawed while uplifted, hence consolidating under its own saturated weight (Chapter 5).



Numerous cores from the fen reveal an average peat thickness of 1.5 m, considerably less than that of the frozen peat. While some of this difference can be ascribed to decomposition, consolidation is indicated by the ubiquitous presence of small ponds and lakes over the thawed zone (Plate 1). Such a concentration of ponds is not found elsewhere in the peatlands. Svensson (1969) has also remarked that circular lakes often mark sites of former palsas in Northern Norway. The observation of a water moat around thawing palsas has also been made in numerous case studies (Lundqvist, 1959; Salmi, 1970; Svensson, 1969). With aggradational theories of palsa development, the water moats have been ascribed to depressions of the mineral soil by the increasing weight of the growing palsa (Svensson, 1969). By perceiving palsas as degrading landforms, the moats are recognized as features created by consolidation of the thawing peat.

A persistent theory in palsa development is the notion of cyclical aggradation and degradation of palsas. There is no evidence, in the Fort Simpson area, for more than the present occurrence of palsas. As discussed above, ground ice development is the net result of the unique evolution of the peatland. Permafrost appears to have developed during a single interval approximately 2000 - 3000 years B.P., when there was the right combination of climate, hydrology and vegetation. Over the past few hundred years it has been continually degrading. The present occurrence of the palsa complex is due only to the insulative properties of the peat cover. Recognition of this will necessitate a change in the classification of palsas. The terms 'young', 'mature', and 'overmature' (Zoltai and Tarnocai, 1975) are



not applicable to this situation.

It is recognized that some palsas are in fact probably aggradational. This would certainly appear to be the case for small frozen mounds found in the middle of Sphagnum bogs or for the 'esker palsas' (Jahn, 1975) found along streams in Northern Europe. Certainly, two types of classification are needed. On an areal basis however, the degradational type of palsa is, in the author's opinion, the most prevalent.

In summary, palsa complexes in the study area are erosional remnants of a once much larger, thermally degraded, permafrost landform. The observed relief is due to thaw consolidation of both the mineral soil and the peat. There is no evidence for cyclical aggradation and degradation.

### 6.3 Open System Moisture Migration in Permafrost

Various lines of evidence presented in this thesis indicate that long term moisture migration through the frozen palsa soils may have occurred. This flux has taken place in spite of a relatively stable frost front over the past few hundred years. First, tritium values in the frozen soils are similar to those in the sub-permafrost groundwater; their anomalously high values indicate mixing of modern water with the older permafrost. Oxygen isotope values in the permafrost are best accounted for by a conceptual model of regelation melting with upward moisture transfer into the frozen soils. Segregated ice





lenses are concentrated in the upper part of the frozen mineral soil with massive zones of reticulate vein ice in the lower core; the opposite of what is normally expected in aggrading permafrost (Mackay, 1974), but consistent with a model of post-freezing, upward moisture flux. A single large ice lens is usually found immediately above the thawed zone in the ice cores, suggesting a continuing moisture supply. Finally, the morphology of the palsa complex, with definite marginal ridges elevated up to a meter above the rest of the palsa, attests to the sustaining water flux from the adjacent ponded fen.

Recently, laboratory tests have proven that water migration occurs in frozen soils due to temperature induced potential gradients (Hoekstra, 1966; Dirksen and Miller, 1966; Ershov et al, 1976; and Mageau, 1978). In a series of theoretical papers Miller (1972, 1978) has advanced a strong conceptual argument that ice regelation is the limiting process in determining rates of water flux through frozen soils containing segregated ice.

The palsa complex environment is precisely the conditions under which thermo-migration of water will most likely occur. The soils are a silty clay with potential unfrozen water contents of approximately 30%; the ground temperatures are around  $-1^{\circ}\text{C}$ ., a nearly optimum temperature for unfrozen water mobility (Hoekstra, 1966). The permafrost is sufficiently shallow that it is effected by seasonal temperature changes and there is abundant water surrounding the permafrost body.





A semi-quantitative analysis can be made to determine whether rates of thermally induced water movement are significant over geologic time. Ice movement by the regelation process constitutes a virtual transport of sensible heat in the direction opposite to the direction of ice movement (Miller, Loch and Bresler, 1975). The governing equilibrium mass and heat transfer equation can be written (Miller, 1978):

$$-K_u \frac{dT}{dz} = -K_f \frac{dT}{dz} - e_i L v_i \quad (1)$$

where  $K_u$  = unfrozen soil conductivity

$K_f$  = frozen soil conductivity

$e_i$  = ice density

$\frac{dT}{dz}$  = thermal gradient in frozen soil

$L$  = latent heat of fusion

$v_i$  = volumetric ice flux

solving for the volumetric ice flux:

$$v_i = \frac{K_u \frac{dT}{dz} - K_f \frac{dT}{dz}}{e_i L} \quad (2)$$

parameters from the palsa soils are:

$$K_u = 1.2 \text{ Cal/m-hr } ^\circ\text{C}$$

$$K_f = 1.7 \text{ Cal/m-hr } ^\circ\text{C}$$

$$\frac{dT}{dz} = .05 \text{ } ^\circ\text{C/m}$$

$$e_i = 910 \text{ kgm/m}^3$$

Substituting these values into (2) yields a volumetric ice flux of approximately  $1 \times 10^{-8}$  cm/sec or  $0.3 \text{ cm}^3/\text{year-cm}^2$ , a rate comparable



to that experimentally measured by Mageau (1978). Within the 1500 year age of the palsa, this represents a total flux of  $450 \text{ cm}^3 / \text{cm}^2$ . As there is an average thickness of 1.5 meters of segregated ice in the palsa, steady state processes could theoretically result in a redistribution of 30% of the mineral soil ground ice.

Many permafrost bodies date from at least the last glaciation. Ground ice in the arctic regions of Canada that escaped glaciation is considerably older. If the steady state regelation rates calculated above are representative values, then much of the natural ground ice must be viewed as a dynamic body subject to continuing mass transfer.



## 6.4 Further Research

In North America, the study of permafrost in discontinuously frozen peatlands has not received the same attention as the more spectacular arctic periglacial features. Many topics remain which require further research. The study described in this thesis involved several different field and laboratory programs, most of which need further refinement or verification.

Refinement in the use of isotopes from peat as paleoclimatic indicators is perhaps the most potentially rewarding avenue of research. Acquisition of site-specific temperature records would be invaluable in deciphering the history of permafrost development. The ubiquity of peat in the sub-arctic would allow regional correlations. If detailed records were obtainable, the potential for mathematically modeling peat development exists. Those topics needing most urgent work, are:

1. an understanding of the plant physiology. Changes in the isotopic content of Sphagnum needs to be determined after growth in a controlled environment.
2. Further correlation of modern Sphagnum isotopes with respective mean and seasonal growth temperatures.
3. Further investigation into the role of microbial decomposition on oxygen isotopes; possibly through the use of nitrogen isotopes.

There seems little further need for immediate work on regional peatland development. Consistent patterns seem to exist throughout temperate and sub-arctic North America. More productive research would



be to analyze and date a series of closely spaced cores across a fen-palsa sequence, trying to determine local plant successions and the role of vegetative and edaphic factors in permafrost development.

Both the theory and testing of thaw consolidation techniques are well established and require little further laboratory work. The techniques should be used to further test the hypothesis that peat consolidation plays a major role in palsa development. Field tests would be particularly useful, though would require considerable imagination to implement.

The upward migration of water through frozen soils is an intriguing problem. While of academic interest for its role in redistribution of ice in permafrost, the subject also has considerable practical importance. The long term stability of cold-temperature pipelines could be affected by post-freezing frost heave. While the phenomenon has been monitored in the laboratory, palsa investigations could verify its long term occurrence and behavior. Isotopic techniques may be particularly useful in this regard.





## BIBLIOGRAPHY



## BIBLIOGRAPHY

- Allen, C.R., O'Brien, R.M.G. and Sheppard, S.M.F. 1976. The chemical and isotopic characteristics of some northeast Greenland surface and pingo waters. *Arctic and Alpine Research*, vol. 8, No. 3, pp. 297-317.
- Anderson, D.M. and Morgenstern, N.R. 1973. Physics, chemistry and mechanics of frozen ground: a review. *In Permafrost: The North American contribution to the 2nd International Conference, Yakutsk, N.A.S.*, pp. 257-288.
- Arnason, B. 1969. Equilibrium constant for the fractionation of Deuterium between ice and water. *J. of Physical Chemistry*, Vol. 73, No. 10, pp. 3491-3494.
- Arnason, B. 1970. Exchange of Deuterium between ice and water in glaciological studies in Iceland. *Isotope Hydrology 1970*. Int. Atomic Energy Agency, pp. 59-71.
- Arvidson, W.D. and Morgenstern, N.R. 1977. Water flow induced by soil freezing. *Can. Geotech. Journal*, Vol. 14, p. 237.
- Barrow, N.J. 1960. A comparison of the mineralization of Nitrogen and Sulphur from decomposing organic materials. *Australian Journal of Agricultural Research*, vol. 11, pp. 960-969.
- Barrow, N.J. 1961. Studies on mineralization of Sulphur from soil organic matter. *Australian Journal of Agricultural Research*, vol. 12, pp. 306-330.
- Biegeleisen, J., Perlman, M.L., and H.C. Prosser. 1952. Conversion of hydrogenic materials to hydrogen for isotopic analysis. *Anal. Chemistry*, vol. 24, pp. 1356-1357.
- Black, R.F. 1969. Thaw depressions and thaw lakes - a review. *Biul. Peryglac.*, No. 19, pp. 131-150.
- Brown, J. 1963. Ice-wedge chemistry and related frozen ground processes, Barrow, Alaska. *Proc. 1st Int. Conf. on Permafrost, Purdue*, pp. 94-97.
- Brown, R.J.E. 1963. Relation between mean annual air and ground temperatures in the permafrost region of Canada. *Proc. 1st Int. Conf. on Permafrost, Building Research Advisory Board, National Research Council*, pp. 241-246.
- Brown, R.J.E. 1965. Some observations on the influence of climatic and terrain features on permafrost at Norman Wells, N.W.T., Canada. *Can. J. Earth Sci.*, vol. 2, pp. 15-30.



- Brown, R.J.E. 1966. Influence of vegetation on permafrost. Nat'l. Acad. of Sci., Nat. Res. Council, Pub. 1287, pp. 20-25.
- Brown, R.J.E. 1968. Permafrost in Canada. Geol. Survey of Canada, Map 1246 A.
- Brown, R.J.E. 1970. Occurrence of permafrost in Canadian peatlands. Proc. 3rd Int. Peat Congress, Quebec, pp. 174-181.
- Brown, R.J.E. 1970. Permafrost in Canada. Univ. of Toronto Press, Toronto, 234 p.
- Brown, R.M. 1970. Distribution of hydrogen isotopes in Canadian waters. Isotope Hydrology 1970. International Atomic Energy Agency, Vienna, Austria, pp. 3-21.
- Bryson, R.A., Irving, W.N. and Larson, J.A. 1965. Radiocarbon and soil evidence of former forest in the southern Canadian tundra. Science, vol. 147, pp. 46-48.
- Burns, B.M. 1973. The climate of the Mackenzie Valley - Beaufort Sea, Canada. Dept. of the Environment, Atmospheric Envir. Service, Climatological studies, No. 24, 230 p.
- Burns, B.M. 1974. The climate of the Mackenzie Valley - Beaufort Sea, Canada. Dept. of Environment, Atmospheric Envir. Service, Climatological studies, No. 24, 240 p.
- Burt, T.P. and Williams, P.J. 1976. Hydraulic conductivity in frozen soils. Earth Surface Processes, vol. 1, pp. 349-360.
- Cajuander, A.K. 1913. Studien uber die Moore Finnlands. Acta for fenn., vol. 2, pp. 1-208.
- Colinvaux, P.A. 1967. Quaternary vegetation history of arctic Alaska. In The Bering Land Bridge. D.M. Hopkins (Ed.), Stanford U. Press, Stanford, CA.
- Craig, B.G. 1965. Glacial Lake McConnell and the surficial geology of parts of Slave River and Redstone River map areas, District of Mackenzie. Geol. Survey of Canada, Bull. 122, 33 p.
- Craig, H. 1961. Isotopic variations in meteoric waters. Science, vol. 133, pp. 1702-1703.
- Croon, I. and Andrews, D.H. 1971. Advances in oxygen bleaching. Tappi, vol. 54, No. 11, pp. 1893-1906.
- Dansgaard, W. 1964. Stable Isotopes in precipitation. Tellus, vol. 16, pp. 436-468.
- Delorme, L.D., Zoltai, S.C. and Kalas, L.L. 1977. Freshwater shelled invertebrate indicators of paleoclimate in northwestern Canada





- during late glacial times. Can. J. Earth Sci., vol. 14.
- Environment Canada, Atmospheric Environment Service. 1973. Canadian Normals, 1941-1970, Temperatures.
- Epstein, S. 1959. Variations of the  $O^{18}/O^{16}$  ratios of fresh waters and natural ice. Nat'l. Acad. Sci., Nucl. Sci. Ser., Report No. 19, pp. 20-25.
- Epstein, S. and Mayeda, T. 1953. Variations of the  $O^{18}$  content of waters from natural sources. Geochim. Cosmochim. Acta 4, pp. 213-224.
- Epstein, S., Thompson, P., and Yapp, C.J. 1977. Oxygen and hydrogen isotopic ratios in plant cellulose. Science, vol. 198, No. 4323, pp. 1209-1215.
- Epstein, S. and Yapp, C.J. 1976. Climatic implications of the D/H ratio of hydrogen in C-H groups in tree cellulose. Earth Planet. Sci. Lett., vol. 30, pp. 252-266.
- Epstein, S., Yapp, C.J. and Hall, J.H. 1976. The determination of the D/H ratio of non-exchangeable hydrogen in cellulose extracted from aquatic and land plants. Earth Planet. Sci. Lett., vol. 30, pp. 241-250.
- Ershov, E., Cheverev, V. and Lebedenko, Y. 1976. Experimental study of moisture migration and ice release in the frozen zone of thawing soils. Vestnik, Geol. Moscow Univ., vol. 37, No. 1, pp. 111-114.
- Forsgren, B. 1966. Tritium determinations in the study of palsa formation. Geogr. Annlr. vol. 46, pp. 343-344.
- Forsgren, B. 1968. Studies of palsas in Finland, Norway, and Sweden - 1964-1966. Biul. Peryglac., vol. 17, pp. 117-123.
- Freidman, I., Redfield, A.C., B. Schoer and Harris, J. 1964. The variations of the Deuterium content of natural waters in the hydrologic cycle. Reviews of Geophysics, vol. 2, No. 1.
- Gat, J. R. 1971. Comments on the stable isotope method in regional groundwater investigations. Water Resources Res., vol. 7, No. 4, pp. 980-993.
- Gell, A. 1976. Underground ice in permafrost, Mackenzie Delta - Tuktoyaktuk Peninsula, N.W.T. Ph.D. thesis (unpub.), U. of British Columbia, 258 pp.
- Gray, J. and Thompson, P. 1976. Climatic information from  $O^{18}/O^{16}$  ratios of cellulose in tree rings. Nature, vol. 262, No. 5568, pp. 481-482.





- Hage, K.D. and Gray, J. 1975. Isotopes in precipitation in North-western North America. *Monthly Weather Review*, vol. 103, pp. 958-966.
- Hallet, B. 1978. Solute redistribution in freezing ground. *Proc. 3rd Int. Permafrost Conf.*, Edmonton, pp. 85-92.
- Harlan, R.L. 1971. Water transport in frozen and partially frozen porous media. *Proceedings Nat'l. Res. Council Symposium on Hydrology*, May 1971.
- Heinselman, M.L. 1963. Forest sites, bog processes, and peatland types in the glacial Lake Agassiz region, Minnesota. *Ecol. Monographs*, vol. 33, pp. 327-374.
- Heinselman, M.L. 1970. Landscape evolution, peatland types, and the environment in the Lake Agassiz peatlands natural area, Minn. *Ecol. Monographs*, vol. 40/z, pp. 235-61.
- Heusser, C.J. 1960. Late Pleistocene environments of North Pacific North America. *Amer. Geog. Soc., Spec. Publ.* 35.
- Hill, D.W. The influence of temperature and load on moisture transfer in freezing soil. M.Sc. thesis (unpubl.) Dept. Civil Eng., U. of Alberta, Edmonton.
- Hoekstra, P. 1966. Moisture movement in soils under temperature gradients with the cold-side temperature below freezing. *Water Resources Res.*, vol. 2, pp. 241-250.
- Hughes, O.L. 1974. Geology and permafrost in relation to hydrology and geophysics. *In Permafrost Hydrology, Proceedings of a Workshop Seminar, Can. Nat. Comm. Int. Hydrological Decade, Environment Canada*, pp. 21-28.
- Iversen, J. 1953. Origin of the flora of Western Greenland in light of pollen analysis. *Oikos*, vol. 4, pp. 85-103.
- Yahn, A. 1975. Problems of the peri-glacial zone. (Translation from Polish) U.S. Dept. Commerce, National Technical Information service, Springfield, Va. TT72-54011, 223 p.
- Jeglum, J.K. 1973. Boreal Forest Wetlands near Candle Lake, Central Saskatchewan. *The Musk-Ox*, No. 11, pp. 41-58.
- Judge, A.S. 1974. The thermal regime of the Mackenzie Valley: Observations of natural state. *Environmental - Social Committee on Northern Pipelines, Task Force on Northern Oil Development*, Report 73-38, 177 p.
- Jumikis, A. 1977. *Thermal Geotechnics*. Rutgers University Press, New Jersey, 372 p.



- Kershaw, K.A. 1969. Quantitative and Dynamic Ecology. William Clowes and Sons, Ltd., London, 183 p.
- Kulczynski, S. 1949. Torfowiska Polesia (Peat bogs of Polesie) Mem. L'Adad. Pol. Sci. Lett., Cl. Sci., Math., Natur., Ser. B, No. 15, 356 p. (in English)
- Lerbekmo, J.F. and Campbell, F.A. 1969. Distribution, composition, and source of the White River Ash, Yukon Territory. Can. J. of Earth Science, vol. 6, pp. 109-116.
- Libby, L.M., and Pandolfi, L.S. 1974. Temperature dependence of isotope ratios in tree rings. Proc. Nat'l. Acad. Sci., U.S.A., vol. 71, p. 2482.
- Linnel, K.A. and Kapler, G.W. 1959. The factor of soil and material type in frost action. Highway Res. Bd., HRB Bull. 225, NAS/NRC Washington, D.C. pp. 81-126.
- Livingstone, 1957. Not seen. Cited in Ritchie and Hare (1971), Quaternary Research, vol. 1, pp. 331-342.
- Lock, J.P.G. and Miller, R.D. 1975. Tests of the concept of secondary frost heaving. Soil Science Society of America, Proc., vol. 39, pp. 1036-1041.
- Lundqvist, J. 1962. Patterned ground and related frost phenomena in Sweden: Sveriges Geol. Undersokning Arsbok 55(7), 101 p.
- Lundqvist, G. 1951. En palsmyr sydast om kebnekaise. Geol. For. Stockh. Forh., vol. 73 (2), pp. 209-225.
- Luscher, and Afifi. 1973. Thaw consolidation of Alaskan silts and granular soils. Proc. 2nd International Conf. on Permafrost, Yakutsk, Nat'l. Acad. of Sciences, pp. 325-334.
- Mackay, J.R. 1963. The Mackenzie Delta area, N.W.T. Can. Dept. Mines Tech. Surv., Geog. Br., Mem. 8, 202 p.
- Mackay, J.R. 1971. The origin of massive icy beds in permafrost, western arctic coast, Canada. Can. J. Earth Sci., vol. 8 pp. 397-422.
- Mackay, J.R. 1972. The world of underground ice. Ann. Assoc. Am. Geog., vol. 62, pp. 1-22.
- Mackay, J.R. 1974. Reticulate ice veins in permafrost, Northern Canada. Can. Geotech. J., vol. 11 (2), pp. 230-237.
- Mackay, J.R. and Lavkulich, L. 1974. Ionic and Isotopic fractionation in permafrost. Geol. Surv. Canada Paper 74-1B.





- Mackay, J.R. 1975. Reticulate ice veins in permafrost - reply to McRoberts, E.C. and Nixon, J.F., Can. Geotech. J., vol. 12, p. 163.
- Mackay, J. R. 1978. Discussion: Freshwater shelled invertebrate indicators of paleoclimate in northwestern Canada - by L.E. Delorme et al. Can. J. Earth Science, vol. 15.
- Mageau, D.W. 1978. Moisture migration in frozen soil. M.Sc. Thesis (unpubl.) U. of Alberta, Edmonton, Alberta. 160 p.
- Matthews, J.V., Jr. 1974a. Quaternary environments at Cape Deceit (Seward Peninsula, Alaska); evolution of a tundra ecosystem. Bulletin of the Geol. Soc. of America, vol. 85, pp. 1353-1384.
- Matthews, J.V., Jr. 1974b. Wisconsin environment of interior Alaska: pollen and macrofossil analysis of a 27 meter core from the Isabella Basin (Fairbanks, Alaska). Can. J. Earth Science, vol. 11 pp. 828-841.
- May, R.W. and Thomson, S. 1978. The geology and geotechnical properties of till and related deposits in the Edmonton, Alberta area. Can. Geotech. J., vol. 15, pp. 362-371.
- McCulloch and Hopkins. 1966. Evidence for an early recent warm interval in northwestern Alaska. Geol. Soc. of Amer. Bull. vol. 77, pp. 1089-1107.
- McRoberts, E.C. and Morgenstern, N.R. 1974. The stability of thawing slopes. Can. Geotech. J., vol. 11, pp. 447-469.
- McRoberts, E.C. and Morgenstern, N.R. 1975. Pore water expulsion during freezing. Can. Geotech. J., vol. 12, pp. 131-139.
- McRoberts, E.C. and Nixon, J.F. 1975. Reticulate ice veins in permafrost, northern Canada: Discussion. Can. Geotech. J., Vol. 12, pp. 159-162.
- Michel, F.A. and Fritz, P. 1978. Environmental Isotopes in permafrost related waters along the Mackenzie Valley Corridor. Proc. 3rd International Permafrost Conf., Edmonton, pp. 207-212.
- Miller, R.P. 1972. Freezing and heaving of saturated and unsaturated soils. Highway Res. Rec. 393, pp. 1-11.
- Miller, R.D. 1978. Frost heaving in non-colloidal soils. Proc. 3rd International Permafrost Conf., vol. 1, Nat. Res. Council of Canada, pp. 707-713.
- Miller, R.D., Loch, J.P. and Bresler, E. 1975. Transport of water in a frozen permeameter. Soil Sci. Soc. of Amer. Proc., vol. 39, pp. 1029-1036.



- Morgenstern, N.R. and Nixon, J.F. 1971. One-dimensional consolidation of thawing soils. *Can. Geotech. J.*, vol. 8(4), pp. 558-565.
- Morgenstern, N.R. and Smith, C.B. 1973. Thaw consolidation tests on remoulded clays. *Can. Geotech. J.*, vol. 10, pp. 25-40.
- Nichols, H. 1967. Pollen diagrams from sub-arctic central Canada. *Science*, vol. 155, pp. 1665-1668.
- Nixon, J.F. 1973. Thaw-consolidation of some layered systems. *Can. Geotech. J.*, vol. 10, pp. 617-631.
- Nixon, J.F. and McRoberts, E.C. 1973. A study of some factors affecting the thawing of frozen soils. *Can. Geotech. J.*, vol. 10(3) pp. 439-452.
- Nixon, J.F. and Morgenstern, N.R. 1973. Thaw consolidation tests on undisturbed fine-grained permafrost. *Can. Geotech. J.*, vol. 11(1) pp. 202-214.
- O'Neil, J.R. 1968. Hydrogen and oxygen isotopic fractionation between ice and water. *J. Phys. Chem.*, vol. 72, p. 3683.
- O'sullivan, J.B. 1963. Geochemistry of Permafrost: Barrow, Alaska. *Proc. 1st International Permafrost Conf.*, Purdue, pp. 30-37.
- Payette, S., Samson, S. and Lagarec, D. 1976. The evolution of permafrost in the taiga and in the forest-tundra, Western Quebec-Labrador Peninsula. *Can. J. Forest Res.*, vol. 6, pp. 203-220.
- Penner, E. and Ueda, T. 1978. A frost-susceptibility test and a basis for interpreting heaving rates. *Proc. 3rd International permafrost Conf.*, Edmonton, Alberta, pp. 721-727.
- Penner, E. and T. Walton. 1978. Effects of pressure and temperature on frost heave. *Proc. Int. Symp. on Ground Freezing*, Ruhr-Univ. Bochum, Germany.
- Pettapiece, W.W. and Zoltai, S.C. 1974. Soil environments in the western Canadian Subarctic. *Quaternary Environments Proc.*, York U.
- Pewe, T. and Sellman, P.V. 1972. Geochemistry of permafrost and Quaternary stratigraphy. *Proc. Int. Symp. on Geomorphology*, U. Liege, Begium, pp. 231-233.
- Radforth, N.W. 1962. Organic terrain and geomorphology. *Can. Geographer*, vol. 1(3-4), pp. 166-171.
- Railton, J.B. and J.H. Sparling. 1973. Preliminary studies on the ecology of palsa mounds in northern Ontario. *Can. J. Botany*, vol. 51, pp. 1037-1044.





- Rampton, V.N. 1971. Late Quaternary vegetational and climatic history of the Snag-Klutlan area, southwestern Yukon Territory, Canada. *Geol. Soc. of Amer. Bull.*, vol. 4, pp. 959-978.
- Reid, D.E. (Ed). 1977. Vegetation survey and disturbance studies along the proposed Arctic Gas Route. Biological Report Series. Can. Arctic Gas Study Ltd., Calgary, Alberta, vol. 37, 179 p.
- Rennie, J.A., Reid, D.E. and Henderson, J.D. 1978. Permafrost extent in the southern fringe of the discontinuous permafrost zone, Ft. Simpson, N.W.T. *Proc. 3rd. Int. Permafrost Conf.*, Edmonton, Alberta, pp. 438-445.
- Ritchie, J.C. and Hare F.K. 1971. Late-Quaternary vegetation and climate near the arctic tree line of northwestern North America; *Quat. Res.*, vol. 1, pp. 331-342.
- Roggensack, W.D. 1977. Geotechnical properties of fine-grained permafrost soils. Ph.D. Thesis (unpubl.), Dept. of Civil Eng., U. of Alberta, Edmonton, Alberta.
- Rutter, N.W., Boydell, A.N., Savigny, K.W. and van Everdingen, R.O. 1973. Terrain evaluation with respect to pipeline construction, Mackenzie Transportation Corridor, southern part, Lat. 60° to 64° N. Environmental-Social Committee on Northern Pipelines, Task Force on Northern Oil Development, Report 73-36, 135 p.
- Ruuhijärvi, R. 1960. Regional distribution of north Finnish bogs. *Ann. Bot. Soc. Zool. Bot. Fenn. 'Vanamo'*, vol. 31 (1).
- Salmi, M. 1970. Investigations on palsa in Finnish Lapland. In *Ecology of the Subarctic Regions*. UNESCO, Paris, pp. 143-153.
- Salmi, M. 1972. Present developmental stages of palsas in Finland. *Proc. 4th Int. Peat Congress*, pp. 121-141.
- Samuelson, O. and Sjoberg. 1979. Oxygen bleaching of kraft and polysulfide pulps. *Tappi*, vol. 62, No. 12, pp. 43-50.
- Samuelson, O. and Stolpe, L. 1969. Aldonic acid end groups in cellulose after oxygen bleaching. *Tappi*, vol. 52, No. 9, pp. 1709-11.
- Schiegl, W.E. 1972. Deuterium content of peat as a paleoclimatic recorder. *Science*, vol. 175, pp. 512-513.
- Schwerdtfeger, W. (Ed.). 1976. *Climates of North America; World Survey of Climatology*, vol. 11, Elsevier Publ.
- Schwerdtfeger, W. (Ed). 1976. *Climates of Central and South America; World Survey of Climatology*, vol. 12, Elsevier Publ.
- Seppälä, M. 1976. Seasonal thawing of a palsa at Enontekiö, Finnish Lapland (1974). *Periglacial Bull.*, No. 26, pp. 2-26.



- Simard, G. 1977. Carbon  $^{14}$  and Tritium measurements of groundwaters in the Eaton River Basin and in the Mirabel area, Quebec. Can. J. Earth Science, vol. 14, pp. 2325-2338.
- Sjors, H. 1961. Forest and peatland at Hawley Lake, northern Ontario. Nat. Mus. Can. Bull. 171, pp. 1-31.
- Sjors, H. 1963. Bogs and fens on Attawapiskat River, northern Ontario. Nat. Mus. Can. Bull. 186, pp. 45-133.
- Smith, L.B. 1972. Thaw consolidation tests on remoulded clays. M.Sc. Thesis (unpubl.), U. of Alberta, Edmonton, Alberta, 157 p.
- Sollid, J.L. and Sorbel, L. 1974. Palsa bogs at Haugtjørn, Dourefjell, South Norway. Norsk geogr. Tidsskr., vol.28, pp. 53-60.
- Speer, T.L., Watson, G.H. and Rowley, R.K. 1973. Effects of ground-ice variability and resulting thaw settlements on buried oil pipelines. In Permafrost: The North American Contribution to the 2nd Int. Conf., Yakutsk, pp. 746-752.
- Spolanskaya, N.A. and Evseyev, V.P. 1972. Domed hummocky peat bogs of the northern taiga in western Siberia. Biuletyn Perglcen vol. 22, pp. 271-283.
- Stanek, W. and J.K. Jeglum. 1977. Comparisons of peatland types using macro-nutrient contents of peat. Vegetatio vol. 33, 2/3: pp. 163-173.
- Svensson, H. 1962. Tundra polygons. Photographic interpretation and field studies in the northern Norwegian polygon areas. Norg. Geol. Undersikelse, vol. 223, pp. 298-327.
- Svensson, H. 1969. A type of circular lake in northern-most Norway. Lund Stud. in Geogr. Ser. A 40, pp. 1-12.
- Tarnocai, C. 1970. Classification of peat landforms in Manitoba. Canada Dept. of Agric. Res. Station Pedology Unit, Winnipeg. 45 p.
- Tarnocai, C. 1974. Soils of the Mackenzie River area. Envir. Soc. Comm.; North. Pipelines, Task Force on N. Oil Dev., Gov't. of Canada, Report 73-26, 136 p.
- Terasmae, J. 1972. Muskeg as a climate controlled ecosystem. Proc. 14th Muskeg Res. Conf., 1971, Nat. Res. Council Tech. Memo, No. 102, pp. 147-158.
- Theander, O. 1954. Acta. Chem. Scand. vol. 8, pp. 989-1000.
- Thie, J. 1974. Distribution and thawing of permafrost in the southern part of the discontinuous permafrost zone in Manitoba. Arctic vol. 27, No. 3, pp. 189-200.





- Thompson, P. and Gray, J. 1977. Determination of  $^{18}\text{O}/^{16}\text{O}$  ratios in compounds containing C,  $\text{H}_3$  and O. Int. Appl. Radiat. Isotopes vol. 28, pp. 411-415.
- Toth, J. 1971. Groundwater discharge: a common denominator of diverse geologic and morphologic phenomena. Bulletin Int. Assoc. Scientific Hydrology, vol. 16, pp. 7-24.
- Tsyтович, N.A. 1976. Mechanics of Frozen Ground. McGraw-Hill, New York, 427 p.
- Veillette, J. 1975. Geological Survey of Canada, Paper 75-1A.
- Vorren, K. D. 1972. Stratigraphical investigations of a palsa bog in northern Norway. Astarte, vol. 5, pp. 39-71.
- Walmsley, M.E. 1977. Physical and chemical properties of peat. In Muskeg and the Northern Environment in Canada, U. of Toronto Press, pp. 82-129.
- Watson, G.H., W.A. Slusarchuk and Rowley, R.K. 1973. Determination of some frozen and thawed properties of permafrost soils. Can. Geotech. Journal, vol. 10, pp. 592-605.
- Weston, R.E. 1955. Hydrogen Isotope fractionation between ice and water. Geochim. Cosmochim. Acta, vol. 8, pp. 281-284.
- Wigley, T.M.L., Gray, B.M., and Kelly, P.M. 1978. Climatic interpretation of  $\delta^{18}\text{O}$  and  $\delta\text{D}$  in tree rings. Nature, vol. 271, p. 92-93.
- Williams, G.P. 1968. The thermal regime of a Sphagnum peat bog. Proc. 3rd. Int. Peat Congr., Quebec, pp. 195-200.
- Wramner, P. 1967. Studier av palsmyrar i Laivadalén, Lappland. In Eriksson, K.G.(Ed) Teknik Och Natur, Göteborg, 457 p.
- Wramner, P. 1973. Palsmyrar; Tasvavuoma Lappland. Goteborg Univ. Naturgeogr. Inst. Rapport 3, 140 pp.
- Wu, T.H. 1977. Soil Mechanics. Allyn and Bacon, Inc. Boston, 438 p.
- Yapp, C.J. and Epstein, S. 1977. Climatic implications of D/H ratios of meteoric water over North America (9500-22,000 B.P.) as inferred from ancient wood cellulose C-H hydrogen. Earth Planet Sci. Lett. vol. 34, pp. 333-350.
- Zoltai, S.C. 1971. Southern limit of permafrost features in peat landforms Manitoba and Saskatchewan. Geol. Assoc. Can., Spec. Paper No. 9, pp. 305-310.



- Zoltai, S.C. 1972. Palsas and peat plateaus in central Manitoba and Saskatchewan. Can. J. For. Res., vol. 2, pp. 291-302.
- Zoltai, S.C. and Pettapiece, W.W. 1978. Age of cryoturbated organic materials in earth hummocks from the Canadian Arctic. Proc. 3rd Intl. Conf. Permafrost, Edmonton.
- Zoltai, S.C. and Tarnocai. 1971. Properties of a wooded palsa in Northern Manitoba. Arctic Alpine Res., vol. 3, pp. 115-129.
- Zoltai, S.C. and Tarnocai, C. 1975. Perennially frozen peatlands in the western Arctic and Subarctic of Canada. Can. J. Earth Science, vol. 12, pp. 28-43.





## APPENDICES



## APPENDIX 1: Thermistor Construction

The thermistors were calibrated in the lab at 5 °C. intervals from -20 °C. to +20 °C. against a previously calibrated thermistor. The thermistor leads were soldered at low temperatures to copper wires, sheathed in 1.5 mm 'Heat Shrink' rubber tubing, and then inserted into 3 mm copper tubing and packed in liquid fiberglass. The thermistor head was allowed to protrude .5 mm out of the copper tube. The tube was sheathed in 3 mm Heat Shrink tubing, and the copper wires soldered to PVC triple insulated dipole cable. Several layers of self-vulcanizing electrical tape were wrapped around the cable. Finally, the entire thermistor plus several centimeters of the cable was dipped in 'Scotchchkote' several times.

The needle probe thermistor is initially prepared in a similar way to the permanent thermistors. The thermistor head is then inserted into a pointed, threaded brass rod, 12 cm in length. A rubber insulated handle is screwed into the rod, the thermistor cable exiting at the other end of the handle. This device completely protects the thermistor head from moisture and shock. The pointed rod can be inserted into the end of the large diameter core immediately after removal from the drill hole or can free fall to the bottom of the hole. This allows more continuous temperature logging, but not to the accuracy of permanent thermistors. The needle probe thermistor was also fitted to a flexible steel rod which was inserted to various depths in the unfrozen bog and fen.



Five permanent thermistors were installed in the frozen palsa and four in the unfrozen bog. The thermistor cables were securely taped to the outside of the PVC pipe used for the installation of piezometers, and lowered into the drill holes. Holes were back-filled and sealed in the usual manner.



Appendix 2 : Results of chemical analysis of ground ice in  
cores S78, E3, and E11.





| Core Sample | Depth (cm) | pH   | Conductivity (micro) | $\text{HCO}_3^-$ (epm.)* | $\text{SO}_4^{--}$ | $\text{Cl}^-$ | Na <sup>+</sup> | Ca <sup>+</sup> | K <sup>+</sup> | Mg <sup>+</sup> |
|-------------|------------|------|----------------------|--------------------------|--------------------|---------------|-----------------|-----------------|----------------|-----------------|
| S78-06      | 30         | 5.47 | 170                  | .131                     | 1.81               | .10           | .140            | 1.52            | .040           | .34             |
| " -15       | 76         | 5.93 | 300                  | .243                     | 3.22               | ---           | .190            | 2.40            | .032           | .64             |
| " -23       | 127        | 5.38 | 250                  | .197                     | 2.29               | .20           | .175            | 2.04            | .028           | .45             |
| " -30       | 175        | 5.19 | 250                  | .171                     | 2.44               | .10           | .183            | 2.00            | .032           | .49             |
| " -38       | 230        | 6.43 | 171                  | .446                     | .89                | .20           | .24             | 1.00            | .030           | .27             |
| " -45       | 267        | 5.74 | 135                  | .295                     | .95                | .20           | .18             | 1.00            | .017           | .25             |
| " -52       | 310        | 5.21 | 240                  | .262                     | 1.83               | .10           | .21             | 1.54            | .026           | .41             |
| " -56       | 333        | 4.98 | 490                  | .131                     | 4.00               | .10           | .27             | 2.97            | .025           | .84             |
| " -59       | 350        | 4.00 | 690                  | .100                     | 7.28               | .10           | .32             | 5.72            | .073           | 1.27            |
| " -71       | 406        | 8.15 | 416                  | 2.250                    | 2.52               | .10           | .42             | 2.54            | .081           | 1.27            |
| " -79       | 470        | 8.07 | 386                  | 2.257                    | 1.93               | .10           | .29             | 2.79            | .086           | .86             |
| " -83       | 508        | 8.18 | 350                  | 2.401                    | .53                | .10           | .49             | 1.82            | .086           | .86             |
| " -106      | 700        | 8.44 | 300                  | 2.247                    | .17                | .20           | .60             | 1.07            | .095           | .96             |
| E3 -3       | 170        | 5.77 | 115                  | .282                     | .25                | ---           | .13             | .32             | .016           | .06             |
| " -4        | 220        | 6.47 | 130                  | .440                     | .40                | ---           | .23             | .50             | .022           | .09             |
| " -5        | 266        | 7.03 | 200                  | .394                     | 1.11               | ---           | .24             | 1.00            | .026           | .23             |
| " -6        | 315        | 7.85 | 240                  | 1.863                    | .66                | ---           | .26             | 1.47            | .340           | .45             |
| " -7        | 340        | 8.06 | 208                  | 2.171                    | .04                | ---           | .17             | 1.54            | .079           | .37             |
| " -8        | 405        | 7.46 | 70                   | 1.577                    | .04                | ---           | .09             | .43             | .015           | .06             |
| " -10-5     | 530        | 8.15 | 265                  | 2.027                    | .61                | ---           | .47             | 1.43            | .095           | .68             |
| " -11-4     | 620        | 7.95 | 160                  | 1.502                    | .04                | ---           | .17             | .93             | .059           | .36             |
| E11-2       | 95         | 4.64 | 51                   | 0                        | .33                | .20           | .08             | .33             | .017           | .10             |
| " -3        | 130        | 5.02 | 82                   | .131                     | .54                | .10           | .07             | .35             | .024           | .13             |
| " -4        | 250        | 6.67 | 123                  | .748                     | .04                | .10           | .07             | .36             | .027           | .10             |
| " -5        | 300        | 6.73 | 117                  | .518                     | .04                | .10           | .07             | .48             | .022           | .10             |
| " -6        | 375        | 6.88 | 79                   | 1.128                    | .04                | .10           | .06             | .54             | .013           | .10             |
| " -7        | 420        | 7.90 | 365                  | 3.044                    | .04                | .10           | .16             | 2.63            | .070           | .55             |
| " -9        | 560        | 8.30 | 283                  | 2.558                    | .04                | .10           | .36             | 1.86            | .173           | .61             |
| " -10       | 620        | 8.24 | 230                  | 2.224                    | .04                | .10           | .22             | 1.36            | .060           | .62             |
| " -11       | 675        | 8.50 | 300                  | 3.448                    | .13                | .10           | .37             | 1.61            | .082           | 1.62            |
| " -12       | 740        | 8.40 | 248                  | 2.973                    | .04                | .10           | .37             | 1.07            | .088           | .62             |

\* All ionic measurements in equivalents per mole (epm.)



| Sites                               | pH   | (mhos)<br>Conductivity | (epm.) <sup>*</sup><br>$\text{HCO}_3^-$ | $\text{SO}_4^{--}$ | $\text{Cl}^-$ | $\text{Na}^+$ | $\text{Ca}^+$ | $\text{K}^+$ | $\text{Mg}^+$ |
|-------------------------------------|------|------------------------|---|--------------------|---------------|---------------|---------------|--------------|---------------|
| Thaw pond, surface water            | 6.92 | 113                    | 1.528                                   | ---                | .10           | .03           | .82           | .02          | .22           |
| Pals lag                            | 6.62 | 108                    | 1.115                                   | ---                | ---           | .39           | .46           | .02          | .11           |
| <u>Sphagnum</u> bog                 | 5.98 | 54                     | .590                                    | ---                | .10           | .11           | .29           | .02          | .12           |
| Groundwater beneath thaw pond       | 7.35 | 570                    | 4.848                                   | 2.05               | .10           | .91           | 3.40          | .08          | 1.78          |
| <u>Sphagnum</u> bog                 | 4.80 | 36                     | .016                                    | .021               | .10           | .05           | .07           | .035         | .03           |
| Fen                                 | 7.91 | 260                    | 3.090                                   | ---                | ---           | .31           | 2.25          | .005         | .62           |
| Groundwater beneath thaw pond       | 7.28 | 560                    | 5.995                                   | 1.16               | .10           | 1.80          | 3.20          | .08          | 1.20          |
| Groundwater beneath collapsed palsa | 7.35 | 300                    | 3.241                                   | .06                | .10           | .24           | 2.18          | .13          | .62           |
| Groundwater beneath collapsed palsa | 7.41 | 440                    | 5.268                                   | ---                | .10           | .09           | 3.49          | .06          | .8            |
| Groundwater beneath palsa E 3       | 7.42 | 595                    | 6.527                                   | .53                | .10           | 2.81          | 2.43          | .168         | 1.64          |
| Groundwater beneath palsa N 9       | 7.55 | 510                    | 4.766                                   | .50                | .10           | .90           | .89           | .13          | 1.85          |
| Collapsed pond, surface water       | 6.13 | 45                     | .289                                    | ---                | .10           | .03           | .32           | .006         | .11           |
| Pals lag drainage                   | 6.10 | 57                     | .426                                    | ---                | .10           | .10           | .57           | .023         | .07           |

\* All ionic measurements in equivalents per mole (epm.)



Appendix 3: A. Results of thaw consolidation tests on core  
S100

B. Results of tests using empirical relationships  
to predict total thaw settlement in organic  
and mineral soils



TABLE A3-1

SUMMARY OF THAW CONSOLIDATION DATA OBTAINED IN PERMODE FOR ORGANIC SOILS

| SAMPLE | DEPTH<br>(m) | FROZEN<br>BULK<br>DENSITY<br>(Mg/m <sup>3</sup> ) | MOISTURE<br>CONTENT<br>(%) | VOLUMETRIC<br>WATER<br>(%) | VOLUMETRIC<br>ICE<br>(%) | MAXIMUM<br>EFFEC.<br>STRESS<br>(kN/m <sup>2</sup> ) | UNDRAINED<br>VERTICAL<br>STRAIN<br>(%) | DRAINED<br>VERT.<br>STRAIN<br>(%) | RESIDUAL<br>STRESS<br>(kN/m <sup>2</sup> ) | B    | PERMEABILITY<br>(m/sec) | GROUND ICE DESCRIPTION |
|--------|--------------|---|----------------------------|----------------------------|--------------------------|---|--|-----------------------------------|--|------|-------------------------|------------------------|
| 1      | .25          | .55   | 340                        | 40                         | 44                       | 2.2   | 0                                      | 0                                 |  |      |                         | active layer ice       |
| 2      | .68          | .90   | 932                        | 33                         | 35                       | 4.4   | 2.3                                    | 3.5                               |  |      | $2 \times 10^{-4}$      | active layer ice       |
| 3      | .80          | .82   | 945                        | 58                         | 63.2                     | 5.0   | 5.6                                    | 10.2                              |  |      |                         | active layer ice       |
| 4      | 1.00         | .96   | 748                        | 24                         | 26.2                     | 5.6   | 2.1                                    | 28.9                              |  |      | $3 \times 10^{-5}$      | pore ice               |
| 5      | 1.50         | .90   | 651                        | 44                         | 48                       | 11.0  | 2.5                                    | 54.2                              | 0  | .96  | $4.2 \times 10^{-5}$    | veins to 2 mm          |
| 6      | 2.00         | .87   | 996                        | 40                         | 43.6                     | 12.6  | 3.7                                    | 42.2                              |  |      |                         | veins to 2.5 mm        |
| 7      | 2.30         | .84   | 940                        | 16                         | 17.4                     | 15.1  | 2.0                                    | 45.3                              |  |      | $3.2 \times 10^{-7}$    | num. veins to 3 mm     |
| 8      | 2.60         | .70   | 1400                       | 38                         | 42                       | 16.3  | 2.7                                    | 37.0                              |  |      |                         | num. veins to 3 mm     |
| 9      | 2.78         | .89   | 1805                       | 32                         | 35                       | 18.2  | 2.5                                    | 33.8                              | 0  | 1.00 | $3.5 \times 10^{-6}$    | num. veins to 2 mm     |
| 10     | 2.95         | .76   | 1013                       | 44                         | 48                       | 19.2  | 4.0                                    | 36.2                              |  |      |                         | lenses to 3 mm         |
| 11     | 3.10         | .89   | 940                        | 43                         | 25                       | 20.4  | 4.1                                    | 35.4                              | 0  | 1.01 | $4.0 \times 10^{-6}$    | peat dispersed in ice  |
| 12     | 3.40         | .70   | 1356                       | 41                         | 45.5                     | 21.7  | 3.6                                    | 40.1                              |  |      | $3.2 \times 10^{-6}$    | lenses to 2 mm         |
| 13     | 3.50         | .80   | 850                        | 60                         | 65                       | 22.6  | 8.1                                    | 71.0                              |  |      |                         | lenses to 2 mm         |
| 14     | 3.85         | .83   | 995                        | 64                         | 70                       | 23.9  | 6.9                                    | 90.0                              | 0  | 1.02 | $1.5 \times 10^{-6}$    | lenses to 2.5 mm       |
| 15     | 4.15         | .81   | 1030                       | 39                         | 43                       | 25.1  | 2.9                                    | 45.7                              |  |      |                         | lenses to 2 mm         |
| 16     | 4.30         | .76   | 1340                       | 26                         | 28.7                     | 25.7  | 2.0                                    | 37.0                              |  |      | $1.8 \times 10^{-7}$    | little visible ice     |
| 17     | 4.40         | 1.02  | 845                        | 41                         | 45.2                     | 32.3  | 4.4                                    | 25.0                              |  |      |                         | vein ice               |
| 18     | 4.50         | .65   | 790                        | 22                         | 24                       | 34.2  | 3.7                                    | 32.1                              |  |      |                         | little visible ice     |





TABLE A3-2

SUMMARY OF THAW CONSOLIDATION DATA OBTAINED IN PERMODE FOR MINERAL SOILS

| SAMPLE | DEPTH<br>(m) | FROZEN<br>BULK<br>DSTY <sub>3</sub><br>(Mg/m <sup>3</sup> ) | MOISTURE<br>CONTENT<br>(%) | MAX. EFFEC.<br>STRESS<br>(kN/m <sup>2</sup> ) | VERTICAL<br>STRAIN<br>(%) | RESIDUAL<br>STRESS <sub>2</sub><br>(KN/m <sup>2</sup> ) | B    | PERMEABILITY<br>(m/sec) | COEFF. of<br>Consol.<br>(C <sub>v</sub> )<br>(cm <sup>2</sup> /sec) | COEFF. of<br>COMPRES.<br>(m <sup>2</sup> /kN)<br>( $\frac{e}{\sigma} = 0$ ) | THAW SETTLE-<br>MENT PARAMETER<br>(%) | GROUND ICE<br>DESCRIPTION           |
|--------|--------------|---|----------------------------|---|---------------------------|---|------|-------------------------|---|---|---------------------------------------|-------------------------------------|
| 20     | 4.60         | 1.60  | 30.1                       | 33.6  | 11.7                      |   |      | 6.2x10 <sup>-8</sup>    |   | 1.2   | 11.05                                 | pore ice (sand)                     |
| 21     | 5.25         | 1.55  | 41.0                       | 37.7  | 24.0                      |   |      | 4.3x10 <sup>-9</sup>    | 6.3x10 <sup>-3</sup>  | 6.8   | 21.4                                  | 1 cm ice lens<br>ret. veins to 4 mm |
| 22     | 5.60         | 1.84  | 25.1                       | 38.9  | 4.5                       |   |      | 1.6x10 <sup>-9</sup>    | 4.2 x10 <sup>-3</sup>   | 3.5   | 3.2                                   | vein ice to 1 mm                    |
| 23     | 5.80         | 1.37  | 49.2                       | 39.9  | 41.0                      | 0   | 1.00 | 1.0x10 <sup>-9</sup>    | 5.0x10 <sup>-4</sup>  | 20.5  | 32.9                                  | 1 cm lens and<br>.3 cm lens         |
| 24     | 5.96         | 1.87  | 22.2                       | 40.5  | 8.1                       | 10  | .70  |                         |   | 12.5  | 3.1                                   | massive silt                        |
| 25     | 6.12         | 1.53  | 44.3                       | 41.1  | 20.6                      | 3   | .94  | 6.1x10 <sup>-9</sup>    | 3.6x10 <sup>-4</sup>  | 17.0  | 13.6                                  | num. veins to 7 mm                  |
| 26     | 6.35         | 1.51  | 46.9                       | 42.4  | 30.7                      | 0   | .97  | 4.3x10 <sup>-9</sup>    | 8.6x10 <sup>-4</sup>  | 5.0   | 28.5                                  | 1.5 cm lens and<br>num. ret. veins  |
| 27     | 7.10         | 1.87  | 20.3                       | 45.8  | 3.0                       | 13  | .71  | 6.8x10 <sup>-10</sup>   | 1.2x10 <sup>-4</sup>  | 5.5   | 0.2                                   | veins to 2mm                        |
| 28     | 7.45         | 1.67  | 36.2                       | 48.7  | 14.3                      |   |      |                         |   | 9.0   | 8.9                                   | 7 mm lens, num.<br>ret. veins       |
| 29     | 8.40         | 1.50  | 48.7                       | 53.7  | 28.6                      | 5   | .91  |                         |   | 2.3   | 27.3                                  | num. ret. veins                     |
| 30     | 9.50         | 1.66  | 26.5                       | 60.3  | 8.5                       |   |      |                         |   | 7.0   | 3.9                                   | num. ret. veins                     |
| 31     | 6.25         | 1.45  | 47.1                       | 42.0  | 35.2                      |   |      |                         |   |   |                                       | num. lenses to 3 m                  |
| 32     | 6.50         | 1.59  | 42.0                       | 43.0  | 17.5                      |   |      |                         |   |   |                                       | 1 cm ice lens                       |
| 33     | 6.73         | 1.80  | 27.2                       | 44.2  | 5.0                       |   |      |                         |   |   |                                       | massive silt                        |
| 34     | 7.00         | 1.72  | 29.3                       | 45.1  | 7.5                       |   |      |                         |   |   |                                       | ret. vein ice                       |
| 35     | 7.65         | 1.45  | 48.3                       | 49.4  | 31.1                      |   |      |                         |   |   |                                       | num. lenses to 5 m                  |
| 36     | 7.90         | 1.31  | 59.1                       | 51.0  | 46.1                      |   |      |                         |   |   |                                       | massive ice, minor<br>silt          |



TABLE A3-4  
Predicted thaw settlements for core S 78 using derived relationships.

| Sample interval (cm) | Frozen bulk density<br>(Mgm/m <sup>3</sup> ) -- $\gamma_f$ | Volumetric water<br>content (%) -- $W_v$ | Moisture content (%)<br>-- $W$ | Predicted settlement -- $E^o$<br>(%) | Predicted settlement -- $E^o$<br>(cm) |
|----------------------|--|--|--------------------------------|--------------------------------------|---------------------------------------|
| 0-2.5                | .60  | 30.0                                     | 340                            | 41                                   | 1.02                                  |
| 2.5-7.5              | .76  | 35.1                                     | 375                            | 49                                   | 2.46                                  |
| 7.5-15.0             | .55  | 43.8                                     | 712                            | 52                                   | 3.90                                  |
| 15.0-20.0            | .86  | 39.0                                     | 700                            | 80                                   | 3.99                                  |
| 20-28.0              | .35  | 28.6                                     | 900                            | 34                                   | 2.72                                  |
| 28-33.0              | .45  | 35.2                                     | 578                            | 43                                   | 2.16                                  |
| 33-38.0              | .46  | 36.0                                     | 570                            | 44                                   | 2.09                                  |
| 38-43.0              | .72  | 53.8                                     | 444                            | 64                                   | 3.20                                  |
| 43-48                | .57  | 40.6                                     | 354                            | 49                                   | 2.46                                  |
| 48-55.5              | .66  | 52.9                                     | 731                            | 63                                   | 4.72                                  |
| 55.5-61              | .74  | 62.3                                     | 1155                           | 67                                   | 3.68                                  |
| 61-63.5              | .71  | 60.0                                     | 1310                           | 71                                   | 5.31                                  |
| 63.5-76              | .90  | 74.3                                     | 933                            | 87                                   | 6.50                                  |
| 76-81                | .82  | 58.1                                     | 1100                           | 69                                   | 3.43                                  |
| 81-86                | .74  | 58.1                                     | 1100                           | 69                                   | 3.43                                  |
| 86-88                | 1.09   | 93.0                                     | 1570                           | 100                                  | 2.00                                  |
| 88-90.5              | 1.30   | 95.8                                     | 1430                           | 100                                  | 2.00                                  |
| 90.5-93              | 1.30   | 95.8                                     | 1430                           | 100                                  | 2.00                                  |
| 93-98                | 1.14   | 94                                       | 1450                           | 100                                  | 2.00                                  |
| 98-103               | .91  | 69                                       | 650                            | 81                                   | 4.04                                  |
| 103-110.5            | .89  | 74                                       | 900                            | 86                                   | 6.48                                  |
| 110.5-117            | .84  | 70                                       | 890                            | 79                                   | 5.13                                  |
| 117-124.5            | .78  | 65                                       | 930                            | 68                                   | 5.08                                  |
| 124.5-129            | .84  | 68                                       | 940                            | 69                                   | 3.11                                  |
| 129-135              | .88  | 71                                       | 785                            | 77                                   | 4.65                                  |
| 135-140              | .89  | 71                                       | 651                            | 83                                   | 4.65                                  |
| 140-145              | 1.02   | 81                                       | 662                            | 94                                   | 4.70                                  |
| 145-154              | .86  | 69                                       | 728                            | 60                                   | 5.36                                  |
| 154-161.5            | .78  | 61                                       | 609                            | 71                                   | 5.36                                  |
| 161.5-169            | .79  | 61                                       | 609                            | 86                                   | 6.53                                  |
| 169-176              | .87  | 67                                       | 542                            | 77                                   | 5.41                                  |
| 176-186              | .83  | 57                                       | 317                            | 68                                   | 6.78                                  |
| 186-195              | .77  | 55                                       | 374                            | 64                                   | 5.72                                  |
| 195-203              | .82  | 67                                       | 827                            | 84                                   | 6.86                                  |
| 203-208              | .74  | 60                                       | 800                            | 70                                   | 3.56                                  |
| 208-213              | .69  | 60                                       | 800                            | 70                                   | 3.56                                  |
| 213-217              | .86  | 65                                       | 820                            | 75                                   | 2.87                                  |
| 217-222              | .80  | 65                                       | 848                            | 75                                   | 3.81                                  |
| 222-227              | .85  | 70                                       | 996                            | 81                                   | 4.09                                  |
| 227-232              | .71  | 60                                       | 1356                           | 70                                   | 3.56                                  |
| 232-238              | .83  | 67                                       | 1030                           | 77                                   | 4.42                                  |



TABLE A3-4 (Continued)

| Sample interval (cm) | $\gamma_F$ | $W_V$ | $W$  | %   | $E^O$ | cm    |
|----------------------|------------|-------|------|-----|-------|-------|
| 238-243              | .75        | 63    | 1256 | 67  |       | 2.54  |
| 243-245              | .67        | 57    | 1560 | 57  |       | 3.25  |
| 245-249              | .62        | 48    | 1260 | 64  |       | 5.31  |
| 249-257              | .70        | 55    | 1200 | 80  |       | 6.58  |
| 257-265              | .83        | 69    | 1170 | 62  |       | 4.34  |
| 265-272              | .66        | 53    | 710  | 67  |       | 3.38  |
| 272-277              | .83        | 66    | 682  | 80  |       | 4.04  |
| 277-282              | .67        | 84    | 1435 | 91  |       | 2.90  |
| 282-287              | .82        | 69    | 1131 | 86  |       | 4.93  |
| 287-290              | .96        | 80    | 1103 | 100 |       | 3.18  |
| 290-295              | .87        | 75    | 1805 | 86  |       | 4.93  |
| 295-303              | .77        | 64    | 1013 | 74  |       | 6.58  |
| 303-308              | .80        | 66    | 1061 | 77  |       | 3.89  |
| 308-313              | .68        | 55    | 833  | 65  |       | 3.28  |
| 313-318              | .81        | 66    | 943  | 77  |       | 3.89  |
| 318-323              | .98        | 80    | 908  | 90  |       | 4.57  |
| 323-326              | .91        | 76    | 1035 | 97  |       | 4.32  |
| <u>End of Peat</u>   |            |       |      |     |       |       |
| 326-330              | .90        |       | ice  | 100 |       | 3.81  |
| 330-333              | 1.70       |       | 200  | 81  |       | 3.10  |
| 333-337              | 1.15       |       | 180  | 71  |       | 2.72  |
| 337-341              | 1.51       |       | 72   | 27  |       | 1.04  |
| 341-344              | 1.60       |       | 59   | 16  |       | .61   |
| 344-349              | 1.52       |       | 60   | 26  |       | 1.32  |
| 349-354              | 1.64       |       | 32   | 12  |       | .61   |
| 354-358              | 1.59       |       | 33   | 15  |       | .66   |
| 358-362              | 1.60       |       | 69   | 16  |       | .61   |
| 362-370              | 1.68       |       | 43   | 6   |       | .53   |
| 370-372              | 1.40       |       | 85   | 40  |       | 1.27  |
| 372-377              | 1.67       |       | 48   | 8   |       | .46   |
| 377-382              | 1.79       |       | 42   | 3   |       | .15   |
| 382-392              | 1.89       |       | 27   | 3   |       | .58   |
| 392-399              | .91        |       | ice  | 100 |       | 8.00  |
| 399-407              | 1.27       |       | 120  | 56  |       | 4.27  |
| 407-412              | .95        |       | 232  | 95  |       | 4.83  |
| 412-420              | .91        |       | ice  | 100 |       | 8.00  |
| 420-430              | .91        |       | ice  | 100 |       | 10.00 |
| 430-433              | 1.74       |       | 39   | 3   |       | .18   |
| 433-438              | .91        |       | ice  | 100 |       | 5.00  |
| 438-443              | 2.00       |       | 26   | 3   |       | .15   |
| 443-452              | 1.83       |       | 30   | 3   |       | .28   |
| 452-457              | 1.23       |       | 170  | 61  |       | 3.10  |
| 457-467              | .91        |       | ice  | 100 |       | 10.00 |



TABLE A3-4 (Continued)

| Sample interval (cm) | $\gamma_f$ | $W_v$ | W   | %  | $E^o$ | cm   |
|----------------------|------------|-------|-----|----|-------|------|
| 467-472              | 2.33       | —     | 27  | 3  |       | .15  |
| 472-478              | 1.95       |       | 44  | 3  |       | .18  |
| 478-483              | 1.69       |       | 66  | 6  |       | .30  |
| 483-488              | 1.45       |       | 68  | 34 |       | 1.73 |
| 488-492              | 1.93       |       | 39  | 3  |       | .13  |
| 492-498              | 1.57       |       | 50  | 20 |       | 1.27 |
| 498-506              | 1.64       |       | 47  | 13 |       | 1.00 |
| 505-511              | 2.29       |       | 32  | 3  |       | .15  |
| 511-521              | 1.50       |       | 39  | 28 |       | 2.84 |
| 521-531              | 1.92       |       | 29  | 3  |       | .30  |
| 531-546              | 1.97       |       | 27  | 3  |       | .46  |
| 546-556              | 2.05       |       | 31  | 3  |       | .30  |
| 556-567              | 1.90       |       | 28  | 3  |       | .36  |
| 567-577              | 2.00       |       | 27  | 3  |       | .30  |
| 577-584.5            | 2.01       |       | 27  | 3  |       | .23  |
| 584.5-592            | 1.88       |       | 30  | 3  |       | .23  |
| 592-600              | 1.86       |       | 30  | 3  |       | .24  |
| 600-608              | 1.80       |       | 32  | 3  |       | .28  |
| 608-619              | 1.90       |       | 28  | 3  |       | .36  |
| 619-630              | 1.88       |       | 30  | 3  |       | .36  |
| 630-636              | 1.60       |       | 48  | 16 |       | 1.02 |
| 636-644              | 1.10       |       | 190 | 78 |       | 5.94 |
| 644-652              | 1.20       |       | 153 | 64 |       | 5.69 |
| 652-658              | 1.82       |       | 33  | 3  |       | .20  |
| 658-666              | 1.89       |       | 31  | 3  |       | .23  |
| 666-673              | 1.94       |       | 29  | 3  |       | .23  |
| 673-681              | 1.88       |       | 30  | 3  |       | .23  |
| End of Mineral Soil  |            |       |     |    |       |      |

1. Mineral soil settlement based on:  $E^o = -103.53 \gamma_f + 187.06$

2. Peat settlement based on:  $E^o = 1.09 W_v + 4.36$

SUMMARY

Field Observations

Frozen mineral soil relief = 152.0 cm.

Frozen palasa relief = 284.0 cm.

Thaw Consolidation Test Results

Total settlement in peat = 245.95 cm.

Total settlement in mineral soil = 105.95 cm.

Total core settlement = 350.3 cm.

CONCLUSIONS

Thawed mineral soil: residual relief = 46.9 cm.

Thawed palasa: depression = 66.0 cm.





#### APPENDIX 4: Testing Methods for Thaw Consolidation

Methods of preparing samples for thaw consolidation testing and the apparatus and instrumentation used in the tests have been described by Roggensack (1978) in considerable detail, and will be only briefly described here.

The permafrost oedometer or permode was the basic piece of equipment (Figure A5). It is of the split barrel design to facilitate the testing of undisturbed samples. The permode walls are constructed of low thermal conductivity PVC and lined with Teflon to eliminate side friction. De-aired sintered stainless steel porous stones permitted drainage through the top or bottom of the sample. The lower porous stone was connected to a pressure transducer with a resolution of  $.15 \text{ KN/m}^2$  and monitored with a Budd Strain gauge. This was used to monitor pore water pressures during thaw and for constant head permeability tests. A linearly variable displacement transducer (LVDT) measured sample settlements to an accuracy of better than  $2 \times 10^{-6}$  meters.

The soil sample is turned on a lathe to a diameter of  $.064 \text{ m}$  to closely fit the permode. Samples are then milled to an average length of  $.07 \text{ m}$ , inserted into a vacuum-greased rubber membrane and placed in the permode. Rubber O-rings at the load cap and base pedestal prevented leakage. Care was taken to eliminate any trapped air between the specimen and the loading cap and base. The apparatus is de-aired, removed from the cold room, and then mounted in the loading frame.



Thawing was uncontrolled at room temperature and under undrained conditions. After complete thawing at a stress equal to approximately one-third the overburden stress, the permeable, still in the undrained condition, was sequentially loaded with weights up to the overburden stress. Maximum pore pressures with each load increment were recorded. This technique allows the determination of the residual stress of a soil (see Roggensack, 1977; Nixon and Morgenstern, 1973). The weights were then removed, and the undrained consolidation recorded. The drains at top and bottom of the sample were opened and the permeable re-loaded. Coefficients of consolidation were determined in the usual manner. The soil was allowed to consolidate for 24 hours under each load increment and the relative settlement recorded. The coefficients  $A_0$  and  $a_0$  were determined using the technique outlined by Luscher and Afifi (1973). After total overburden stress had been reached the sample was allowed to consolidate for 72 hours and the total thaw consolidation,  $E^0$ , recorded.

The overburden pressures were determined from the relationship

$$\sigma_e = X_1 \gamma_p + X_2 \gamma_p' + X_3 \gamma_s'$$

where  $X_1$  = height of palsa above water table

$X_2$  = depth of frozen peat beneath the water table

$X_3$  = depth of mineral soil beneath the water table to the thaw front

$\gamma_p$  = thawed unit weight of peat

$\gamma_p'$  = submerged unit weight of peat

$\gamma_s'$  = submerged unit weight of mineral soil



## APPENDIX 5: Stefan's formula.

The simplest method for calculating frost penetration depth, X, in a homogeneous soil is Stefan's formula:

$$X = \sqrt{\frac{2 K dT \cdot t}{L}}$$

where: K - coefficient of thermal cond.

dT - step temperature

t - time

L - latent heat of fusion





## APPENDIX 6: Testing Methods and Apparatus for Frost Heave Characteristics of Palsa Soil

The experimental apparatus and methods used to obtain the basic frost heave data is identical to that described by Hill and Morgenstern (1977) and very similar to that used by Penner and Ueda (1977). Briefly, the test cell is a PVC lined, heavily insulated chamber capable of holding a pre-consolidated soil sample 0.10 m in diameter and up to .15 m in height. The sample is sheathed in a thin rubber membrane to prevent side friction. Four thermocouples are imbedded in the cell walls. Consolidation and overburden pressures were provided by a hanging weight loading apparatus mounted above the freezing cell. Freezing cold side temperatures were introduced at the upper plate by a circulating ethylene glycol bath. The lower plate was kept at temperatures slightly above freezing by a circulating water bath. The freezing cell was kept in a constant temperature (+2 °C.) cold room to reduce thermal effects from the sides. The base of the sample had free access to de-ionized, de-aired water with the water table maintained at the level of the base of the sample.

After consolidation was complete, the pressure was reduced to a selected value and a freezing temperature imposed at the top of the specimen. Heaving was "open system" throughout the test.

Temperatures at the top, base and sides of the sample, rates of vertical heave and rates of water intake by the freezing soil were measured every hour by a data acquisition system with printing and plotting facilities.





## APPENDIX 7: Frost Heave Characteristics of the Palsa Soils

The frost heave susceptibility of the soil is an extremely important characteristic of northern terrain. This parameter is of significance to geomorphic process studies in that it defines the upper limits for the development time of permafrost features and allows an assessment of the relative importance of the various environmental parameters in the development of a cryogenic landscape. In this Appendix, the frost heave characteristics of the palsa complex mineral soil are determined. Results from these tests are applied to the problem of the rate of development of the ground ice profile in Chapter 5.

The testing method involves placing a temperature gradient across a frozen soil under a specified overburden pressure. After steady state temperature conditions in the sample are achieved, the frost cell is opened to drainage and frost heaving begins. The rate of heaving of the soil is monitored under different cold side temperatures and various overburden pressures. The temperature gradient in the frozen portion of the soil is approximately linear, hence the position of the 0 °C. isotherm is determined by the cold side temperature (Figure A8-1). Two sets of tests were completed; typical cumulative heaving rates, water intake rates and temperature profiles for the tests are included in Appendix 6. The testing results have been summarized in Table A8-1.

During freezing of soils in the field, the position of the free water table beneath the frost front varies according to the suction



TABLE A8-1

| Test Number | Pre-consolidation pressure (Kg / cm <sup>2</sup> ) | Pressure during heaving (Kg / cm <sup>2</sup> ) | Cold Side temperature | Temp. gradient in frozen zone (°C/cm) | Total heave rate x 10 <sup>-3</sup> (mm/min) | Water intake x 10 <sup>-4</sup> (cm <sup>3</sup> /sec) |
|-------------|--|---|-----------------------|---------------------------------------|--|--|
| BB-1        | 3.0  | 1.0   | -1.0                  | .434                                  | 2.53   | 2.67   |
|             | 3.0  | 1.0   | -2.0                  | .571                                  | 3.45   | 3.97   |
|             | 3.0  | 1.0   | -4.0                  | .916                                  | 6.67   | 6.81   |
| BB-2        | 3.0  | 3.0   | -1.0                  | .434                                  | 1.37   | 1.58   |
|             | 3.0  | 3.0   | -2.0                  | .571                                  | 2.53   | 2.58   |
|             | 3.0  | 3.0   | -4.0                  | .916                                  | 3.52   | 4.58   |



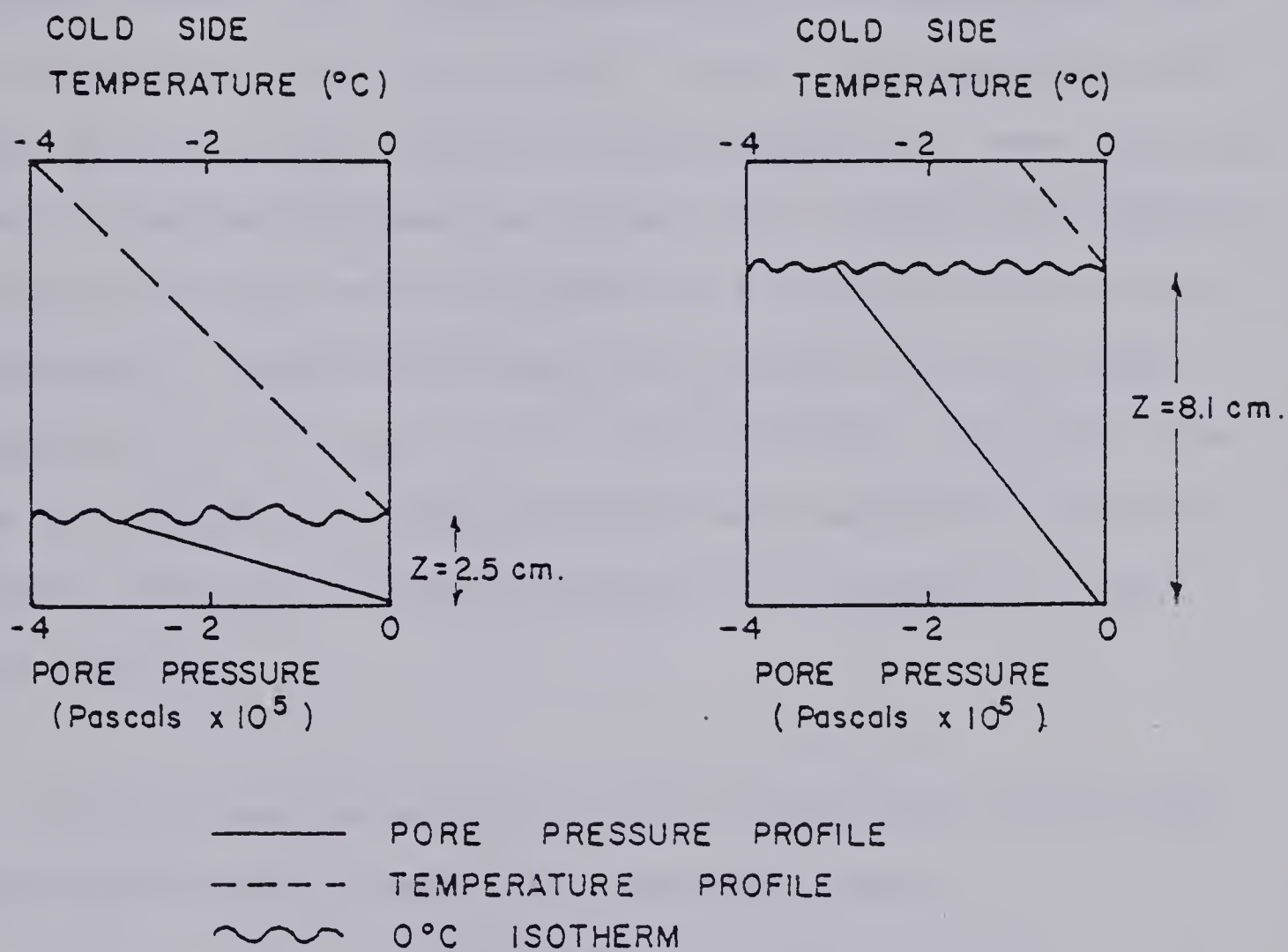


FIGURE A8-1: CHANGES IN PORE PRESSURE GRADIENT  
WITH CHANGES IN COLD SIDE  
TEMPERATURE .



potential, the soil permeability and the rate of advance of the freezing front (see McRoberts and Nixon, 1973). In the frost permeode however, a stationary freezing front, hence quasi steady state condition, are achieved in a few hours. Throughout the tests the water table is held constant at the base of the sample, creating two water pressure boundary values:  $P = -$  suction potential at the freezing front and  $P =$  atmospheric at the porous stone. The cold side temperature determines the steady state position of the freezing front, hence with samples of identical thickness the distance,  $dX$ , over which the hydraulic pressure difference,  $dH$ , is dissipated is a function of the cold side temperature. Figure A8-1 illustrates the situation for a cold side temperature of  $-4^{\circ}\text{C}$ . and of  $-1^{\circ}\text{C}$ . from test BB-1. It is clear that the thickness of soil through which the water must flow to reach the freezing front is considerably greater (3.3 X) for the  $1^{\circ}\text{C}$ . cold side temperature.

Suction pressures generated at the freezing front can be calculated from the data in Table A8-1 using Darcy's law:

$$dH = Q \frac{dX}{kA}$$

where  $k$  = soil permeability ( $1.2 \times 10^{-8}$  cm/sec)

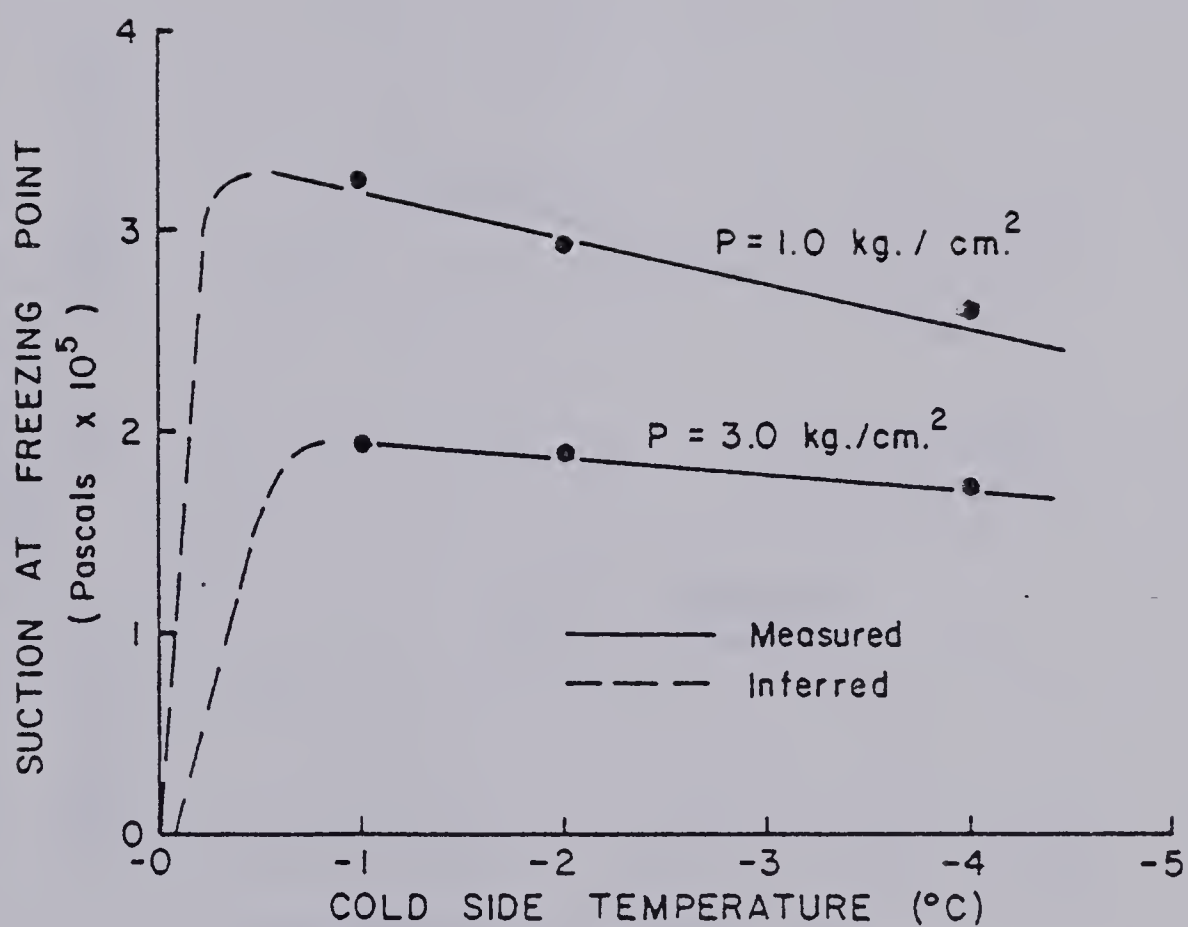
$A$  = cross sectional area of soil sample

$dX$  = distance between the frost front and the porous stone

The suction pressures are listed in Table A8-1. They are plotted as a function of cold side temperature in Figure A8-2 and as a function of the temperature gradient in the frozen zone in Figure A8-3. The plots are very similar in form. There appears to be a limiting



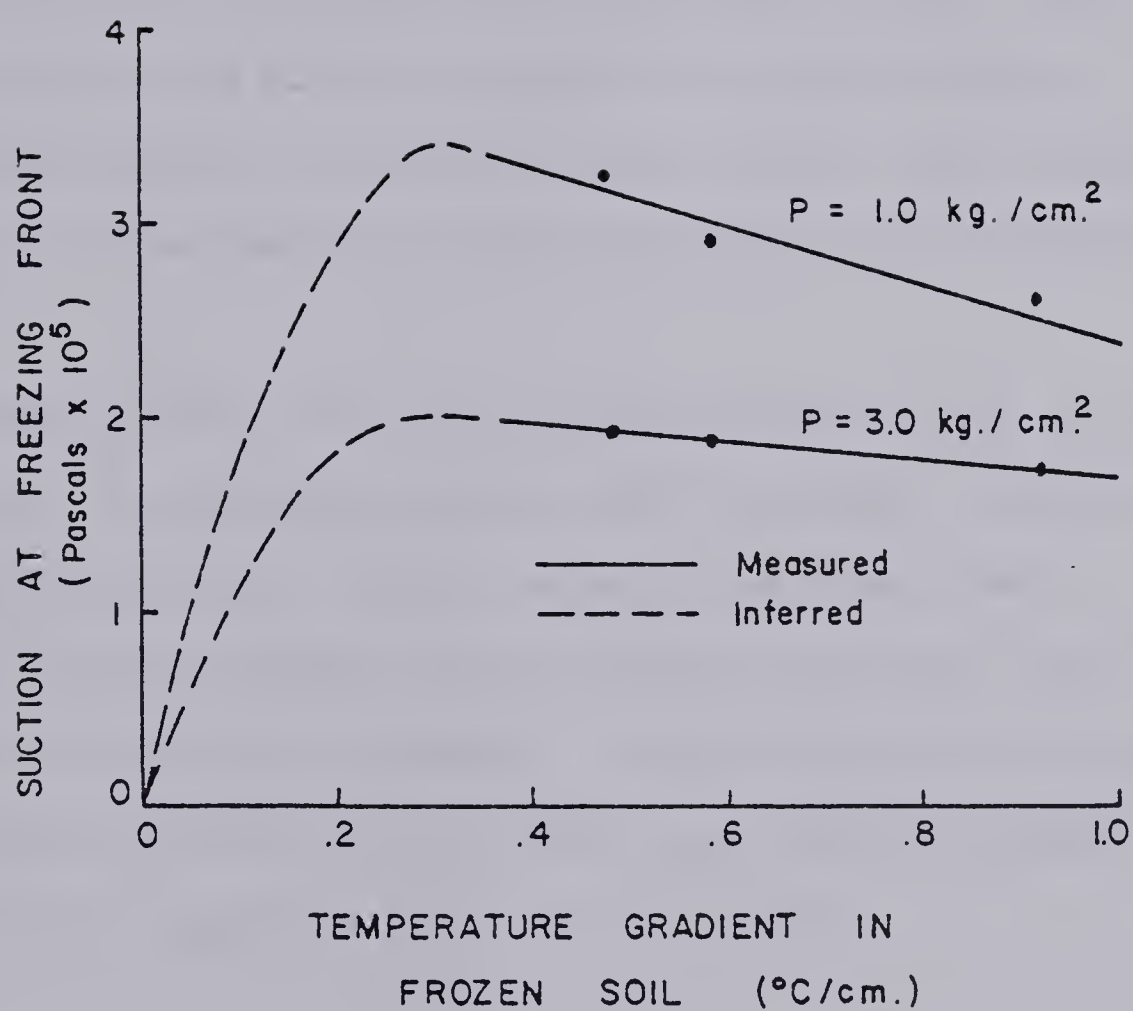




CALCULATED SUCTION AT THE FREEZING FRONT AS A FUNCTION OF COLD SIDE TEMPERATURE .

FIGURE A8-2





CALCULATED SUCTION AT FREEZING FRONT  
AS A FUNCTION OF TEMPERATURE  
GRADIENT IN THE FROZEN SOIL.

FIGURE A8-3



suction potential at some temperature between  $0^{\circ}\text{C.}$  and  $-1^{\circ}\text{C.}$  At cold side temperatures below  $-1^{\circ}\text{C.}$ , suction potentials are nearly constant. This conclusion agrees with those of Hill (1976) who also found a limiting suction in freezing soils. At cold side temperatures below  $-1^{\circ}\text{C.}$ , pressure is the dominant variable in determining heave rates. The relationship derived by Linnel and Kepler (1959) between  $\ln$  heave rate and overburden pressure is supported (see Appendix 9). In the temperature range  $0^{\circ}$  to  $.5^{\circ}\text{C.}$ , the temperature variable is by far the most important variable. Small temperature depressions at the freezing front or small changes in the temperature gradient of the frost fringe (Miller, 1978) produce large increases in the interfacial suction potential in the vicinity of  $0^{\circ}\text{C.}$

Penner and Ueda (1977) and Penner and Walton (1978) have maintained that the hydraulic potential ( $dH$ ) is a direct function of the cold side temperature. Results presented above show that it is the hydraulic gradient ( $dH/dX$ ) and not hydraulic potential that is a function of cold side temperature. Further discussion of the ramifications of this error in the frost heave theory developed by Penner et al is beyond the scope of this thesis.

In the palsa soils, a maximum overburden pressure of  $1 \text{ kg/cm}^2$  will occur. Approximate suction potentials at the freezing front of  $3 \times 10^5$  Pascals occur at this pressure; this result was used in Chapter 5 to approximate the development time for the observed ground ice in the palsa complex.





**B30314**